Comprehensive studies on the genome-edited hybrid rice line with dual truncations in the calmodulin-binding domains of OsGAD1 and OsGAD3

OsGAD1 と OsGAD3 のカルモジュリン結合ドメインの欠損を二重に持つゲノム編集ハイブリッドイネ系統に関する総合的研究

A Dissertation

Presented to the Graduate School of Natural Science and Technology

Of Shimane University

In Partial Fulfilment of the Requirements for the Degree

Doctor of Philosophy in Science

(Doctoral Program in Science and Engineering for Innovation)

By

UMMEY KULSUM

N22D204

August 2025

Thesis Supervisor

Professor Kazuhito Akama

Co-supervisors

Associate Professor Sadanobu Katoh

Professor Noritaka Hirohashi

Professor Yuuki Kodama

Acknowledgements

With sincere gratitude, I thank Allah (SWT) for granting me the strength, patience, and guidance to complete this PhD journey.

I would like to express my deepest and most heartfelt appreciation to my supervisor, Professor Kazuhito Akama**,** for his exceptional mentorship, continuous encouragement, and unwavering support throughout my doctoral studies. His thoughtful guidance, patience, and insight have had a profound impact on the direction and quality of my research. I am truly honored and grateful to have worked under his supervision.

I am also deeply thankful to my co-supervisors, Associate Professor Sadanobu Katoh, Professor Noritaka Hirohashi, and Professor Yuuki Kodama, for their invaluable guidance, advice, and support. My sincere appreciation extends to Professor Tsuyoshi Nakagawa and Associate Professor Kohji Nishimura, members of my thesis examination committee.

I extend my gratitude to the Ministry of Education, Culture, Sports, Science and Technology (MEXT), Japan, for granting me the scholarship that made it possible to pursue my PhD studies in Japan. The financial and academic support I received through this program enabled me to fully engage in my research and academic development during these years.

To my dear friends in Japan and Bangladesh, I am incredibly thankful for your friendship, support, and encouragement during both the joyful and challenging moments of this journey. Whether it was a warm conversation, a shared meal, a kind word, or simply your presence, it helped me feel at home in a foreign land. I am especially grateful to my friends from Pakistan, Oman, Nepal, and India, as well as the Bangladeshi community in Matsue, who became like family to me.

To my lab mates and fellow researchers**,** thank you for creating a collaborative and supportive environment. I have learned much from our shared experiences, discussions, and teamwork. Your kindness, patience, and help, whether in the lab or outside, made this long academic journey much easier and more fulfilling.

Above all, I owe the deepest thanks to my family**.** To my beloved parents**,** whose endless love, sacrifices, and prayers have been my greatest source of strength, thank you for always believing in me and encouraging me even from afar. To my brother and sister-in-law**,** thank you for your support, patience, and the comfort your words brought in challenging moments.

This achievement is not mine alone; it is a reflection of the collective support, prayers, and love that I have been blessed with.

UMMEY KULSUM

Abbreviations

GABA = Gamma-Aminobutyric Acid
GAD = Glutamate Decarboxylase
CaMBD = Calmodulin-Binding Domain
CaM = Calmodulin
CRISPR/Cas9 = Clustered Regularly Interspaced Short Palindromic Repeats / CRISPR-associated protein 9
GC-MS = Gas Chromatography–Mass Spectrometry
DAB = 3,3′-Diaminobenzidine
RT-qPCR = Reverse Transcription Quantitative Real-Time PCR
TBP-2 = TATA-binding Protein 2
RNA-seq = RNA Sequencing
DEGs = Differentially Expressed Genes
KEGG = Kyoto Encyclopedia of Genes and Genomes
GO = Gene Ontology
FPKM = Fragments Per Kilobase of Transcript per Million Mapped Reads
TCA = Trichloroacetic Acid
TE = Tris-EDTA Buffer
N6D = N6 Medium with 2,4-Dichlorophenoxyacetic Acid
MS = Murashige and Skoog Medium
SD = Standard Deviation
NADPH = Nicotinamide Adenine Dinucleotide Phosphate
HISAT2 = Hierarchical Indexing for Spliced Alignment of Transcripts
DESeq2 = Differential Expression Sequencing version 2
PCR = Polymerase Chain Reaction
CTAB = Cetyltrimethylammonium bromide
FW = Fresh weight
DW = Dry weight
H_2O_2 = Hydrogen peroxide
dNTP = Deoxynucleotide triphosphate
EDTA = Ethylenediaminetetraacetic acid

Table of contents

List of Tables

List of Figures

Chapter 1: Introduction

1.1 The global importance of rice and agricultural challenges

1.1.1 Rice as a staple crop

Rice (*Oryza sativa* L.) ranks among the most important cereal grains on the planet, providing sustenance for over half of the world's population (FAO, 2023). It accounts for approximately 21% of the energy consumed per person globally and contributes 15% of the protein intake per capita (Rice Production Course, n.d.). In many Asian countries, rice is not only a dietary staple but also a central component of cultural identity and economic livelihood. The importance of rice transcends regional boundaries, with global annual consumption exceeding 500 million metric tons (USDA, 2024). Due to its adaptability to different agro-ecological zones, rice is cultivated across diverse climatic regions. However, rice is particularly vulnerable to environmental disturbances. Its sensitivity to various environmental cues makes it an excellent model organism for studying plant stress responses (Radha et al., 2023).

1.1.2 Current and future challenges in rice production

Despite its crucial role in global food security, rice production faces mounting challenges due to the increasing demand from population growth, urban expansion, and changing dietary preferences. The pressure to increase rice yields without compromising environmental sustainability necessitates innovative agricultural approaches (Ray et al., 2013). In addition, rice yields have plateaued in several major producing regions, raising concerns about the ability to meet future food demands (Pingali, 2012).

Another pressing concern is abiotic stress, which has emerged as one of the most significant and persistent threats to rice productivity. Environmental factors such as drought, salinity, flooding, and extreme temperatures increasingly affect rice at critical growth stages, causing severe reductions in yield and grain quality (Yin et al., 2024). These stressors are often unpredictable, overlapping, and intensified by ongoing climate variability (Ahmed et al., 2017)

Traditional breeding has contributed to yield improvements under optimal conditions, but progress in enhancing abiotic stress tolerance has been limited due to the complex and polygenic nature of stress-responsive traits (Sabar et al., 2024). As a result, there is an urgent need for new approaches that integrate molecular breeding, functional genomics, and biotechnology to develop rice varieties with enhanced resilience to adverse environments.

1.1.3 Climate change and abiotic stresses: a growing threat

A major challenge facing rice production today is climate change, which has heightened the occurrence and severity of abiotic stresses like drought, salinity, flooding, and extreme temperature variations. These environmental stressors greatly hinder plant growth and productivity, frequently resulting in significant reductions in crop yields (Sarma et al., 2023).

For instance, drought stress can lead to up to 50% yield reduction in rainfed rice-growing areas by inhibiting photosynthesis, reducing water-use efficiency, and impairing reproductive development (Amin et al., 2022). Salinity affects over 20% of irrigated lands globally and disrupts ion homeostasis, leading to toxic accumulation of sodium ions in plant tissues (Majeed & Muhammad, 2019). Similarly, cold stress impairs seedling establishment and panicle development, particularly in temperate and high-altitude areas (Kruthika & Jithesh, 2023). Flooding causes oxygen deficiency, leading to metabolic disruption and root damage, especially during early vegetative stages (Singh et al., 2017). The cumulative impact of these stresses not only diminishes yields but also affects grain quality, thus impacting food and nutritional security. Therefore, enhancing abiotic stress tolerance in rice has become a primary objective of molecular breeding programs.

1.2 Plant responses to abiotic stress

1.2.1 Overview of abiotic stress in plants

Abiotic stresses refer to the non-living environmental factors that negatively affect plant growth, development, and productivity. These include temperature extremes, water scarcity (drought), excess water (flooding), salinity, nutrient deficiencies, and oxidative stress (H. Zhang et al., 2025). Unlike biotic stresses such as pathogen or pest attacks, abiotic stresses act by disrupting fundamental physiological and biochemical processes within plant cells (Pandey et al., 2017).

In rice, exposure to abiotic stress can compromise every developmental stage, from seed germination to grain filling (Thapa et al., 2023; Zhang et al., 2025). For instance, drought and salinity reduce cell turgor pressure, inhibit stomatal conductance, and impair photosynthesis (Radha et al., 2023). In contrast, cold temperatures can destabilize membrane fluidity, restrict enzymatic activities, and affect the formation of reproductive organs (A. Sharma et al., 2020). Plant responses to these stresses are not uniform; instead, they are highly dynamic and vary based on the stress intensity, duration, developmental stage, and genotype (Rahman et al., 2022).

To adapt and survive under unfavorable environmental conditions, plants have evolved complex defense mechanisms that include morphological changes (e.g., root elongation) (Sun et al., 2020),

physiological adjustments (e.g., stomatal regulation) (Melotto et al., 2017), metabolic reprogramming (Lu & Xia, 2025), and transcriptional modulation of stress-responsive genes (Sahil et al., 2021).

1.2.2 Molecular and biochemical responses

At the molecular level, plants respond to abiotic stress through signal perception, transduction, and the activation of stress-responsive transcription factors and downstream genes. Signal perception often involves membrane-bound receptor-like kinases (RLKs), calcium channels, and reactive oxygen species (ROS) sensors (G. Xu et al., 2022). Upon perception, intracellular second messengers such as calcium ions (Ca^{2+}), ROS, and nitric oxide (NO) are rapidly generated (Jain et al., 2018); (Wdowiak et al., 2024)and activate cascades such as mitogen-activated protein kinase (MAPK) pathways (K. Kumar et al., 2020).

Transcription factors such as DREB (Dehydration Responsive Element Binding) (Lata & Prasad, 2011), NAC (NAM, ATAF, and CUC) (Nuruzzaman et al., 2013), MYB (Ma et al., 2023), bZIP (basic leucine zipper) (Guo et al., 2024), and WRKY families (Phukan et al., 2016) play central roles in regulating stress responses by binding to cis-regulatory elements in the promoters of target genes. These genes encode for osmolyte biosynthesis enzymes, late embryogenesis abundant (LEA) proteins, detoxifying enzymes, and molecular chaperones that protect cellular structures.

Biochemically, plants increase the synthesis of compatible solutes such as proline, glycine betaine, sugars, and polyamines that stabilize proteins and membranes under osmotic stress (Paliwal et al., 2021). Antioxidant defense mechanisms involving enzymatic components such as superoxide dismutase (SOD), catalase (CAT), ascorbate peroxidase (APX), and non-enzymatic molecules such as glutathione and tocopherols also play vital roles in scavenging harmful ROS generated during stress (Aslam et al., 2022).

1.2.3 Role of osmoprotectants and antioxidants

Osmoprotectants are low molecular weight, highly soluble compounds that accumulate in plant cells under stress and confer protection by maintaining osmotic balance, stabilizing cellular structures, and detoxifying ROS (Zulfiqar et al., 2019). Common osmoprotectants include proline, trehalose, mannitol, and gamma-aminobutyric acid (GABA). Among these, GABA has gained increasing attention due to its multifunctional role in stress response. It functions not only as an osmoprotectant but also as a signaling molecule that integrates metabolic and environmental cues (Islam et al., 2024). GABA metabolism intersects with both the carbon and nitrogen pathways through the GABA shunt, providing metabolic flexibility and promoting energy production under stress conditions (Michaeli & Fromm, 2015).

Antioxidants play a crucial role in safeguarding plant cells from oxidative harm by countering the effects of excess reactive oxygen species (ROS). During periods of abiotic stress, significant amounts of ROS, including hydrogen peroxide (H_2O_2), superoxide (O_2^-), and hydroxyl radicals (OH•), are generated, which can lead to damage in lipids, proteins, and nucleic acids. To maintain cellular redox balance and ensure the health and stability of the cells, mechanisms such as the ascorbate-glutathione cycle and other antioxidant systems are essential. Given the vital functions of osmoprotectants and antioxidants, enhancing the biosynthetic and regulatory pathways for these compounds presents a valuable approach for improving crop resilience to abiotic stress, particularly in rice.

1.3 GABA metabolism in plants

1.3.1 Overview of GABA biosynthesis and the GABA shunt

Gamma-aminobutyric acid (GABA) is a non-protein amino acid that is widely present in plants, animals, and microorganisms (Hu et al., 2024). In plants, GABA is primarily synthesized via the decarboxylation of L-glutamate by the enzyme glutamate decarboxylase (GAD), which is considered the rate-limiting step in the GABA shunt (Li et al., 2021). The GABA shunt is a metabolic pathway that bypasses two steps of the tricarboxylic acid (TCA) cycle and comprises three key enzymatic reactions: (1) the conversion of glutamate to GABA by GAD, (2) the transamination of GABA to succinic semialdehyde (SSA) by GABA transaminase (GABA-T), and (3) the oxidation of SSA to succinate by succinic semialdehyde dehydrogenase (SSADH) (Michaeli & Fromm, 2015).

This pathway plays a central role in maintaining carbon–nitrogen balance, pH regulation, and providing intermediates for the TCA cycle under both normal and stress conditions (Ansari et al., 2021). Because it can rapidly convert excess glutamate into succinate, the GABA shunt serves as an important route for energy production when glycolysis or the TCA cycle is impaired during stress (Dabravolski & Isayenkov, 2023).

1.3.2 Functions of GABA in plant stress tolerance

Accumulation of GABA in plant tissues is one of the earliest responses to various abiotic stresses including salinity, drought, hypoxia, temperature extremes, and mechanical damage (Sita & Kumar, 2020). GABA contributes to stress tolerance through multiple mechanisms:

- **Osmotic regulation:** As a compatible solute, GABA helps maintain cell turgor and hydration by contributing to osmotic adjustment (Seifikalhor et al., 2019).
- **Redox homeostasis:** GABA indirectly supports the antioxidant system by enhancing the cellular redox state through the GABA shunt, thus limiting oxidative damage (Aswathi et al., 2025).

- **pH buffering:** The decarboxylation of glutamate consumes protons, which helps buffer cytosolic pH under acidic conditions caused by cellular damage (Islam et al., 2024).
- **Metabolic flexibility:** By feeding into the TCA cycle, GABA allows metabolic continuity even when primary metabolism is disrupted (Michaeli & Fromm, 2015).

Furthermore, GABA has been implicated in cell signaling (Seifikalhor et al., 2019), growth regulation (Abdullah et al., 2025), pollen tube development (Yu & Chen, 2008), and modulation of stomatal movement (B. Xu et al., 2021). It also interacts with phytohormonal signaling pathways such as abscisic acid (ABA), ethylene, and salicylic acid, further broadening its impact on plant stress physiology (Islam et al., 2024).

1.3.3 Signaling and cross-talk with phytohormones

Recent research has shown that GABA serves not only as a metabolic intermediate but also acts as a signaling molecule that can affect gene expression and engage with various signaling pathways (Fromm, 2020). A key function of GABA as a signaling agent is its capacity to modulate anion channels like aluminum-activated malate transporters (ALMTs), which in turn influences stomatal closure and ion movement in response to stress (Ramesh et al., 2018).

The interplay between GABA and phytohormones, especially ABA, has been of particular interest. Under drought or salinity stress, ABA accumulation is associated with GABA synthesis. In turn, GABA modulates ABA-responsive gene expression, suggesting a feedback mechanism between the two. GABA has also been shown to mitigate the effects of ethylene-induced senescence and to influence auxin-related development under stress (Michaeli & Fromm, 2015).

Thus, the multifunctional role of GABA in metabolism, signaling, and hormonal crosstalk positions it as a critical integrator of plant responses to abiotic stress. Enhancing GABA levels via metabolic engineering or targeted gene editing of *GAD* genes thus represents a promising avenue to improve crop resilience under changing environmental conditions.

1.4 Glutamate decarboxylase (*GAD*) genes in rice

1.4.1 *GAD* gene family: structure and regulation

In rice and other plant species, the glutamate decarboxylase (*GAD*) gene family encodes enzymes that catalyze the conversion of L-glutamate to gamma-aminobutyric acid (GABA), forming the first and rate-limiting step in the GABA shunt (Akama et al., 2001). These enzymes are pyridoxal-5'-phosphate (PLP)-dependent and localized predominantly in the cytosol. In rice, five GAD isoforms have been identified, OsGAD1 through OsGAD5, each exhibiting distinct expression patterns and regulatory mechanisms (Akama & Takaiwa, 2007; International Rice Genome Sequencing Project, 2005).

OsGAD1, OsGAD3, OsGAD4, and OsGAD5 contain a calmodulin-binding domain (CaMBD) at their C-terminal ends, which plays a pivotal role in modulating GAD activity via calcium/calmodulin interactions (Akama et al., 2020; Akter et al., 2024). This domain acts as an autoinhibitory segment, which suppresses enzymatic activity under basal conditions. Upon calcium influx triggered by environmental stress, CaM binds to the CaMBD, relieving the inhibition and activating GAD (Akama & Takaiwa, 2007). By contrast, OsGAD2 lacks this CaMBD (Akama et al., 2001). Transcriptional regulation of *GAD* genes is influenced by both developmental and environmental stimuli. For instance, *OsGAD3* is highly expressed in developing seeds, while OsGAD1 shows prominent expression in vegetative tissues and under stress conditions (Akama et al., 2020). Expression is also regulated by stress-induced signaling pathways involving calcium ions, abscisic acid (ABA), and reactive oxygen species (ROS).

1.4.2 The role of the calmodulin-binding domain (CaMBD)

Calmodulin is a universally conserved calcium-binding protein present across all eukaryotic organisms (Davis et al., 1986; McCormack et al., 2005; Kim et al., 2009). Interestingly, recent evolutionary studies indicate that the development of the CaMBD in certain early streptophyte lineages might have provided a beneficial adaptation for the shift to life on land. This development seems to align with the emergence of additional regulatory elements that are crucial for managing the more challenging and variable conditions encountered in terrestrial environments (Stéger & Palmgren, 2023).

The calmodulin-binding domain (CaMBD) found in many plant GADs is a conserved region that fine-tunes GAD activity through Ca^{2+}/CaM-dependent interactions. Structurally, it comprises basic amphiphilic α-helices rich in tryptophan and lysine residues, which facilitate electrostatic and hydrophobic binding to calmodulin (Baum et al., 1996). This interaction is calcium-dependent and essential for regulating the activity of the enzyme in response to fluctuations in cytosolic Ca^{2+} concentrations.

In unstressed cells, the CaMBD maintains GAD in a low-activity state, acting as a built-in brake to prevent excess GABA synthesis. Upon perception of environmental stress signals that elevate intracellular Ca^{2+} levels, calmodulin is activated and binds to the CaMBD, removing the inhibitory effect and enhancing GAD activity (Baum et al., 1993). This mechanism ensures that GABA is produced only when necessary, conserving metabolic resources during normal growth.

Recent studies have demonstrated that removing the C-terminal region or truncating the CaMBD leads to constitutive activation of GAD, resulting in elevated GABA levels regardless of external stimuli (Akama & Takaiwa, 2007; Akama et al., 2020). This genetic strategy has proven beneficial for

developing genome-edited plants with improved abiotic stress tolerance and increased GABA content in grains, a desirable trait for nutritional enhancement (Akter et al., 2024; Akama et al., 2020).

1.4.3 Genetic manipulation of GADs to enhance GABA

Recent advances in molecular biology, including both transgenic and genome editing technologies, have facilitated precise manipulation of glutamate decarboxylase (*GAD*) genes to enhance GABA biosynthesis. Transgenic approaches have traditionally employed constitutive or tissue-specific promoters to overexpress GAD genes or introduced foreign genes to increase GABA levels. For example, transgenic rice lines overexpressing *OsGAD2* under the control of a constitutive promoter showed significant increases in GABA content, particularly in roots and developing seeds (Akama & Takaiwa, 2007). Similarly, heterologous expression of *AtGAD1* from *Arabidopsis thaliana* in maize resulted in elevated GABA levels (Rajani et al., 2021). In tobacco, overexpression of GAD also led to increased GABA content and conferred improved resistance against biotic stressors, highlighting the role of GABA in plant defense mechanisms (McLean et al., 2003).

Even though transgenic approaches have successfully enhanced GABA accumulation in various plant species, they are often met with regulatory restrictions and public concerns due to the incorporation of foreign DNA. In contrast, CRISPR/Cas9-mediated genome editing presents a precise and transgene-free alternative for modifying endogenous genes. This technique enables targeted manipulation of specific regulatory domains, such as the calmodulin-binding domain (CaMBD) in GAD enzymes, without the need for constitutive overexpression. For example, Akter et al. (2024) demonstrated that genome editing of the CaMBD in OsGAD4 led to increased GABA accumulation and improved abiotic stress tolerance in rice, underscoring the functional relevance of this regulatory region. Similarly, Akama et al. (2020) reported that CRISPR/Cas9-mediated truncation of the CaMBD in OsGAD3 significantly elevated GABA content in rice seeds, accompanied by enhanced seed weight and protein concentration.

Similarly, manipulation of OsGAD1, a gene more prominent in vegetative tissues, holds potential for improving stress tolerance during early plant development. While OsGAD3 is more seed-specific, editing both OsGAD1 and OsGAD3 simultaneously could potentially confer both stress resilience and nutritional benefits. This approach exemplifies the power of precise, multi-target genome editing for complex trait improvement in crops. The rice *GAD* gene family represents a valuable molecular target for enhancing GABA biosynthesis and abiotic stress tolerance. Disruption of the CaMBD emerges as a key strategy to derepress GAD activity, offering a scalable method to improve rice performance under adverse environmental conditions.

1.5 Biotechnological approaches for enhancing stress tolerance

1.5.1 Conventional breeding vs genetic engineering

For decades, conventional breeding has been the cornerstone of crop improvement, relying on phenotypic selection and hybridization to enhance desirable traits such as yield, disease resistance, and abiotic stress tolerance. While effective, traditional breeding is time-consuming and limited by the genetic diversity within cross-compatible species. Moreover, the polygenic nature of stress tolerance traits, along with strong environmental interactions, often complicates selection and slow progress.

Genetic engineering emerged as a transformative alternative, allowing the direct introduction of novel genes from diverse species into crops. This approach enabled the development of transgenic plants expressing stress-responsive genes such as transcription factors (e.g., DREB, MYB), osmolyte biosynthesis enzymes (e.g., P5CS), and detoxifying proteins (e.g., glutathione-S-transferases) (Pandita, 2023). However, concerns over biosafety, public acceptance, and regulatory restrictions have constrained the widespread adoption of transgenic crops, especially in food staples like rice (OECD, 2023). To address these limitations, modern approaches such as genome editing have been developed, offering precision, speed, and non-transgenic modifications that align better with current regulatory and public expectations.

1.5.2 CRISPR/Cas9 in rice research

The clustered regularly interspaced short palindromic repeats (CRISPR)/CRISPR-associated protein 9 (Cas9) system has revolutionized plant biotechnology by enabling site-specific genome editing with unparalleled precision and efficiency. In rice, CRISPR/Cas9 has been successfully used to edit a wide array of genes involved in stress tolerance, yield, grain quality, and disease resistance (Chen et al., 2024). Compared to RNA interference (RNAi) and overexpression strategies, CRISPR/Cas9 allows for the generation of stable, heritable mutations without foreign DNA integration (Bhattacharjee et al., 2023).

Applications in rice include the knockout of negative stress regulators (e.g., OsERF922) (Wang et al., 2016), editing of drought-tolerance regulators (e.g., OsPYL1) (Usman et al., 2020), and targeted modification of grain quality traits (e.g., *Wx* gene for amylose content) (Huang et al., 2020). Moreover, multiplex genome editing has facilitated simultaneous modifications of multiple loci, a strategy well-suited for complex traits like abiotic stress tolerance (Bahariah et al., 2021). CRISPR/Cas9 has also been applied to genes related to GABA metabolism. Deletion of the CaMBD region in OsGAD3 via CRISPR/Cas9 led to increased GABA content in seeds, demonstrating its utility in metabolic engineering (Akama et al., 2020). Similarly, targeted truncation of the CaMBD in OsGAD4 has been shown to enhance GABA accumulation and improve abiotic stress tolerance in rice seedlings, further

validating the role of *GAD* genes in stress-responsive metabolic pathways (Akter et al., 2024). This highlights the potential of genome editing not just for trait enhancement but also for nutritional fortification.

1.5.3 Previous studies on genome editing of stress-response genes

Several studies have employed CRISPR/Cas9 and related technologies to improve rice tolerance to abiotic stresses by targeting stress-inducible or regulatory genes. For instance, the deletion of the *OsDST* gene, a negative regulator of drought and salt stress tolerance, improved water-use efficiency and survival under adverse conditions (Santosh et al., 2020). Similarly, disruption of OsRR22, a type-B response regulator involved in cytokinin signaling, enhanced salinity tolerance (Zhang et al., 2019). Together, these advances underscore the power of genome editing technologies like CRISPR/Cas9 in dissecting stress-related pathways and generating elite rice varieties capable of thriving under challenging environmental conditions. When combined with knowledge from functional genomics, transcriptomics, and metabolic profiling, genome editing can be strategically deployed for precise trait stacking and robust crop improvement.

1.6 Knowledge gaps and rationale for this research

1.6.1 Underexplored potential of OsGAD1 and OsGAD3

Despite significant advancements in plant stress biology, the OsGAD gene family in rice, particularly OsGAD1 and OsGAD3, remains underutilized in the context of abiotic stress tolerance. While GABA metabolism has been extensively studied for its role in osmotic regulation, antioxidant defense, and metabolic flexibility, few studies have explored the direct manipulation of OsGAD genes through genome editing for dual benefits: stress resilience and metabolic enhancement.

Previous research has largely focused on stress-responsive transcription factors and signaling components such as OsDREB, OsNAC, and OsHKT1;5 (Yuan et al., 2016), often neglecting primary metabolic regulators like GADs that integrate both stress signaling and energy homeostasis. OsGAD3 has been manipulated to increase grain GABA content (Akama et al., 2020), and OsGAD4 truncation has demonstrated improved stress tolerance (Akter et al., 2024). However, a comprehensive assessment of OsGAD1 and OsGAD3 either individually or in combination, for abiotic stress mitigation has not been thoroughly investigated. Furthermore, while the role of the calmodulin-binding domain (CaMBD) in regulating GAD activity is well-established, its targeted removal using CRISPR/Cas9 in rice to modulate GABA synthesis under stress conditions represents a novel strategy. A dual-editing approach targeting both OsGAD1 and OsGAD3, aimed at generating a synergistic or additive effect, has not been documented prior to this research.

1.7 Need for combinatorial editing and hybrid development

Single-gene modifications may offer limited improvements in complex traits like abiotic stress tolerance, which are controlled by networks of interconnected pathways. Therefore, a combinatorial editing strategy that targets multiple genes within the same pathway, such as OsGAD1 and OsGAD3, is more likely to produce robust phenotypic outcomes.

The rationale behind combining mutations in *OsGAD1* and *OsGAD3* is based on their complementary expression profiles and physiological roles. *OsGAD1* is predominantly expressed in vegetative tissues and may be critical during early developmental stages and environmental adaptation (Luo et al., 2024). Conversely, OsGAD3 is more active in seeds and reproductive tissues, thus potentially contributing to long-term fitness and nutritional value (Akama et al., 2020). By developing a hybrid line that inherits edited versions of both genes, it becomes possible to harness the benefits of hybrid vigor along with enhanced GABA biosynthesis and stress tolerance. This strategy aligns with broader trends in plant biotechnology, where stacking beneficial alleles through precise editing or crossing is increasingly viewed as a powerful approach to address multifactorial agricultural challenges.

1.8 Research aims and anticipated significance

This research aims to:

- Utilize CRISPR/Cas9 technology to truncate the calmodulin-binding domain (CaMBD) of *OsGAD1*, generating a genome-edited rice line with constitutively active GAD enzyme activity.
- Cross genome-edited *OsGAD1* and *OsGAD3* lines to develop a hybrid line combining both modifications, with the hypothesis that dual truncation will result in additive or synergistic increases in GABA accumulation and abiotic stress tolerance.
- Evaluate the resulting genotypes under multiple abiotic stresses (cold, drought, salinity, and flooding) to assess physiological performance and GABA accumulation.
- Conduct transcriptomic analysis to identify differentially expressed genes and enriched biological pathways associated with enhanced stress tolerance.

The anticipated significance of this study lies in its novel approach to manipulating GABA metabolism through the simultaneous editing of two key regulatory genes. It not only expands the functional understanding of *OsGAD1* and *OsGAD3* in stress physiology but also demonstrates the utility of CaMBD truncation as a generalizable tool for metabolic and stress engineering.

Chapter 2: Materials and Methods

2.1 Plant materials and growth conditions

Oryza sativa L. cv. Nipponbare (Ni) was used in this study as a control plant. For *in vitro* tissue culture, rice seeds were prepared using the following steps:

i. The rice seeds were dehulled using an automatic rice husker (Model TR-260; Kett Electric Laboratory Co. Ltd., Tokyo, Japan).
ii. Immediately after dehulling, the seeds were immersed in 70% (v/v) ethanol for 1 minute and then thoroughly rinsed with double-distilled water (ddH_2O).
iii. The dehulled seeds were surface sterilized by treating them with a 50% (v/v) bleach solution (Kao Co. Ltd., Tokyo, Japan) for 30 minutes while gently shaking.
iv. After this treatment, the seeds were washed five times with ddH_2O to remove any residual bleach.
v. Following surface sterilization, the seeds were transferred to 0.5× Murashige and Skoog (MS) agar medium (Murashige & Skoog, 1962) for germination.
vi. The seeds were placed in a growth chamber at 25°C (SANYO, Osaka, Japan) with illumination provided by white fluorescent tubes for a duration of 2 weeks.
vii. After 2 weeks of germination, the seedlings were carefully moved into a commercially available soil medium (JA, EPOCH Co., Ltd., Izumo, Japan) and maintained in a growth room under a photoperiod of 16 hours of light and 8 hours of darkness at the same temperature of 25°C.

2.2 Generation of genome-edited OsGAD1ΔC lines

2.2.1 Design and Cloning of gRNAs for Rice Transformation

To achieve truncation of the C-terminal region of OsGAD1, we employed the CRISPR-P program (http://crispr.hzau.edu.cn/CRISPR2/) for the design of single guide RNAs (gRNAs). This process involved identifying multiple target sequences within the 3'-terminal coding region of OsGAD1. Specifically, we developed three distinct gRNAs: gRNA-F1 and gRNA-F2, which were strategically placed upstream of the calmodulin-binding domain (CaMBD), and gRNA-R1, which was located downstream of this domain (Table 2). Each of these gRNAs consisted of a 20-nucleotide sequence targeted at the *OsGAD1* gene.

The next steps involved the synthesis and annealing of these gRNA sequences to form double-stranded DNA, which was a critical precursor for cloning. Subsequently, these double-stranded gRNAs were inserted into the *BbsI* restriction site of the gRNA cloning vector pU6gRNA. This procedure resulted in the generation of three distinct plasmids designated as pU6gRNA_F1, pU6gRNA_F2, and

pU6gRNA_R1. The methodologies followed were consistent with the established protocols as detailed by (Mikami et al., 2015).

To assemble the gRNA expression cassette containing gRNA-R1, the pU6gRNA_R1 plasmid was digested with the restriction enzymes *Pvu*II and *Asc*I. The resultant fragment was then ligated into either pU6gRNA_F1 or pU6gRNA_F2 at their respective *Eco*RV and *Asc*I sites. This ligation step facilitated the formation of two new constructs: pU6gRNA_F1_R1 and pU6gRNA_F2_R1. These constructs were essential for the next phase of our research, which involved rice transformation.

2.2.2 *Agrobacterium*-mediated transformation

Following the creation of the constructs, we introduced them independently into the Ti plasmid pZH_gYSA_MMCas9 at the *Asc*I and *Plm*I sites to construct a binary vector necessary for *Agrobacterium tumefaciens*-mediated transformation of rice. The introduction of the binary vector into the *Agrobacterium tumefaciens* strain EHA105 was then accomplished through electroporation. (Hood et al., 1993).

After successfully transforming the *Agrobacterium*, we proceeded with the rice calli transformation. This process was carried out by co-cultivating *Agrobacterium* with the rice calli and subsequently selecting for transformants on N6D medium, which was supplemented with 50 mg/L of hygromycin B, in alignment with the rice transformation protocol outlined by Ozawa (2009). The selection medium allowed for the survival of only those cells that had integrated the gRNA constructs, thereby promoting the development of transgenic lines.

Following selection, the rice calli were cultured under appropriate conditions to regenerate into whole plants. After the regeneration phase, four distinct transgenic lines were identified and selected as successful candidates for genome-edited OsGAD1ΔC lines.

Table 1. List of media

Media	Composition
Growth media 0.5x MS (Murashidge and Skoog) media (Murashige & Skoog, 1962)	2.35 g/L of MS powder (Wako, Japan) dissolved in deionized water, pH adjusted to 5.8, addition of 4 g/L Gelrite, and autoclave at 121°C, 15 psi for 20 minutes.
Selection media N6 (Chu) media (Lei et al., 2014)	Sucrose (30g/L), N6 basal salt (Sigma, Japan) (3.98g/L), *Myo*-inositol (100mg/L), Casamino acids (300mg/L), Proline (1150mg/L) dissolved in deionized water, pH adjusted at 5.8. Addition of Gelrite (Wako, Japan) (4g/L). Autoclave at 121°C, 15 psi for 20 minutes. Addition of 2,4-D (200µl/L), PPM (plant preservative mixture) (500µl/L), N6D Vitamin (1 ml/L).
Regeneration media (Mikami et al., 2015)	MS powder (4.70g/L), Sucrose (30.0g/L), Sorbitol (30.0g/L), Casamino acid (2.0g/L), pH adjusted at 5.8. Gelrite (4.0g/L) After autoclave the media was supplemented with NAA (α-naphthaleneacetic acid) (0.2mg/L), Kinetin (2.0mg/L), Meropenem (1ml/L), Hygromycin (1ml/L), PPM (500µl/L).
Hormone free media	MS powder (2.35g/L), adjust pH at 5.8. Gelrite (4g/L), After autoclave the media was supplemented with PPM (500 µl) and Hygromycin (500mg/L).

2.3 Analysis of the OsGAD1ΔC rice line

A mixture of six rice grains from each of the selected four transgenic T_1 lines was collected and finely ground using a MicroSmash (Tomy, Tokyo, Japan). From this powdered sample, 20 mg was taken for the isolation of free amino acids, following the protocol established by Akama et al. (2009), which involves an 8% (v/v) solution of trichloroacetic acid (TCA). In parallel, another portion of the rice powder was used to extract total DNA through the cetyltrimethylammonium bromide (CTAB) method as detailed by Murray & Thompson (1980). The specific region coding for *OsGAD1* was then PCR-amplified using designated primer pairs (Table 2) to verify successful genome editing in the transgenic rice lines.

2.3.1 Genomic DNA isolation

Genomic DNA isolation from leaf tissue using the CTAB (Cetyl trimethylammonium bromide) method involved the following steps:

i. ~50mg fresh leaf sample from each of the plants, was frozen on liquid nitrogen and crushed in screw cap tubes (2ml) containing small (5mm) stainless steelbeads (Microsmash TOMY, Tokyo, Japan).
ii. 2% CTAB buffer (5M NaCl, 0.5M EDTA, 1M Tris-HCl, 2% (w/v) CTAB) was mixed with 0.2% 2-mercaptoethanol in a 2 ml tube, and 400 µL of the CTAB buffer was added to the leaf sample and shaken gently.
iii. Then placed in a heat-block incubator, CLUBIO (60°C) for 30 minutes, shaken occasionally.
iv. 400 µL of Chloroform: Isoamyl alcohol (24:1) mixture was added and mixed well.
v. Centrifuged at 14000 x *g* for 10 minutes at 4°C to transfer the aqueous phase to a new 1.5 ml clean micro centrifuge tube.
vi. After that, 200 µL of cold isopropanol was added for DNA precipitation and mixed well.
vii. Centrifuged at 14000 x *g* for 10 minutes at 4°C, and the supernatant was discarded, keeping the pellet.
viii. Then, air-dried the DNA pellet and dissolved it in 100ul TE (including 10ug/ml RNaseA), mixed well by vortex (IWAKI), then incubated 30 minutes at 30°C.
ix. Afterward, 100ul TE (10mM Tris-1mM EDTA) buffer (pH 8), 100ul 7.5M Ammonium Acetate (pH 5.5), and 750 uL 100% (v/v) Ethanol were added, mixed well, and vortexed for 5 min.
x. Again centrifuged at 14000 x *g* for 20 minutes at 4°C, and the supernatant was discarded, keeping the pellet.
xi. Washed with 1 mL 70% (v/v) cold Ethanol, centrifuged at 14000 x *g* for 5 minutes at 4°C. and discarded the ethanol.
xii. The DNA pellet was allowed to dry and dissolved in 100 µL TE.
xiii. The concentration of DNA was confirmed by electrophoresis of the individual samples on a 1% agarose gel and also using Qubit™ fluorometer (Q32857, Invitrogen, USA). After that, genomic DNA was used for PCR reaction and DNA sequencing.

2.3.2 PCR screening

Isolated DNA was used for PCR amplification using EmeraldAmp® PCR Master Mix (TAKARA, Japan), followed by 30 cycles of denaturation at 98°C for 10 s, annealing at 55°C for 30 s, and extension at 72°C for 30 s. Target-specific primers for *OsGAD1* were employed to amplify the regions of interest (Table 2).

Table 2. List of primers

Primer	Sequence (5'-3')	Purpose
OsGAD1gRNA F1	GTTGGCCCGATTGCTGCTTCGCGA	Genome editing
OsGAD1gRNA R1	AAACTCGCGAAGCAGCAATCGGGC	
OsGAD1gRNA F2	GTTGGCAATCGGGCGACGATGGCG	
OsGAD1-329 F	TCGTCATCAGGGAGGACTTC	Confirmation of genome editing
OsGAD1-329 R	CGTACACCGCCAGTCAGTC	
OsGAD3-F57	GTCCTCGACATCGAGAAGGT	
OsGAD3-R379	AGAATCGAAGGCTCCACTCA	
OsHSP70-F	ACCGTCTTTGATGCCAAG	RT-qPCR analysis
OsHSP70-R	CTCAGCAATCTCACGCAT	
OsNAC3-F	GAAGAACGAGTGGGAGAAGATG	
OsNAC3-R	GCGAGCATGGAGAGGTC	
OsMYB30-F	GTGGATCAACTACCTCCGC	
OsMYB30-R	TTCTTGATCTCGTTGTCCGTC	
OsERF68-F	TCATCTACGACTACATCCCGG	
OsERF68-R	GTTCTTCCGCTCCCTCTTC	
OsHAK5-F	CCAAAGCCATACAGCCAAG	
OsHAK5-R	TCCTTGATCCCGTTGGTAAAG	
OsRAB16A-F	GCTCAAGCTCGTCTGAGG	
OsRAB16A-R	GTGTCGGTGGTGGTGGTG	
OsTAF2-F	CTTGCTTTACCAGGTCTTAAGC	
OsTAF2-R	GACACTGTGGAAAAATGAGATG	
OsADC1-F	TCCCGATCATCCCAATCCAG	
OsADC1-R	GAGGAACATGCCGAGGTAGT	
OsSGL-F	CACAGCAGAAGAAGCAGAGC	
OsSGL-R	CTAATAGGCGGTGTGGTGTTG	
OsSAP1-F	CGCGACAAGAAGGATCAGGA	
OsSAP1-R	GGTGACGACAAAGAAGACGG	
OsGolS1-F	TGTGCAGCGGGTTCGAAG	
OsGolS1-R	GGAAGTACTTGACGGCGC	
OsDST-F	AAGTTCTTGAAGTCGCAGGC	
OsDST-R	CCCCAACGCCAGCAGTAG	
OsDSR-1 F	CAGATTCATGGGTTATGG	
OsDSR-1 R	GACAGCAGCTTCTTGATA	
OsHSF13-F	AACACCTACGGATTTAGGAAAG	

OsHSF13-R	CTCAATCTCTTCTTCCATCC	
OsDREB2B-F	GTGGAGGCGAGGAAAGTACTGGA	
OsDREB2B-R	CCTGTGGATCAAGCTCCTGC	
OsGAD1-F	ATGGGACTGACTGGCGGTGTA	
OsGAD1-R	AGGAGGAAGGAGATTGGCAAGC	
OsGAD2-F	AACCAAGGGCGTTTGCTAGAC	
OsGAD2-R	AAGAAGGTTTAGTACGCTCCCA	
OsGAD3-F	TCCACAAATCAAGACGCTGCTG	
OsGAD3-R	GGACCTAGAATCGAAGGCTCCA	
OsGAD4-F	ACCGTCTCAAGTCTGCTCTCAT	
OsGAD4-R	TCAATTCACTGCTACACACCCA	
TBP2-F	TGGTCTGGAGGAGCGTATAGCA	Internal control for RT-qPCR
TBP2-R	CAAGTCTCTCAGTCACCCAAGC	

2.3.3 DNA sequencing

To further validate the CRISPR/Cas9-mediated edits in *OsGAD1,* DNA sequencing was carried out through a series of steps, including enzymatic purification of the PCR product, cycle sequencing, and post-reaction cleanup, followed by capillary electrophoresis in ABI 3130xl genetic analyzer (Thermo Fisher Scientific, USA).

PCR product purification

Purification of PCR products was conducted using ExoSAP-IT (Thermo Fisher Scientific, USA) to degrade remaining primers and unincorporated nucleotides. The purified mix consisted of:

- 6 µL PCR product
- 14 µL nuclease-free water (dMQ)
- 4 µL diluted ExoSAP-IT (1 µL enzyme diluted in 40 µL water)

Cycle Sequencing Reaction

The cleaned PCR products were used as templates for cycle sequencing using the BigDye Terminator v3.1 Kit (Applied Biosystems, USA). Each 10 µL reaction included:

- 1 µL purified DNA
- 1.9 µL sequencing buffer
- 0.2 µL BigDye terminator mix
- 0.3 µL primer (Forward or Reverse)
- dMQ water

The thermocycling protocol included an initial denaturation at 95°C for 5 minutes, followed by 30 cycles of denaturation at 95°C for 30 seconds, annealing at 52°C for 10 seconds, and extension at 60°C for 4 minutes.

Post-Sequencing Cleanup and Analysis

To remove residual salts and dyes, ethanol precipitation was performed. Each sample was mixed with 1 µL of 3 M sodium acetate (pH 5.2) and 25 µL of 100% ethanol, gently pipetted, and left to stand at room temperature in the dark for 15 minutes. After centrifugation at 14,000 × *g* for 20 minutes at 4°C, the supernatant was discarded. The pellet was washed with 20 µL of 70% ethanol, followed by another spin at 14,000 × *g* for 10 minutes. After drying, the pellet was resuspended in 15 µL of Hi-Di Formamide, briefly vortexed, and heat-denatured at 95°C for 5 minutes before rapid cooling on ice.

Samples were analyzed using the ABI PRISM 3130xl Genetic Analyzer (Applied Biosystems), and the sequence data were interpreted using GENETYX-MAC software version 22.0.1 (GENETYX Corporation, Japan).

2.3.4 Amino acid isolation

The isolation of free amino acids was performed using the following steps

i. The plant sample, ~30mg was collected from each plants and frozen on liquid nitrogen and crushed in 2ml screw cap tubes containing small (5mm) stainless steel beads.
ii. 400ul of 8% TCA (Trichloroacetic acid) (10:1 volume ratio) was added to the sample.
iii. Shook the mixture for 30 min using IWAKI TUPLE MIXER.
iv. Centrifuged 20 min at 14,000 x *g* at 20°C.
v. The supernatant was transferred to a new 1.5 mL tube.
vi. Addition of diethyl ether at a volume close to the top of the tube.
vii. Again, shook for 30 minutes.
viii. Centrifuged for 20 minutes at 14,000 x *g* at 20°C.
ix. Repeated the process from the addition of diethyl ether and shaking for 30 minutes.
x. Air dried the solution of amino acid for 15 minutes to remove the extra diethyl ether.

2.3.5 GABA quantification using GABase enzymatic assay

The concentration of GABA in rice tissues was measured using a fluorescence-based enzymatic assay involving GABase (Sigma-Aldrich), a commercial enzyme preparation containing GABA transaminase (GABA-T) and succinate semialdehyde dehydrogenase (SSADH) from *Pseudomonas fluorescens,* following the method outlined by Akama et al. (2009). These enzymes facilitate the two-step conversion

of GABA to succinate with concomitant reduction of $NADP^+$ to NADPH, which is measurable via fluorescence. To generate a standard curve for accurate quantification, twelve GABA standards of known concentrations were prepared: 0.1, 0.25, 0.5, 1.0, 1.5, 2.0, 2.5, 3.0, 5.0, 10.0, and 20.0 nmol per 20 µL. These standards were analyzed under the same conditions as the unknown samples to ensure calibration across the full range of expected GABA concentrations.

A 150 µL reaction mixture was prepared for each sample or standard, consisting of:

- 142 µL of 0.1 M pyrophosphate buffer (pH 10.5)
- 4 µL of 60 mM 2-mercaptoethanol
- 2 µL of 60 mM α-ketoglutarate
- 2 µL of 50 mM $NADP^+$

The prepared mixture was added to a 96-well plate already containing 20 µL of either the extracted amino acid sample or a GABA standard, bringing the total volume to 170 µL per well. A GABase working solution (10 µL per well) was freshly prepared by mixing 2 µL GABase (2 units/ml) with 8 µL of buffer, then added to initiate the reaction. The plate was incubated at 37°C for 1 hour.

Following incubation, the plate was placed into a fluorescence microplate reader (TECAN Wako Genios FL, Austria). Absorbance was measured before and after incubation to determine NADPH formation. The difference in absorbance values corresponds to the GABA concentration in each sample. Fluorescence readings were compared against the standard curve to calculate the GABA content.

2.3.6 Amino acid assessment by gas chromatography-mass spectrometry (GC-MS)

Free amino acid contents were quantified using gas chromatography–mass spectrometry (GC-MS) (Shimadzu, Kyoto, Japan) with the EZ:Faast™ GC-MS Free Amino Acid Analysis Kit (Phenomenex, USA), following a modified version of the method by Kowaka et al. (2015).

Standard and Calibration

Amino acid standards (SD1–SD3) at 200 nmol/mL were used. GABA standards were manually prepared at 1, 5, 10, 50, 100, and 200 nmol/mL. Calibration levels were prepared by mixing standard solutions with derivatization reagent to achieve final concentrations of 50, 100, and 200 nmol/mL.

Internal Standard

Norvaline was used as the internal standard at 200 nmol/mL to correct for variability in sample handling.

GC-MS Conditions

Analysis was performed on a Shimadzu GC/MS-QP2010 system with a ZB-AAA column (10 m × 0.25 mm). Injection volume was 1 µL (split mode, 280°C). Helium was the carrier gas at 3.0 mL/min. The oven was programmed from 110°C to 320°C. Detection was done in EI mode using full scan and SIM (m/z 45–450).

Data Analysis

Peak identification and quantification were done using Shimadzu software based on calibration curves and normalized to the internal standard. Results were expressed as nmol/mL fresh weight.

2.4 Development of genome-edited hybrid line

In this study, two independently developed genome-edited rice lines were utilized: OsGAD1ΔC #5, generated via CRISPR/Cas9 genome editing in the present research, and OsGAD3ΔC #8, a previously established line reported by Akama et al. (2020). Both lines carry targeted deletions at the C-terminal calmodulin-binding domain (CaMBD) of their respective genes, OsGAD1 and OsGAD3.

To combine the genetic modifications of both truncated *GAD* genes into a single plant, a classical cross-breeding approach was employed. The OsGAD1ΔC #5 line, confirmed to be homozygous for the intended deletion, was used as the female parent, while the homozygous OsGAD3ΔC #8 line served as the male parent. Controlled pollination was conducted to produce F1 hybrid seeds that were expected to carry heterozygous alleles for both modified genes.

The resulting F_1 hybrid plants were grown under standard greenhouse conditions, and self-pollination was carried out to advance the population to the F_2 generation. Screening of the F_2 progeny was performed using PCR-based genotyping to identify individuals that were homozygous for both OsGAD1ΔC and OsGAD3ΔC alleles. Among these, one line designated as Hybrid #78 was selected for further experimentation. The genotype of Hybrid #78 was reconfirmed using amplicon-based PCR analysis as described in earlier sections.

2.5 Abiotic stress treatments

To investigate the physiological, biochemical, and molecular responses of genome-edited rice lines to environmental stress, a series of abiotic stress treatments were conducted on seedlings, followed by tissue sampling for amino acid analysis.

Seedling growth prior to stress exposure

Rice seeds were surface-sterilized and germinated on half-strength 0.5X MS agar medium. Seedlings were grown under controlled temperature and 60–70% relative humidity for two weeks. Uniform seedlings at 14–16 days old were selected for stress treatments.

Abiotic stress conditions

The following stress treatments were applied to simulate common abiotic challenges encountered during rice growth:

- **Cold Stress**: 15-day-old seedlings were transferred to fresh 0.5X MS media and kept at 4°C.
- **Flooding Stress**: 15-day-old seedlings were submerged completely in 0.1× liquid MS medium in transparent containers to simulate waterlogging.
- **Drought Stress**: 16-day-old seedlings were removed from agar medium, residual media was gently cleaned from the roots, and seedlings were placed on dry plastic trays under room temperature to induce dehydration.
- **Salinity Stress**: 14-day-old seedlings were immersed in 150 mM NaCl solution prepared in distilled water.

Each stress treatment was applied for a specific duration, depending on the experimental purpose (biomass loss or survival rate), as detailed below.

2.5.1 Biomass loss assessment

To quantify biomass reduction under stress, seedlings were harvested after the following durations:

- Cold, flooding, and salinity: 2 days
- Drought: 6 hours

Fresh weight (FW) was recorded immediately after stress treatment. Seedlings were then dried at 65°C for 24 hours to measure dry weight (DW). Biomass loss was expressed as a percentage compared to control seedlings grown without stress.

2.5.2 Survival rate evaluation

Separate sets of seedlings were exposed to prolonged stress conditions to assess survival capacity:

- Cold: 5 days at 4°C
- Flooding: 3 days submerged in MS liquid
- Drought: continued exposure until ~65% FW was lost
- Salinity: 2 days in 150 mM NaCl solution

Post-treatment, seedlings were rehydrated in water for 3 hours, then transplanted into soil pots and grown under normal conditions for an 18-day recovery period. Survival was determined based on new leaf emergence and visible regrowth.

2.5.3 Tissue collection for amino acid analysis

To analyze stress-induced changes in free amino acid content, both shoot and root tissues were collected from untreated control seedlings as well as those subjected to the abiotic stress conditions described above. Samples were harvested at multiple time points (1, 3, 6, 12, and 24 hours) after the onset of stress to monitor temporal changes in amino acid accumulation. For each time point and treatment, approximately 30 mg of fresh tissue was excised, immediately frozen in liquid nitrogen, and stored at −80°C until further processing. Frozen tissues were later homogenized in extraction buffer, and free amino acids were isolated and derivatized for GC-MS analysis, following the procedure detailed in previous sections.

2.5.4 Detection of hydrogen peroxide accumulation by DAB staining

To evaluate oxidative damage responses in rice leaves under abiotic stress conditions, 3,3′-diaminobenzidine (DAB) staining was performed to detect hydrogen peroxide (H_2O_2) accumulation following Thordal-Christensen et al. (1997). Leaf samples were collected from 14-day-old seedlings of WT Ni, OsGAD1ΔC #5, OsGAD3ΔC #8, and Hybrid #78 following exposure to stress treatments, including cold (4°C for 5 days), salinity (150 mM NaCl for 2 days), flooding (submergence for 3 days), and drought (kept in plastic plate for 6 hours). The procedure was as follows:

i. Leaves were detached and immediately immersed in DAB solution (1 mg/mL DAB in distilled water, adjusted to pH 3.8 with HCl).
ii. Samples were incubated in the dark for 1 hour, followed by light exposure for 8 hours to allow the oxidation reaction to occur.
iii. After staining, leaves were destained in ethanol (95%) until chlorophyll was removed, leaving only brown precipitates indicating the presence of H_2O_2.
iv. Leaves were then rinsed and mounted on glass slides for imaging.
v. Images were captured using a light microscope.

2.5.5 RNA extraction and RT-qPCR

To examine the transcriptional responses of rice seedlings under various abiotic stress conditions, total RNA was extracted from shoot and root tissues collected at defined time points post-treatment. Subsequent gene expression analysis was performed using reverse transcription quantitative real-time PCR (RT-qPCR).

RNA extraction

Total RNA was isolated using the ISOSPIN Plant RNA Kit (Nippon Gene Co., Ltd., Tokyo, Japan), following the manufacturer's protocol. 50–100 mg of frozen plant tissue was homogenized in liquid nitrogen and subjected to lysis and purification steps provided in the kit, which included on-column DNase I treatment to remove potential genomic DNA contamination. The purity and concentration of extracted RNA were assessed using a Qubit™ fluorometer (Q32857, Invitrogen, USA) by measuring absorbance at 260 nm and the A260/A280 ratio. RNA integrity was further verified by agarose gel electrophoresis.

cDNA synthesis

First-strand cDNA was synthesized from 1 μg of total RNA using ReverTra Ace reverse transcriptase (TOYOBO Co., Osaka, Japan) in a 20 μL reaction volume. The reaction mixture included oligo(dT) primers, dNTPs, RNase inhibitor, and reverse transcriptase, and was incubated at 42°C for 60 minutes, followed by enzyme inactivation at 95°C for 5 minutes.

RT-qPCR analysis

Quantitative real-time PCR (qPCR) was performed using the ECO Real-Time PCR System (PCRmax, Staffordshire, United Kingdom) with a standard SYBR Green-based detection method. Each 10 μL reaction contained:

- 5 μL of 2× SYBR Green PCR Master Mix (TOYOBO),
- 1 μL of forward primer (10 μM),
- 1 μL of reverse primer (10 μM),
- 0.2 μL of cDNA template, and
- 2.8 μL of nuclease-free water.

The qPCR cycling conditions were as follows:

- Initial denaturation at 95°C for 30 seconds,

- Followed by 40 cycles of 95°C for 15 seconds and 60°C for 60 seconds.

Normalization and relative quantification

Gene expression levels were quantified using the $2^{-\Delta\Delta CT}$ method (Livak & Schmittgen, 2001). The TATA-binding protein 2 (*TBP-2*) was used as an internal reference for normalization across samples and treatments, as it has been reported to show stable expression in rice under various stress conditions (Zhu et al., 2012). All reactions were conducted in biological triplicate, with technical duplicates for each sample to ensure reproducibility. Primer sequences for all target and reference genes are listed in Table 2.

2.6 RNA sequencing

To examine genome-wide transcriptomic changes in response to abiotic stress, high-throughput RNA sequencing (RNA-seq) was conducted on total RNA extracted from shoot tissues of rice seedlings. The experiment was performed through a commercial sequencing service provided by Nippon Genetics Co., Ltd. (https://n-genetics.com/ngs/), utilizing the Illumina sequencing platform, which is based on the sequencing-by-synthesis technology.

mRNA enrichment and cDNA library preparation

Total RNA was first assessed for quality and concentration using a NanoDrop spectrophotometer and Bioanalyzer (Agilent Technologies) to confirm integrity. Samples with RNA integrity number (RIN) ≥ 7.0 were used for library construction. Messenger RNA (mRNA) was selectively isolated from total RNA using poly-T oligo-attached magnetic beads, which specifically bind to the polyadenylated (poly-A) tails of mature eukaryotic transcripts. The enriched mRNA was subsequently fragmented into short sequences under elevated temperature and divalent cation conditions to enhance transcript coverage.

First-strand complementary DNA (cDNA) synthesis was performed using random hexamer primers and reverse transcriptase. Second-strand synthesis followed a strand-specific (directional) library preparation protocol, incorporating deoxyuridine triphosphate (dUTP) instead of dTTP in the second strand to preserve strand orientation, following the method of Parkhomchuk et al. (2009). The resulting double-stranded cDNA was end-repaired, A-tailed, and ligated to sequencing adapters. After ligation, fragments of a suitable size (typically 250–300 bp) were selected and enriched by PCR to complete the library preparation. Libraries were validated by qPCR and Bioanalyzer, and then sequenced using a paired-end format on an Illumina platform.

Raw data processing and quality control

Raw sequencing reads were initially obtained in FASTQ format. These files were subjected to quality control and filtering using custom Perl scripts, which removed low-quality reads, adapter contamination, and reads containing poly-N sequences. Only high-quality clean reads were retained for downstream analyses.

Reference genome alignment

The high-quality paired-end reads were mapped to the *Oryza sativa* ssp. *japonica* (cv. Nipponbare) reference genome (EnsemblPlants assembly: *Oryza_sativa.IRGSP-1.0*, accession: GCA_001433935.1) using the HISAT2 aligner (version 2.0.5) (Mortazavi et al., 2008). HISAT2 is a fast and sensitive alignment program that utilizes a hierarchical indexing strategy for efficient mapping.

An index of the reference genome was built with HISAT2 prior to alignment. The clean reads were aligned with default parameters, and only reads uniquely mapped to the reference genome were retained for further analysis. Genome and gene annotation files were obtained from the Ensembl Plants database.

Gene expression quantification

After alignment, FeatureCounts (v1.5.0-p3) (Liao et al., 2014) was used to count the number of reads mapped to each annotated gene. Gene expression levels were then normalized and expressed as Fragments Per Kilobase of transcript per Million mapped reads (FPKM), which accounts for both sequencing depth and gene length.

Differential expression analysis

Differential expression between treatment groups and controls was assessed using the DESeq2 package (version 1.20.0) in R (Anders & Huber, 2010). DESeq2 uses a model based on the negative binomial distribution and includes internal normalization to correct for differences in sequencing depth and RNA composition across samples. Genes with an adjusted p-value (Benjamini-Hochberg corrected) < 0.05 and a fold change ≥ 2 or ≤ 0.5 were considered significantly differentially expressed.

Gene Ontology (GO) enrichment analysis

To functionally characterize the differentially expressed genes (DEGs), Gene Ontology (GO) enrichment analysis was conducted using the clusterProfiler R package. This tool identifies overrepresented GO terms among the DEGs compared to the entire genome background, while

correcting for potential gene length biases. GO terms with a false discovery rate (FDR)-adjusted p-value < 0.05 were considered significantly enriched.

2.7 Statistical analysis

All data are presented as the mean ± standard deviation (SD) from three biological replicates. Statistical analysis was performed using Student's *t*-test for pairwise comparisons and one-way ANOVA for multiple group comparisons in Microsoft Excel. Statistical significance was defined as $^{*}P<0.05$ and $^{**}P<0.01$.

Chapter 3: Results

3.1. Generation of CaMBD-truncated OsGAD1 mutant line by CRISPR/Cas9 genome editing

The rice (*Oryza sativa*) genome encodes five glutamate decarboxylase (GAD) isoforms, designated OsGAD1 through OsGAD5 (International Rice Genome Sequencing Project, 2005), all of which catalyze the decarboxylation of glutamate to γ-aminobutyric acid (GABA), a non-protein amino acid implicated in stress responses. Most OsGAD isoforms, including OsGAD1, OsGAD3, OsGAD4, and OsGAD5, share a conserved C-terminal calmodulin-binding domain (CaMBD), which acts as an autoinhibitory regulatory region modulating GAD enzymatic activity in a Ca^{2+}/calmodulin-dependent manner(Akama et al., 2001;Trobacher et al., 2013). In contrast, OsGAD2 is structurally and functionally distinct from the other isoforms. It lacks key conserved residues in its C-terminal region, including the tryptophan (W) residue and lysine (K) cluster that contribute to the amphipathic α-helical structure essential for CaM binding (Arazi et al., 1995; Akama & Takaiwa, 2007). This structural divergence renders OsGAD2 non-responsive to Ca^{2+}/CaM regulation, as confirmed by *in vitro* binding assays (Akama and Takaiwa, 2007). Conversely, OsGAD1, OsGAD3, and OsGAD4 have been biochemically validated to contain functional CaMBDs based on in vitro CaM-binding studies (Akama et al., 2001; Akama et al., 2020; Akter et al., 2024).

Previous reports have demonstrated that C-terminal truncation of OsGAD3 and OsGAD4, results in enhanced GAD enzymatic activity and increased GABA accumulation (Akama et al., 2020; Akter et al., 2024). This observation strongly suggested that OsGAD1, which contains similar conserved residues and structural motifs in its CaMBD (Fig. 1 a, b), may also be negatively regulated by its C-terminal domain. Therefore, removal of the CaMBD in OsGAD1 was hypothesized to yield a constitutively active GAD enzyme with elevated GABA biosynthesis, similar to GAD3 and GAD4 truncation mutants.

(a)

```
OsGAD2      GEEASIRVVKSEAV-PVRKSVPLVAGKTKGVC
OsGAD1      -TKKSVLETEREIFAYWRDQVKK---KQTGIC
OsGAD5      -AKKTVREIEKEVTTYWRSFVARK--KSSLVC
PhGAD       -HKKTDSEVQLEMITAWKKFVEEKKKKTNRVC
OsGAD3      -AKKSELETQRSVTEAWKKFVLAK--RTNGVC
OsGAD4      -ASEREMEKQREVISLWKRAVLAK-KKTNGVC
```

(b)

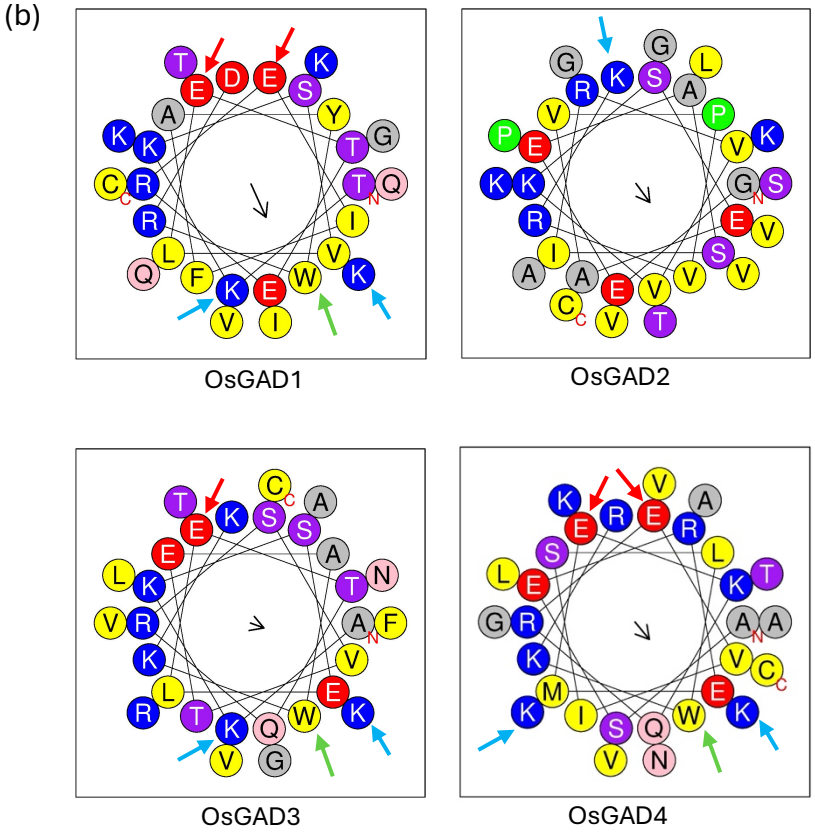

Fig. 1 Comparison of the C-terminal regions of plant glutamate decarboxylases (GADs). (a) Multiple sequence alignment of the C-terminal regions from *Oryza sativa* (*Os*) and *Petunia hybrida* (*Ph*) GADs using Clustal Omega (https://www.ebi.ac.uk/jdispatcher/). Key residues critical for calmodulin (CaM) binding, tryptophan (W) and lysine (K), are denoted using a dot and a bold line, respectively. Pseudosubstrate residues E476 and E480 in *PhGAD*, as reported by Arazi et al. (1995), are indicated with stars. The analyzed sequences include *Os*GAD1 (AB056060), *Os*GAD2 (AB056061), *Os*GAD3 (AK071556), *Os*GAD4 (AK101171), *Os*GAD5 (AK070858), and *Ph*GAD (L16977). (b) α-helical wheel projection of amino acid residues displayed using HeliQuest (https://heliquest.ipmc.cnrs.fr/index.html). The α-helical wheel diagram represents the amphipathic helical structure of the calmodulin-binding domain (CaMBD) of four OsGADs. Amino acid residues are displayed as colored circles, arranged to show their spatial orientation within the helix. Hydrophobic residues (yellow) cluster on one side, forming a hydrophobic face, whereas hydrophilic residues, including positively charged (blue), negatively charged (red), polar (purple), and special residues (pink

and gray), form the opposite face. The arrow in the middle indicates the direction of the hydrophobic face, which interacts with hydrophobic binding pocket of calmodulin in a calcium-dependent manner. Tryptophan (W) (green arrow) plays a key role in anchoring the helix to calmodulin via strong hydrophobic interactions, and lysine (K) (blue arrow) contributes to electrostatic interactions with negatively charged residues of calmodulin, stabilizing the binding. Glutamate (E) (red arrow) residues act as pseudosubstrates. This amphipathic arrangement is essential for the function of CaMBD in facilitating GAD activity in response to calcium signaling. Lines connecting residues highlight spatial proximity and potential interactions within the helix.

To test this hypothesis, CRISPR/Cas9-based genome editing was employed to generate OsGAD1 mutants lacking the CaMBD. Two guide RNAs (gRNAs) were strategically designed to introduce deletions flanking the CaMBD-encoding region of OsGAD1 (AB056060), enabling precise removal of the C-terminal domain (Fig. 2a). *Agrobacterium*-mediated transformation of rice calli resulted in several independent T_0 lines carrying targeted deletions. Following genotyping and sequencing of the target sites, four homozygous OsGAD1ΔC mutant lines were identified, each harboring distinct deletion patterns in both nucleotide and predicted amino acid sequences (Fig. 2 b, c).

These genome-edited lines were advanced to the T_1 generation, and their GABA content and brown rice grain weight were evaluated under standard growth conditions (Table 3). Among the edited lines, OsGAD1ΔC #5 exhibited a nearly complete deletion of the CaMBD and consistently showed the highest GABA levels when compared to wild-type Nipponbare (WT Ni) and the other mutant lines. In addition, this line displayed normal vegetative growth and grain development, indicating that the removal of the CaMBD did not have adverse effects on overall plant morphology or fertility. Based on its superior GABA accumulation and desirable agronomic traits, OsGAD1ΔC #5 was selected as the representative line for subsequent physiological and molecular analyses throughout this study.

(b)

OsGAD1: TCCAGCGCCATCGCGAAGCAGCAATCGGGCGACGATGGCGTGGT//CCGGAATCTGCTAG

OsGAD1ΔC #5: TCCAGCGCCATCG--(-113bp)--TCTGCTAG

OsGAD1ΔC #206: TCCAGCGCCATCGCGAAGCAGCAATCGGGCGACGAT--(-88bp)--TCTGCTAGTGTGGCTCTGTGA

OsGAD1ΔC #210: TCCAGCGCCATCGCGAAGCAGCAATCGGGCGACGAT---(-88bp)---gTCTGCTAG

OsGAD1ΔC #219: TCCAGCGCCATCGCGAAGCAGCAATCGGGCGACGAT--(-88bp)--TCTGCTAa---(-1bp)--TGTGGCTCTGTGA

(c)

OsGAD1-SSAIAKQQSGDDGVVTKKSVLETEREIFAYWRDQVKKKQTGIC

OsGAD1ΔC #5: SSAI*VC*

OsGAD1ΔC #206: SSAIAKQQSGDD*SASVAL*

OsGAD1ΔC #210: SSAIAKQQSGDD*VC*

OsGAD1ΔC #219: SSAIAKQQSGDD*SANVAL*

Fig. 2 CRISPR/Cas9-mediated production of CaMBD-truncated OsGAD1 genome-edited plants. (a) The nucleotide and corresponding amino acid sequences of OsGAD1 (AB056060) are shown. The CaMBD region is underlined. The guide RNA (gRNA) sequence used for editing is highlighted in red, with the complementary sequence of the protospacer adjacent motif (PAM) shown in blue. F1, F2, and R1 mark the targeted cleavage sites within the gene. (b) The nucleotide sequence of wild-type *OsGAD1* and the resulting genome-edited sequences. The dashed line indicates the deletion (bp= base pair), and lowercase letters indicate insertion introduced as a result of the genome editing process. (c)The amino acid sequences of the resulting genome-edited sequences are shown. The wild-type OsGAD1 (Ni) sequence includes the CaMBD region, highlighted in red. OsGAD1ΔC refers to four genome-edited lines with truncated CaMBD regions. The sequence highlighted in teal represents the additional amino acids.

Table 3. Grain weight and relative GABA content in the WT Ni and OsGAD1 genome-edited lines

Rice lines	Brown rice (mg/grain)	GABA (fold change)
WT Ni	18.8	1
OsGAD1ΔC #5	20.8	6.6
OsGAD1ΔC #206	20.7	1.1
OsGAD1ΔC #210	20.3	2.7
OsGAD1ΔC #219	18.7	2

3.2 Characterization of CaMBD-truncated OsGAD1, OsGAD3, and their hybrid line

To investigate the functional consequences of removing the autoinhibitory calmodulin-binding domain (CaMBD) from GAD enzymes in rice, targeted genome editing was performed on the *OsGAD1* and *OsGAD3* loci. Using the CRISPR/Cas9 system, precise deletions were introduced into the C-terminal coding regions of both genes, resulting in 113 bp and 122 bp deletions in OsGAD1ΔC and OsGAD3ΔC (Akama et al., 2020), respectively (Fig. 3a). These deletions led to premature truncation of the corresponding proteins, effectively eliminating the CaMBD, which is responsible for calcium/calmodulin-mediated regulatory control (Akama et al., 2001; Akama et al., 2020). The resulting amino acid sequence alterations are shown in Fig. 3b, confirming loss of the CaMBD-encoded region in both modified isoforms.

To evaluate the combined effects of CaMBD removal from both OsGAD1 and OsGAD3, a hybrid line was developed by crossing two homozygous genome-edited lines: OsGAD1ΔC #5 (selected as the female parent) and OsGAD3ΔC #8 (used as the male parent). This crossing strategy was implemented to integrate both truncated alleles into a single genetic background, thereby allowing assessment of potential additive or synergistic effects on GABA biosynthesis and stress response phenotypes (see materials and methods).

PCR-based genotyping (Fig. 3c) confirmed the successful inheritance of the truncated alleles from both parents in the resulting Hybrid #78, indicating that the crossbreeding strategy effectively combined the OsGAD1ΔC and OsGAD3ΔC mutations.

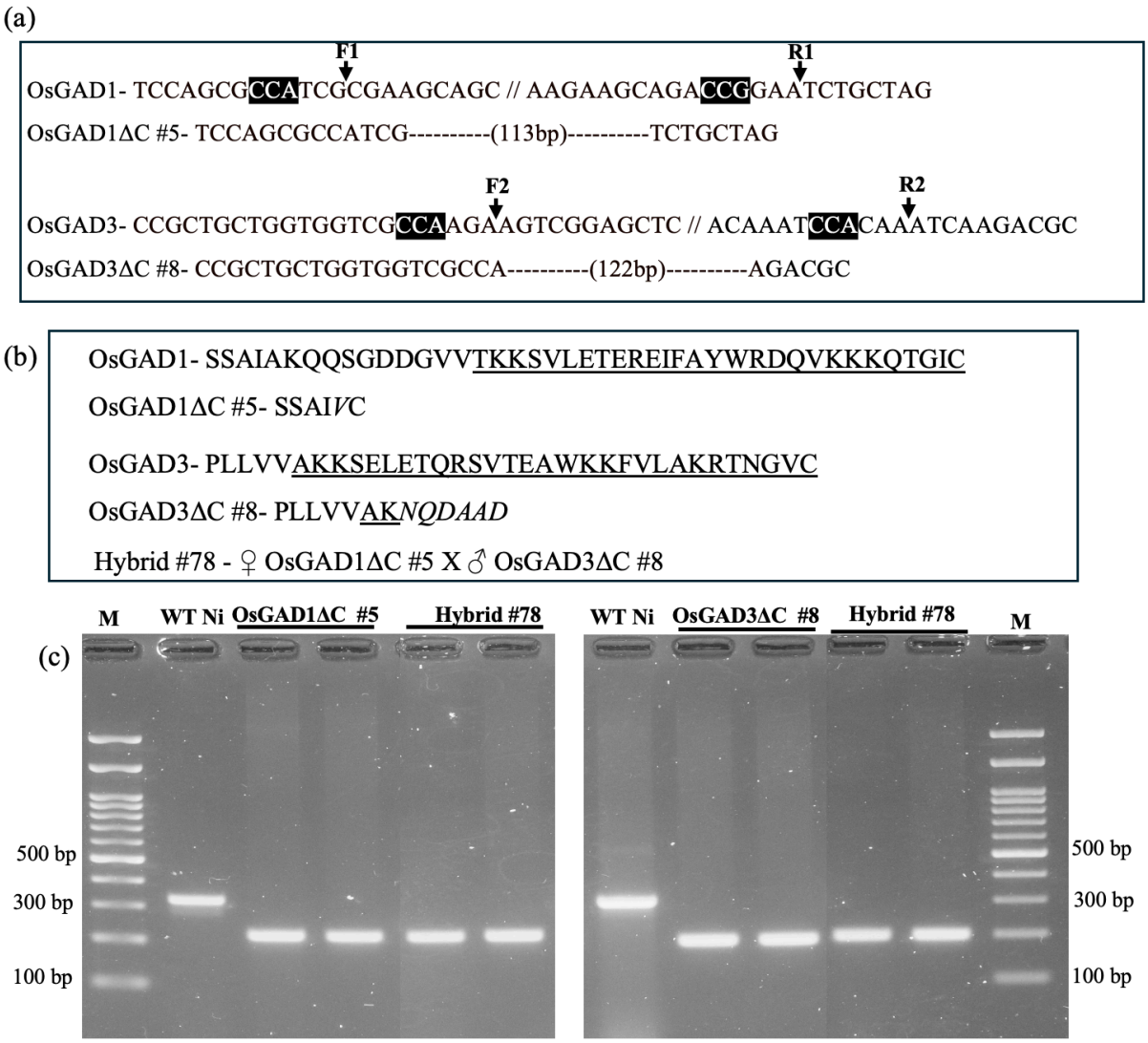

Fig. 3 Establishment of CaMBD-truncated OsGAD1 and OsGAD3 lines by CRISPR/Cas9 genome editing along with their hybrid line. (a) OsGAD1ΔC #5 contains a 113 bp deletion within the target region of wild-type (WT) *OsGAD1*. The positions of F1 and R1 indicate the upstream and downstream CRISPR/Cas9 putative cleavage sites, respectively, within the targeted CaMBD region of OsGAD1; OsGAD3ΔC #8 (Akama et al. 2020) containing a 122 bp deletion; F2 and R2 shows the upstream and downstream CRISPR/Cas9 putative cleavage sites in the OsGAD3 target site, accordingly; letters highlighted in the black box within the WT sequence represents the PAM complementary sequence; (b) Amino acid sequences in WT OsGAD1, OsGAD3, and CaMBD-truncated OsGAD1ΔC #5 and OsGAD3ΔC #8. Underlined letters indicate the CaMBD sequence in the WT C-terminal region. Italics letters indicate the additional amino acids produced by genome editing. Hybrid line #78 indicates the combination of a cross between the OsGAD1 and OsGAD3 genome-edited lines. (c) PCR amplification of OsGAD1 and OsGAD3 in the hybrid line had shorter products, with a 198 bp fragment for OsGAD1 and a 208 bp fragment for OsGAD3, indicating 113 bp and 122 bp deletions in the CaMBD regions of OsGAD1 and OsGAD3, respectively. These truncated products were consistent with those observed in the parental lines OsGAD1ΔC #5 and OsGAD3ΔC #8, compared with the WT Nipponbare (WT Ni). 100 bp DNA marker (indicated with the letter M) was used to identify the PCR product sizes.

To assess whether the genome editing and subsequent hybridization affected plant morphology, a series of agronomic traits were measured in OsGAD1ΔC #5, OsGAD3ΔC #8, and Hybrid #78, alongside wild-type Nipponbare (WT Ni) controls (Table 4). A slight increase in leaf blade length and culm height was

observed in the genome-edited lines and the hybrid compared to the WT. However, these differences suggested that truncation of the CaMBD in OsGAD1 and OsGAD3 does not adversely affect vegetative development or plant architecture under normal growth conditions.

Table 4. Agronomic traits of WT Ni, OsGAD1ΔC #5, OsGAD3ΔC #8, and Hybrid #78.

Rice line	Dry weight (g)	No. of branches	Leaf blade size (cm)	No of panicles	Panicle length (cm)
WT Ni	175 ± 7.0	40.5 ± 6.0	64.36 ± 5.2	37.33 ± 3.9	20.03 ± 2.5
OsGAD1ΔC #5	139.6 ± 19.9	36.3 ± 6.0	60.0 ± 2.9	35.4 ± 4.0	19.5 ± 1.4
OsGAD3ΔC #8	161.2 ± 4.1	32.57 ± 6.7	69.65 ± 2.5	28.71 ± 7.1	20.91 ± 1.2
Hybrid #78	154.42 ± 8.4	33.14 ± 5.1	68.65 ± 6.6	26.42 ± 4.8	23.28 ± 1.8*

Rice line	Culm length (cm)	No of seeds per panicle	Weight of 1000 seeds (g)	Total weight of seeds (g)	Ripening rate (%)
WT Ni	68.9 ± 5.1	119.9 ± 8.5	26.8 ± 1.5	125.9 ± 4.9	92.51 ± 2.9
OsGAD1ΔC #5	70.4 ± 1.6	105.3 ± 10.4	25.7 ± 0.9	101.2 ± 4.7	91.8 ± 3.0
OsGAD3ΔC #8	87 ± 6.2**	111.3 ± 8.2	22.8 ±1.2	75.34 ± 7.2*	81.01 ± 4.4
Hybrid #78	81.82 ± 4.6*	105.93 ± 5.5	27.09 ± 1.4	86.52 ± 6.5*	90.76 ± 2.1

Data represented as mean ± standard deviation (n=5). Asterisks indicate significant differences (*P<0.05, **P<0.01). Significant differences were determined using Student's t-test by comparing the genome-edited lines with wild-type Ni.

To determine whether the observed changes were associated with altered gene expression, transcript levels of the four *OsGAD* genes were analyzed using reverse transcription quantitative real-time PCR (RT-qPCR). As shown in Fig. 4, expression of *OsGAD1* in the leaf (Fig. 4a) and *OsGAD3* in the root (Fig. 3c) was slightly elevated in the hybrid line compared to WT Ni, with expression profiles largely resembling those observed in the respective parental lines. This modest upregulation suggests that the presence of truncated alleles does not substantially disrupt the transcriptional regulation of *GAD* genes in vegetative tissues.

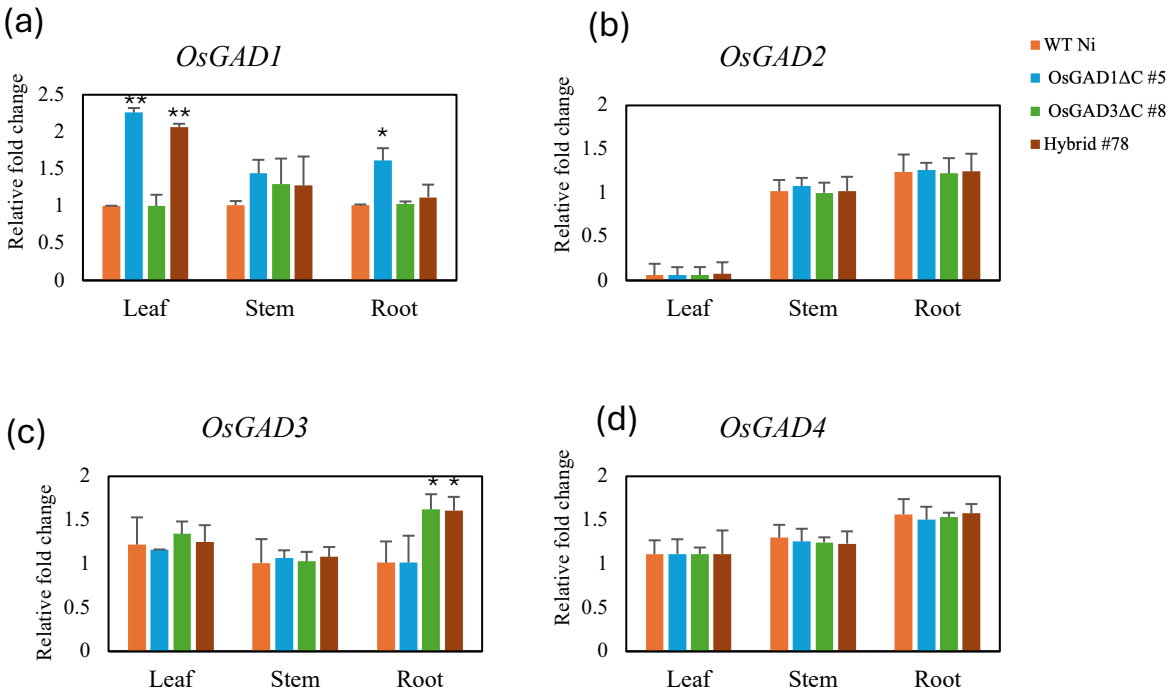

Fig. 4 Relative expression of four *OsGADs* in different vegetative tissues of the rice seedlings. Expression of (a) *OsGAD1* (AB056060), (b) *OsGAD2* (AB056061), (c) *OsGAD3* (AK071556) and (d) *OsGAD4* (AK101171) in leaf, stem, and root tissues of WT Ni, OsGAD1ΔC #5, OsGAD3ΔC #8, and Hybrid #78. Bars represent the mean ± standard deviation (SD) (n=3) of relative fold change. Expression levels were analyzed using the $2^{-\Delta\Delta Ct}$ method, where TATA-binding protein (*TBP-2*) was used as an internal control. Statistical significance was assessed by comparing the values to those of the wild-type. Asterisks denote significant differences (*P<0.05, **P<0.01).

Further expression profiling of the GABA transaminase (*GABA-T*) gene family was performed to examine whether genome editing had downstream effects on GABA catabolism. RT-qPCR analysis revealed that expression levels of all three *GABA-T* genes remained comparable between WT, the single-mutant lines, and the hybrid line (Fig. 5), indicating that the GABA degradation pathway was not significantly altered as a result of CaMBD truncation.

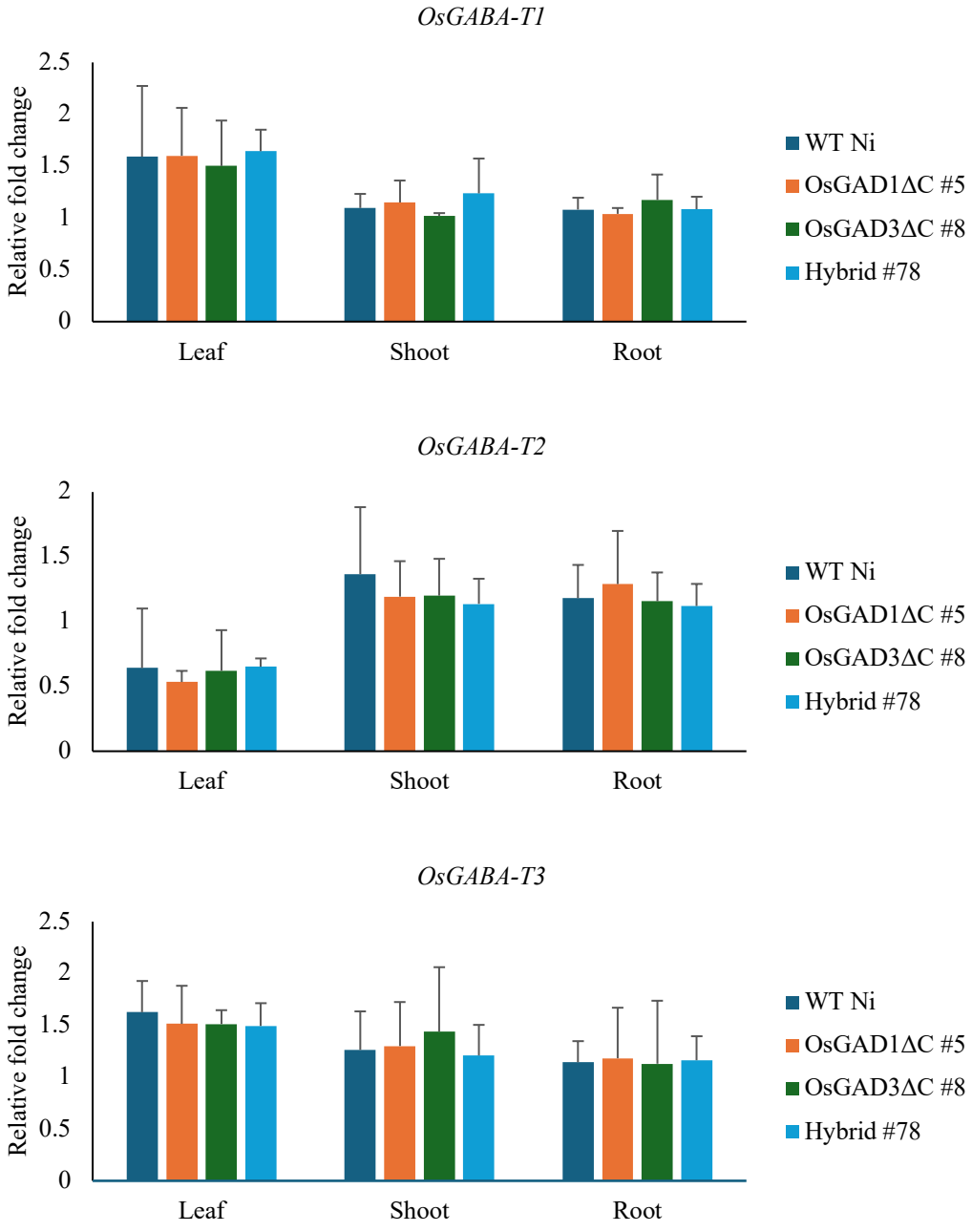

Fig. 5 Relative expression of three *OsGABA-T* in different vegetative tissues of the rice seedlings. Expression of *OsGABA-T1*, *OsGABA-T2*, and *OsGABA-T3* in leaf, stem, and root tissue of WT Ni, OsGAD1ΔC #5, OsGAD3ΔC #8, and Hybrid #78. Bars represent the mean ± standard deviation (SD) (n=3) of relative fold change. Expression levels were analyzed using the $2^{-\Delta\Delta Ct}$ method, where TATA-binding protein 2(*TBP-2*) was used as an internal control.

Biochemical quantification of GABA accumulation (Table 5) revealed that Hybrid #78 accumulated significantly higher levels of GABA compared to its parental lines, OsGAD1ΔC #5 and OsGAD3ΔC #8, across vegetative tissues. This observation supports the hypothesis that simultaneous removal of CaMBDs from both GAD isoforms exerts at least additive effects on GABA biosynthesis, likely due to the constitutive activity of the truncated GAD1 and GAD3 enzymes.

These results collectively suggest that targeted deletion of the CaMBD in OsGAD1 and OsGAD3 not only enhances GABA accumulation without detrimental effects on basic plant morphology but that the combined truncations in the hybrid line may provide a promising strategy to enhance production of GABA in rice.

Table 5. GABA contents of vegetative tissues from WT Ni and genome-edited plants

Rice lines	(GABA nmol/mg)		
	Leaf	**Stem**	**Root**
WT Ni	37.87 ± 1.77	12.82 ± 1.73	49.85 ± 1.20
OsGAD1ΔC #5	62.32 ± 6.10*	28.49 ± 2.29*	78.87 ± 1.14*
OsGAD3ΔC #8	59.51 ± 3.28*	25.56 ± 1.56*	81.56 ± 6.51*
Hybrid #78	79.64 ± 2.88*	32.73 ± 1.82**	104.40 ± 2.61**

Data represented as mean ± standard deviation (n=3). Asterisks indicate significant differences (*P<0.05, **P<0.01). Significant differences were determined using Student's t-test by comparing the genome-edited lines with wild-type Ni.

3.3 GABA accumulation in response to abiotic stress conditions

GABA is widely recognized as a metabolite that accumulates in plants in response to various abiotic stressors, functioning as part of a conserved defense mechanism. Transcriptomic data from the Transcriptome Encyclopedia of Rice (TENOR) database (Kawahara et al., 2016) revealed that OsGAD1 and OsGAD3 transcripts are consistently upregulated under abiotic stresses, including cold, salinity, flooding, and drought (Fig. 6).

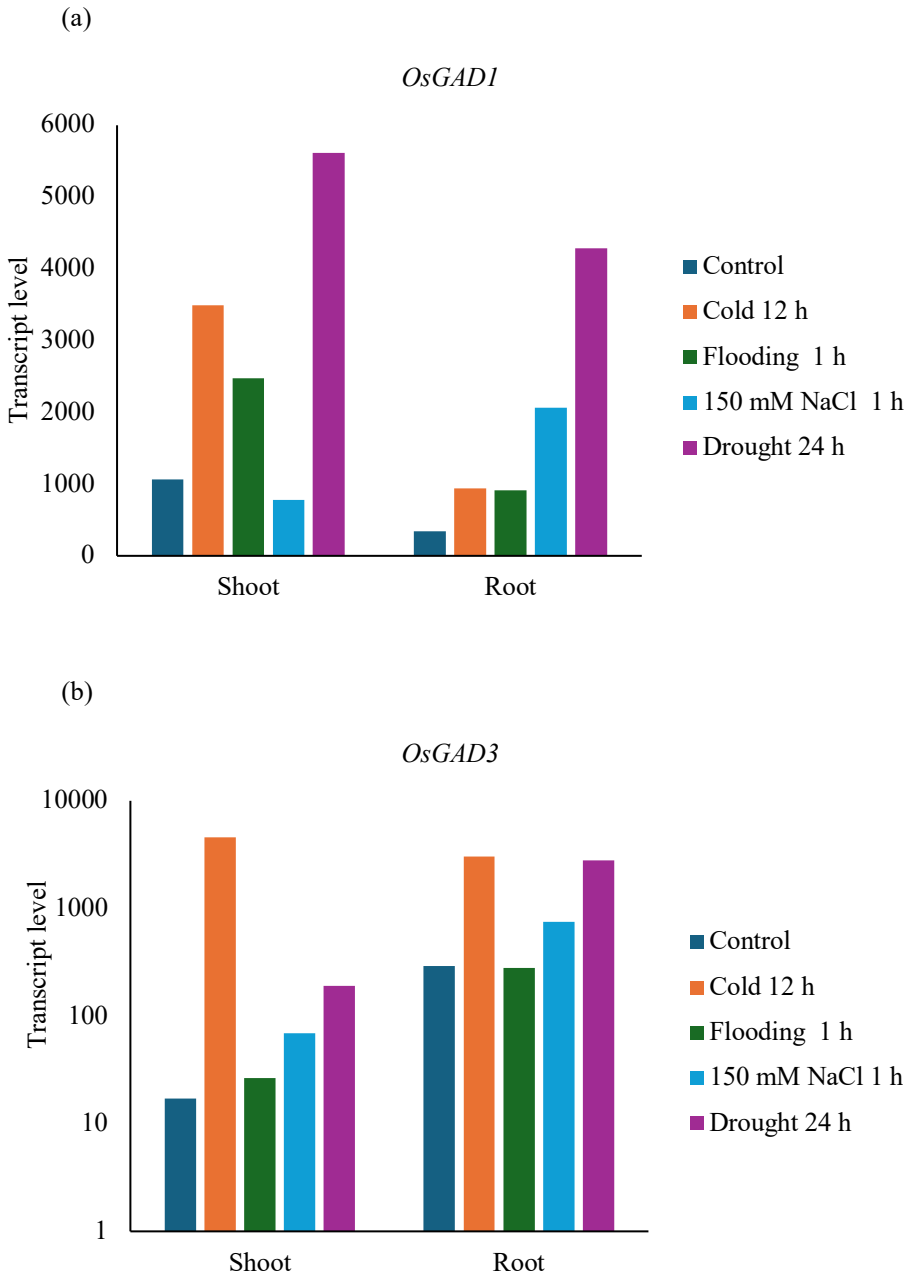

Fig. 6 Analysis of *OsGAD1* and *OsGAD3* transcript levels in response to abiotic stress conditions. The values indicate the abundance of *OsGAD1* and *OsGAD3* transcripts in shoot and root tissues, derived from mRNA-seq data retrieved from the TENOR database (https://tenor.dna.affrc.go.jp/).

These findings imply the hypothesis that enhanced expression of these *GAD* genes may contribute to increased GABA biosynthesis during stress. Consistent with previous observations in several plant species (Zhou et al., 2024; Sita & Kumar, 2020; Kreps et al., 2002), elevated expression of *GAD* genes often correlates with elevated GABA levels under stress conditions. Additionally, truncation of the CaMBD in OsGAD4 was recently shown to significantly enhance GABA accumulation (Akter et al., 2024), reinforcing the notion that GAD enzymatic activity is regulated at both the transcriptional and post-translational levels.

Based on this, we hypothesized that truncating the CaMBDs of OsGAD1 and OsGAD3 would enhance GAD activity and subsequently increase GABA accumulation under abiotic stress. To test this, OsGAD1ΔC #5, OsGAD3ΔC #8, and their hybrid line Hybrid #78 were subjected to four different abiotic stress treatments: cold, salinity, flooding, and drought. GABA concentrations were measured at multiple time points in both shoot and root tissues, and results were compared to the WT Ni control (Fig. 7).

Cold Stress

Upon exposure to 4°C, GABA levels in the shoot tissues of all genome-edited lines increased during the initial 12 hours of treatment, followed by a decline at 24 hours (Fig. 7a). The Hybrid #78 line exhibited the most significant increase, with GABA concentrations reaching approximately 3.5-fold higher than WT Ni. In root tissues, a steady increase in GABA levels was observed in OsGAD3ΔC #8 and Hybrid #78, peaking at 24 hours. In contrast, OsGAD1ΔC #5 showed a transient rise followed by a decline, suggesting differential temporal regulation between the two edited genes. These results aligned with the TENOR database's expression profiles for OsGAD1 and OsGAD3 under cold conditions.

Salinity Stress Response

Salinity stress was simulated by treating 14-day-old seedlings with 150 mM NaCl and collecting tissues at 1, 3, and 6 hours post-treatment (Fig. 7b). Under these conditions, Hybrid #78 showed the most pronounced increase in GABA levels, especially in root tissues at 3 hours, where GABA accumulation reached approximately 3.9 times that of WT Ni and twice as much as the parent lines. Conversely, OsGAD1ΔC #5 and OsGAD3ΔC #8 did not show substantial increases, indicating that simultaneous truncation of both genes in the hybrid line may produce synergistic effects. Similar patterns of GABA accumulation under salt stress have been reported in other species: a 1.5-fold increase in Arabidopsis (Renault et al., 2010), 1.5-fold in tomato (Wu et al., 2020).

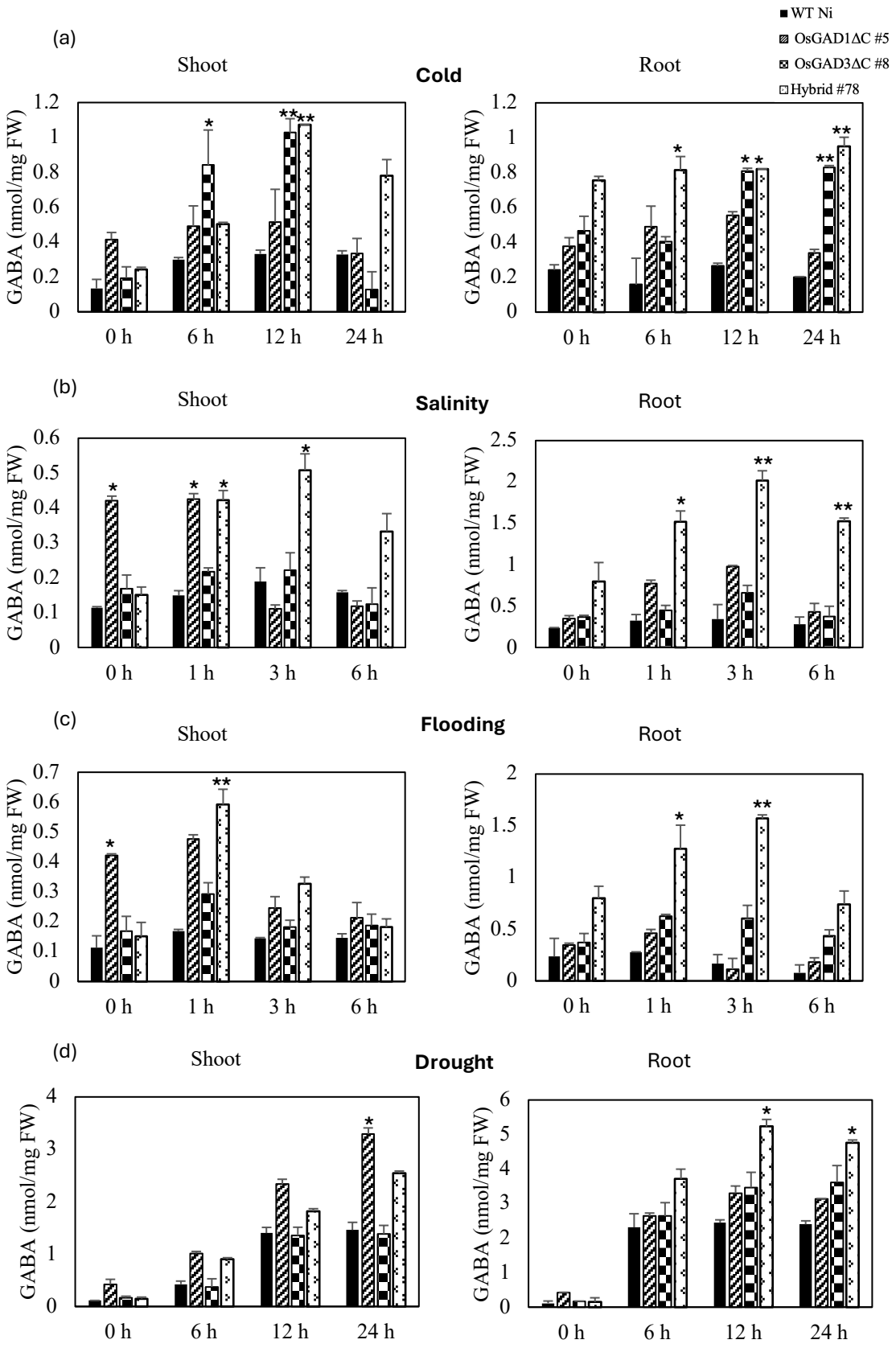

Fig. 7 Quantitative analysis of GABA content in response to abiotic stresses in rice seedlings. (a) **Cold stress response**. GABA levels were assessed in 16-day-old seedlings of WT-Ni, OsGAD1ΔC #5, OsGAD3ΔC #8, and Hybrid #78 after exposure at 4°C. Samples were collected at

intervals of 6, 12, and 24 h after stress induction. (b) **Salinity stress response**. Seedlings aged 14 days were subjected to 150 mM NaCl solution, with tissue samples harvested at 1, 3, and 6 h (c) **Flooding stress response**. 15-day-old seedlings were fully submerged in liquid Murashige and Skoog (MS) media, mirroring the time intervals used for salinity stress, to monitor GABA synthesis in hypoxic conditions. (d) **Drought stress response**. Seedlings aged 16 days were removed from MS media and placed on plastic plates to simulate drought conditions, with sample collection at 6, 12, and 24 h after stress application. The control (0 h) represents baseline GABA content in non-stress conditions. The error bars denote the mean ± standard deviation (SD) based on three biological replicates (n=3). FW = fresh weight. Statistical significance was determined by comparing the values of each rice line with the wild-type in identical stress conditions. Asterisks denote significant differences (*P<0.05, **P<0.01).

Flooding Stress Response

In flooding stress conditions (Fig. 7c), GABA levels in shoot tissues of all genome-edited lines increased during the first hour of submergence, followed by a decline. In root tissues, OsGAD1ΔC #5 showed a modest increase at early time points but later declined sharply. By contrast, Hybrid #78 exhibited a pronounced peak in GABA accumulation at 3 hours, reaching 5-fold higher levels than WT Ni and more than twice that of either parental line. These results suggested that Hybrid #78 maintains a stronger metabolic response under hypoxic stress, likely due to the combined loss of autoinhibitory control in both GAD isoforms.

Drought Stress Response

To simulate drought stress, seedlings were removed from media and placed on dry plastic surfaces. GABA levels increased progressively in both shoot and root tissues across all lines (Fig. 7d). The highest accumulation was observed in Hybrid #78, particularly in the root tissue at 12 hours, indicating a rapid and sustained response to dehydration. Both OsGAD1ΔC #5 and OsGAD3ΔC #8 also showed increased GABA levels compared to WT, but to a lesser extent than the hybrid line. These results suggested that the hybrid exhibits enhanced GABA biosynthetic capacity and a stronger tolerance to dehydration.

These results demonstrated that the genome-edited lines, particularly Hybrid #78, accumulate significantly higher levels of GABA under abiotic stress conditions compared to WT Nipponbare and their respective parental lines. This supports the model in which GABA functions as a key stress-responsive metabolite, accumulating as part of a rapid adaptive response to environmental stressors (Sita and Kumar, 2020; Signorelli et al., 2021). The elevated GABA levels in Hybrid #78 likely reflect the additive effects of removing the CaMBD from both OsGAD1 and OsGAD3, thereby promoting constitutive GAD activity independent of calcium/calmodulin signaling.

3.4 Upregulation of *OsGAD1* and *OsGAD3* under abiotic stress conditions

To understand the transcriptional response of *OsGAD1* and *OsGAD3* under abiotic stress, quantitative real-time PCR (RT-qPCR) was conducted in both shoot and root tissues across four rice lines: wild-type Nipponbare (WT Ni), OsGAD1ΔC #5, OsGAD3ΔC #8, and the hybrid line Hybrid #78. Seedlings were subjected to cold, salinity, flooding, and drought stress, and relative gene expression levels were quantified and normalized against *TBP-2* as the internal control.

The results revealed that both *OsGAD1* and *OsGAD3* were transcriptionally induced under all tested stress conditions, with the most pronounced upregulation observed during drought stress (Fig. 8a, 8b). Among the four genotypes, Hybrid #78 consistently showed the highest expression levels for both genes. Under drought treatment, *OsGAD1* expression in the root tissue of Hybrid #78 increased by approximately 18-fold, while *OsGAD3* expression reached nearly 12-fold relative to non-stressed controls. The parental lines OsGAD1ΔC #5 and OsGAD3ΔC #8 also exhibited moderate induction, but their expression levels were noticeably lower than those of the hybrid line. WT Ni showed the lowest fold change, particularly for *OsGAD3*.

These findings are consistent with previous reports. For example, Chen et al. (2024) demonstrated that drought stress in rice induces *GAD* gene expression, leading to elevated GABA accumulation, which in turn contributed to improved water-use efficiency and enhanced drought tolerance. Similarly, in tomato, Wang et al. (2024) showed that cold stress activated GAD enzymatic activity, resulting in increased GABA production, which played a protective role by stabilizing cellular structures and reducing cold-induced damage.

However, the response to abiotic stress appears to vary among species and gene family members. For instance, Ji et al. (2020) investigated the *GAD* gene family in poplar and found that only two out of six GAD isoforms were transcriptionally responsive to salt stress caused by NaCl exposure. Likewise, Zhang et al. (2022) reported that hypoxia induced a significant increase in GABA levels in tea plants, which was associated with upregulation of *CsGAD1* and *CsGAD2* through activation of the GABA shunt pathway.

In our study, the strong correlation between GABA content and gene expression in the genome-edited lines, particularly in Hybrid #78, suggests that the enhanced stress-responsive GABA accumulation is at least partly driven by upregulation of *OsGAD1* and *OsGAD3*. The data further imply that GABA biosynthesis under stress may involve a positive feedback mechanism, where increased GABA levels potentially reinforce the transcription of *GAD* genes to sustain metabolic adaptation.

These results support the functional role of *OsGAD1* and *OsGAD3* as key regulatory components in rice stress physiology, particularly when their CaMBD domains are removed, enhancing their activity and expression responsiveness.

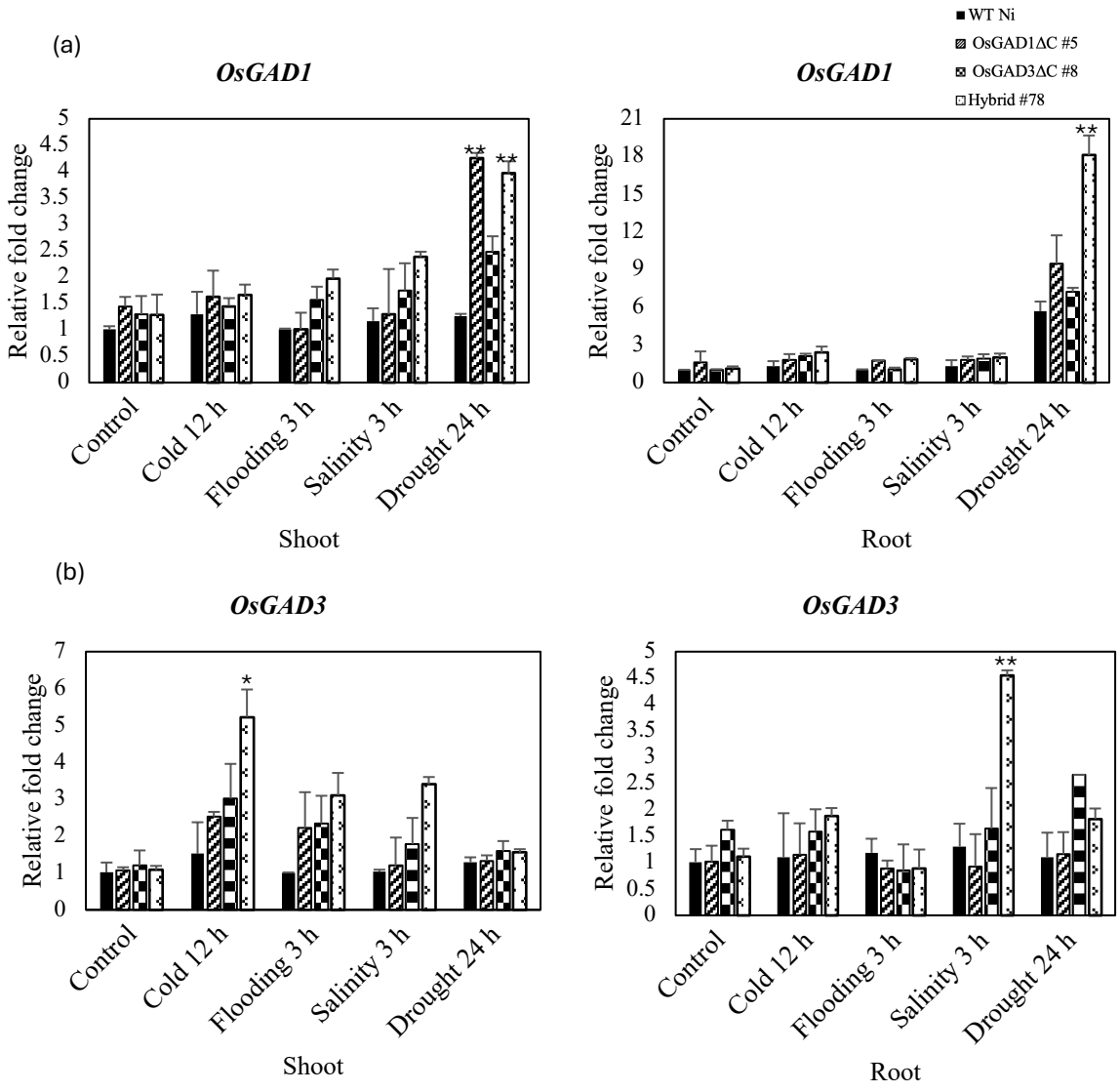

Fig. 8 Relative expression of *OsGAD1* and *OsGAD3* genes in abiotic stress conditions. (a) *OsGAD1* and (b) *OsGAD3* gene expression in shoot and root tissues of WT-Ni, OsGAD1ΔC #5, OsGAD3ΔC #8, and Hybrid #78 in response to control (without stress treatment), cold (12 h), flooding (3 h), salinity (3 h), and drought (24 h) conditions. Bars represent the mean ± standard deviation (SD) of relative fold change. Expression levels were analyzed using the $2^{-\Delta\Delta Ct}$ method, where TATA-binding protein 2 (*TBP-2*) was used as an internal control. Statistical significance was determined by comparing the values of each rice line with WT-Ni in identical stress conditions. Asterisks denote significant differences (*P<0.05, **P<0.01*)*.

3.5 Differential accumulation of free amino acids in response to abiotic stress in rice vegetative tissues

The accumulation of specific free amino acids is a well-recognized metabolic adaptation employed by plants to counteract environmental stresses. These amino acids often serve as osmolytes, antioxidants, or signaling molecules that contribute to cellular protection and stress tolerance (Anzano et al., 2022; Rai, 2002). In this study, the levels of six stress-associated amino acids alanine, serine, aspartic acid, glutamic acid, proline, and valine, were quantified in shoot and root tissues of WT Ni, OsGAD1ΔC #5, OsGAD3ΔC #8, and Hybrid #78. Plants were evaluated under both control conditions and abiotic stress treatments, including cold, salinity, flooding, and drought.

3.5.1 Amino acid profiles in shoot tissues

As shown in Figure 9a, a notable enhancement in amino acid accumulation was observed in Hybrid #78, particularly under drought stress, where levels of all six amino acids increased substantially. Moderate increases were also detected under cold and salt stress, while a slight reduction was noted under flooding conditions. Similarly, OsGAD3ΔC #8 displayed prominent increases in amino acid content under drought and salinity, modest elevation in response to cold, and minor to no changes under flooding. OsGAD1ΔC #5 exhibited more conservative responses, showing moderate increases in drought and salt stress but clear declines in amino acid content during flooding. By contrast, WT Ni showed the least responsive profile, with minor increases observed under cold and salinity, a moderate rise in drought stress, and clear reductions in all amino acids under flooding. These trends highlighted the superior stress responsiveness of the genome-edited lines, especially Hybrid #78, compared to WT, with a particularly strong metabolic adjustment under drought stress. The elevated amino acid levels likely reflect a coordinated effort to maintain cellular osmotic balance and metabolic stability during dehydration and ionic stress (Rossi et al., 2021).

3.5.2 Amino acid profiles in root tissues

The response patterns in root tissues (Figure 9b) generally mirrored those observed in the shoot, though the magnitude of amino acid accumulation was often higher. Hybrid #78 again demonstrated the most pronounced response, especially under drought stress, supporting its enhanced capacity for osmotic adjustment, a known role of amino acid accumulation under water-limiting conditions (Heinemann & Hildebrandt, 2021). In contrast, WT Ni and OsGAD1ΔC #5 showed substantial reductions in several amino acids, including serine, aspartic acid, and glutamic acid, particularly under flooding stress. This suggested that these genotypes may be more susceptible to metabolic disruption during submergence, which is consistent with observations by Komatsu et al. (2024) showing that hypoxic stress conditions alter amino acid biosynthesis and degradation pathways in rice. Both Hybrid #78 and OsGAD3ΔC #8

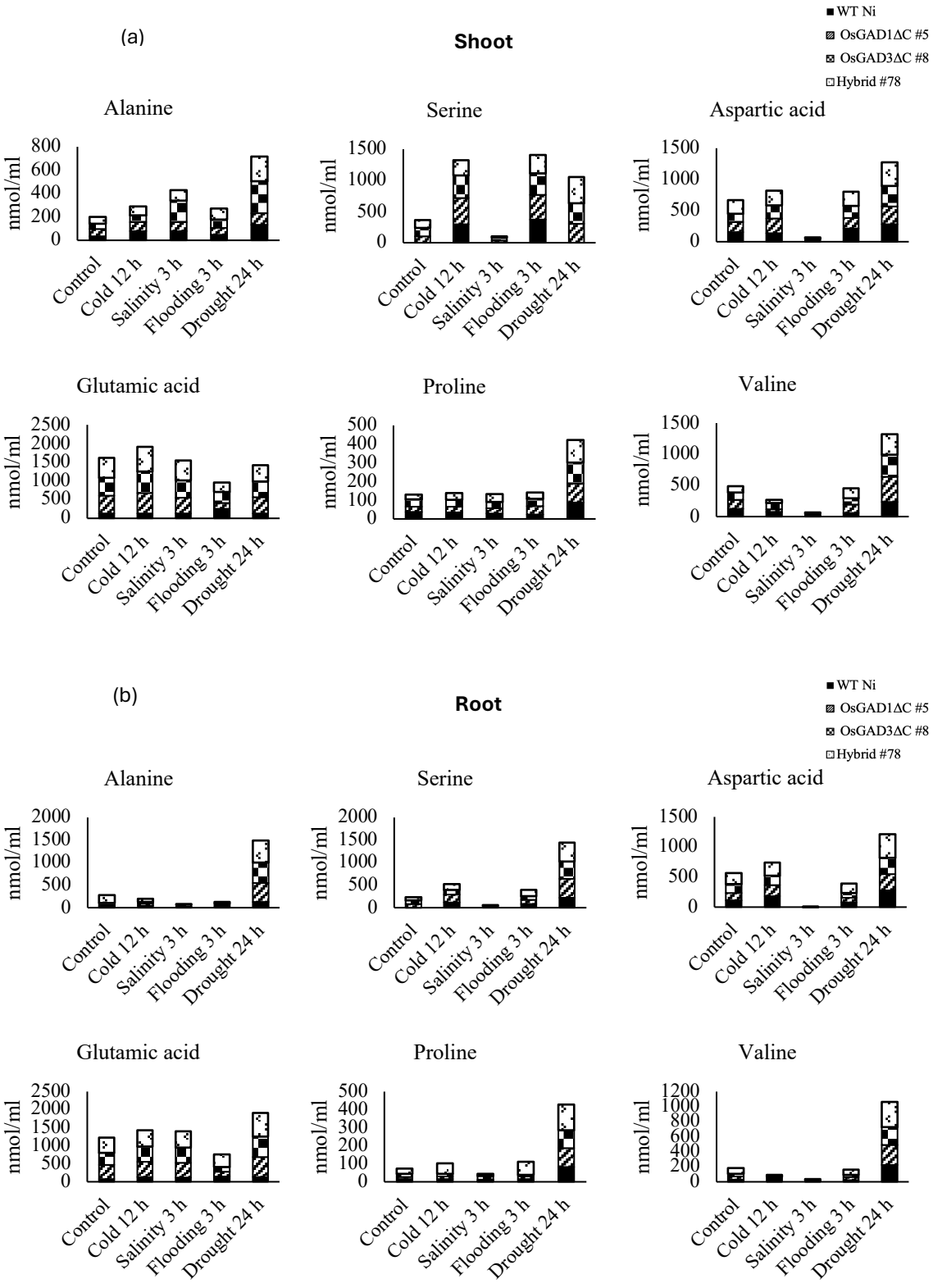

Fig. 9 Comparative analysis of free amino acid content in shoot and root tissues after abiotic stress treatment. This stacked column bar graph represents the quantified levels of free amino acids: alanine, serine, aspartic acid, glutamic acid, proline, and valine, in the vegetative tissues of different rice lines subjected to abiotic stresses. Panel (a) illustrates the amino acid content in shoot tissues, and panel (b) depicts that in root tissues. WT Ni, OsGAD1ΔC #5, OsGAD3ΔC #8, and Hybrid #78 were examined in this analysis.

displayed more resilient metabolic responses, with sustained or enhanced amino acid levels under most stress conditions. These findings align with previous studies that highlight the critical role of amino acid biosynthesis in osmoprotection, redox balance, and stress signaling (Trovato et al., 2021). The ability of these genotypes to maintain higher amino acid levels, particularly under drought and salinity, reflects a robust stress adaptation mechanism likely linked to their enhanced GAD activity and GABA metabolism.

Taken together, these findings reveal genotype-dependent variations in amino acid metabolism under abiotic stress, with Hybrid #78 consistently exhibiting the most pronounced accumulation of stress-related amino acids. This enhanced biochemical response is likely a contributing factor to its superior physiological performance and stress resilience, as observed in other sections of this study. The comparatively lower accumulation in WT Ni and OsGAD1ΔC #5, particularly under flooding stress, emphasizes the complexity of metabolic regulation and the importance of specific gene modifications such as CaMBD truncation, in shaping plant stress responses.

3.6 Enhanced abiotic stress tolerance

To evaluate stress resilience, the survival rates of WT Nipponbare (WT Ni), OsGAD1ΔC #5, OsGAD3ΔC #8, and the hybrid line Hybrid #78 were assessed under four abiotic stress conditions: cold, salinity, flooding, and drought. Following exposure, seedlings were transplanted to soil and allowed to recover for 18 days, and survival rates were recorded (Fig. 10; Table 6). Each treatment was repeated in three biological replicates to ensure accuracy.

3.6.1 Survival rates under stress conditions

Under cold stress (4°C for five days), no surviving plants were observed in WT Ni or OsGAD1ΔC #5, indicating complete sensitivity. OsGAD3ΔC #8 exhibited a 33% survival rate, while Hybrid #78 showed a 25% survival rate, suggesting moderate cold tolerance in both lines. In salinity stress (150 mM NaCl for 48 hours), all lines except Hybrid #78 exhibited 0% survival. Hybrid #78 demonstrated 33% survival, indicating a clear advantage in salt stress resistance. During flooding stress, WT Ni displayed 33% survival, OsGAD1ΔC #5 had 66%, OsGAD3ΔC #8 had 50%, and Hybrid #78 showed the highest survival rate at 83%, indicating strong tolerance to water submergence. In the drought stress assay, Hybrid #78 again exhibited superior performance with an 83% survival rate, followed by OsGAD3ΔC #8 (33%), OsGAD1ΔC #5 (18%), and WT Ni (8%). These results consistently highlighted Hybrid #78 as the most stress-tolerant genotype across all abiotic stress conditions. The enhanced survival of this hybrid is likely attributable to the combined genetic contributions of the two parental lines. The phenomenon of heterosis, where the progeny exhibit superior traits relative to their parents, is well-documented in rice and other crops (Gu & Han, 2024), and likely explains the enhanced performance of Hybrid #78, particularly under salinity stress.

Interestingly, while OsGAD1ΔC #5 exhibited elevated GABA levels under control conditions, it did not translate into improved stress survival. This suggests that constitutive accumulation of GABA may not be sufficient for stress adaptation. Instead, Hybrid #78, which carries both the *OsGAD1* and *OsGAD3* truncations, displayed stress-inducible GABA accumulation, reflecting a more regulated and responsive metabolic adaptation. The contrast in survival between OsGAD1ΔC #5 and Hybrid #78, especially under drought and salinity stress, supports the idea that co-expression of both truncated genes allows for more dynamic GABA regulation, leading to better stress responsiveness. Furthermore, the survival of OsGAD3ΔC #8 and Hybrid #78 under cold stress, in contrast to the complete sensitivity of OsGAD1ΔC #5, suggested that OsGAD3 plays a pivotal role in cold tolerance, which is enhanced in the hybrid background through additive or synergistic effects.

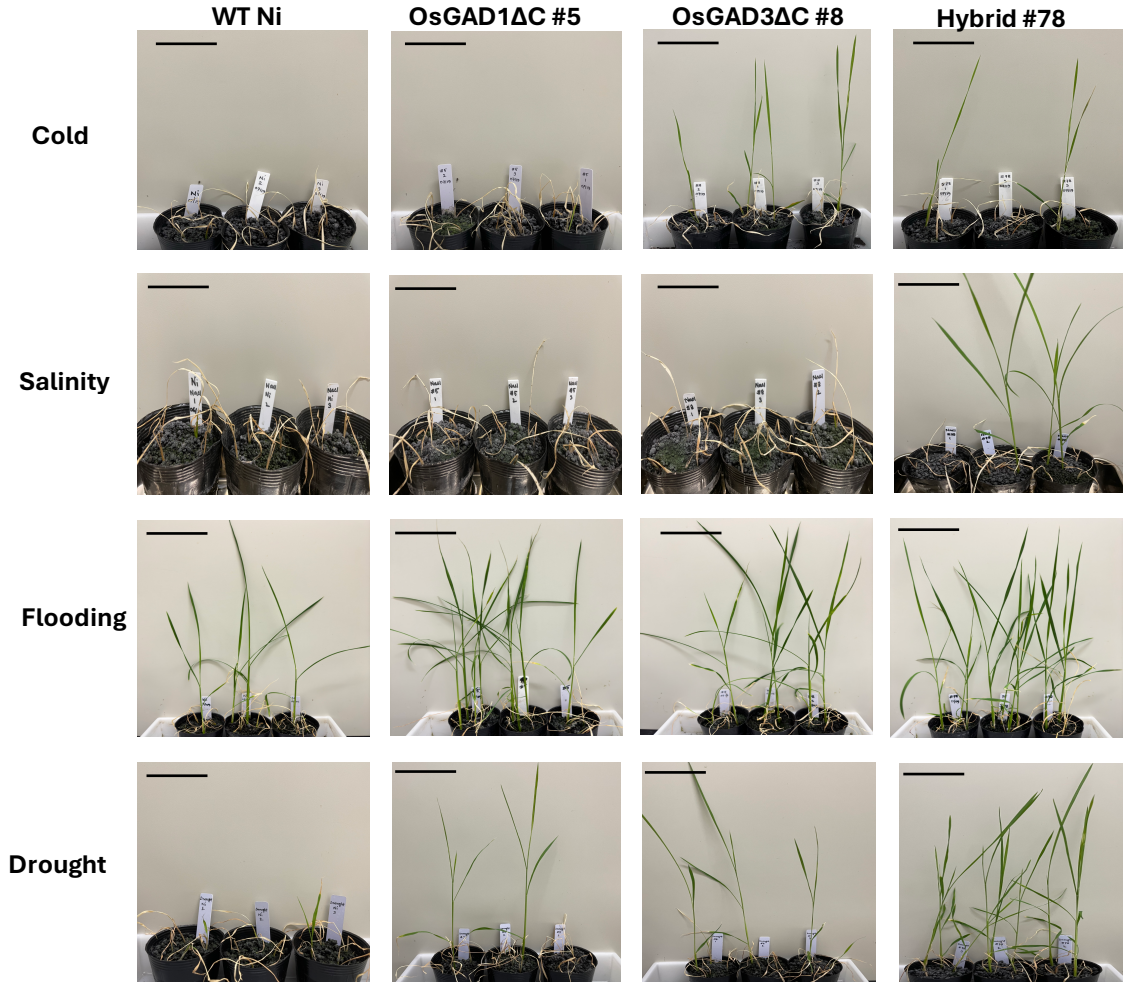

Fig. 10 Abiotic stress tolerance in rice seedlings. Assessments of cold, salinity, flooding, and drought stress responses were conducted on WT Ni, OsGAD1ΔC #5, OsGAD3ΔC #8, and Hybrid #78 at the seedling stage. For cold stress evaluation, 16-day-old seedlings were subjected to 4°C for 5 days prior to soil transplantation. Salinity stress was imposed by immersing 14-day-old seedlings in 150 mM NaCl solution for 48 h, followed by transfer to soil. Flooding stress involved immersion of seedlings in MS liquid media for 72 h, followed by transfer to soil. Drought stress was simulated by keeping seedlings

on plastic plates for 6 h until approximately 65% of their initial fresh weight was lost. (Scale bar = 12 cm).

Table 6. Survival rate (%) after abiotic stresses.

Stress type	Survival rate (%)			
	WT Ni	OsGAD1ΔC #5	OsGAD3ΔC #8	Hybrid #78
Cold	0	0	33.33 ± 4.54**	25.00 ± 6.49**
Salinity	0	0	0	33.33 ± 4.82**
Flooding	33.33 ± 3.76	66.71 ± 6.21	50.31 ± 5.92	83.86 ± 4.27*
Drought	8.33 ± 5.02	18.00 ± 3.76	33.33 ± 7.41*	83.33 ± 7.84**

Post-stress recovery was quantified by calculating the survival rate of seedlings after an 18-day recovery period in soil. Bars represent the mean ± standard deviation (SD) (n= 12 plants). Statistical significance was determined by comparing the values of each rice line with WT Ni in identical stress conditions. Asterisks denote significant differences (*P<0.05, **P<0.01).

3.6.2 Biomass loss under stress conditions

In addition to survival rates, biomass retention was used as an indicator of stress tolerance. Both fresh weight and dry weight were measured post-stress treatment across all four genotypes under cold, salinity, flooding, and drought conditions (Table 7). Consistently, Hybrid #78 experienced the lowest reduction in biomass across all stress types. The most notable difference was observed in drought stress, where the hybrid retained the highest proportion of its biomass, indicating enhanced water stress adaptation. In contrast, WT Ni showed the greatest biomass loss, confirming its susceptibility. The genome-edited parental lines OsGAD1ΔC #5 and OsGAD3ΔC #8 exhibited intermediate tolerance, with OsGAD3ΔC #8 performing slightly better, especially under salinity and drought stress. These findings reinforce the notion that Hybrid #78 has superior physiological stability and is better equipped to maintain growth under stress.

Table 7. Biomass loss (%) after abiotic stresses.

Stress type	**Biomass loss (FW%)**				**Biomass loss (DW%)**			
	WT Ni	OsGAD1 ΔC #5	OsGAD3 ΔC #8	Hybrid #78	WT Ni	OsGAD1 ΔC #5	OsGAD 3ΔC #8	Hybrid #78
Cold	13.54 ± 3.67	11.93 ± 1.41	6.77 ± 4.53*	2.33 ± 3.15**	14.65 ± 3.01	18.52 ± 3.89	10.32 ± 2.25	7.02 ± 3.15*
Salinity	17.41 ± 5.70	14.84 ± 3.68	12.67 ± 4.73	7.32 ± 3.97**	14.12 ± 1.43	11.96 ± 2.35	10.21 ± 1.34	5.16 ± 3.97
Flooding	22.11 ± 3.50	18.05 ± 4.69	12.87 ± 2.22*	6.51 ± 1.84**	17.53 ± 2.06	11.53 ± 1.36	8.82 ± 1.04*	4.97 ± 1.92*
Drought	69.50 ± 2.86	57.49 ± 2.9	55.95 ± 3.54	45.77 ± 3.33*	22.43 ± 3.77	17.26 ± 2.23	14.95 ± 1.61*	10.32 ± 2.29**

Data represented as the mean ± standard deviation (SD) of fresh weight (FW) and dry weight (DW) percentage in cold, salinity, flooding, and drought stress conditions. Statistical significance was

determined by comparing the values of each rice line with the wild type in identical stress conditions. Asterisks denote significant differences (*P<0.05, **P<0.01)

The enhanced survival and biomass retention in Hybrid #78 is closely associated with the increased expression of *OsGAD1* and *OsGAD3*, resulting in significantly higher GABA accumulation under stress. The hybrid's robust salinity tolerance, demonstrated by its 33% survival, correlates with its highest GABA levels among all lines. The improved performance under cold stress in both Hybrid #78 and OsGAD3ΔC #8 also points to a central role of GAD3 in cold adaptation, likely due to stress-inducible expression and functional activity under low-temperature conditions. In both flooding and drought stress, the co-expression of the truncated forms of GAD1 and GAD3 in Hybrid #78 appears to confer an additive effect, boosting GABA biosynthesis and enhancing overall stress resilience.

Previous studies have shown that exogenous application of GABA can improve plant tolerance to abiotic stresses by modulating various physiological and metabolic pathways. Ullah et al. (2023) and Chen et al. (2022) reported that GABA regulates the GABA shunt, secondary metabolism, hormone signaling, carbon/nitrogen balance, and ROS detoxification. Similarly, Zarbakhsh & Shahsavar (2023) demonstrated that exogenous GABA improved photosynthetic efficiency, mineral nutrient uptake, and soluble sugar accumulation in pomegranate plants exposed to drought and salt stress. Additionally, Qian et al. (2024) and Liu et al. (2024) found that GABA enhances antioxidant enzyme activity, helping to alleviate oxidative stress caused by high salinity.

Collectively, these findings support the conclusion that elevated GABA levels, whether through genetic manipulation or exogenous application, enhance abiotic stress tolerance in plants. The superior performance of Hybrid #78 can therefore be attributed to a combination of genetically enhanced GABA biosynthesis, stress-responsive gene expression, and metabolic reprogramming, resulting in increased resilience under adverse environmental conditions.

3.7 Reduced hydrogen peroxide (H_2O_2) accumulation in genome-edited lines under abiotic stress

To assess oxidative damage levels in the rice lines under abiotic stress conditions, DAB staining was performed to detect hydrogen peroxide (H_2O_2) accumulation in leaf tissues. The presence of brown precipitate indicated elevated levels of H_2O_2, a common marker of oxidative stress. As shown in Fig 11 WT Ni displayed intense DAB staining across all four stress conditions, highlighting its higher susceptibility to oxidative damage. In contrast, Hybrid #78 showed the least amount of staining, particularly under drought and flooding conditions, suggesting a more robust antioxidant response.

Both OsGAD1ΔC #5 and OsGAD3ΔC #8 exhibited intermediate staining levels, with OsGAD3ΔC #8 appearing slightly less affected than OsGAD1ΔC #5, especially under cold and salt stress. These results corroborate the survival rate and biomass retention data, further supporting the superior stress tolerance of Hybrid #78, which likely results from enhanced GABA-mediated regulation of ROS homeostasis. This aligns with previous reports that link GABA metabolism to improved antioxidant enzyme activity and reduced ROS accumulation in plants under abiotic stress (Qian et al., 2024; Liu et al., 2024).

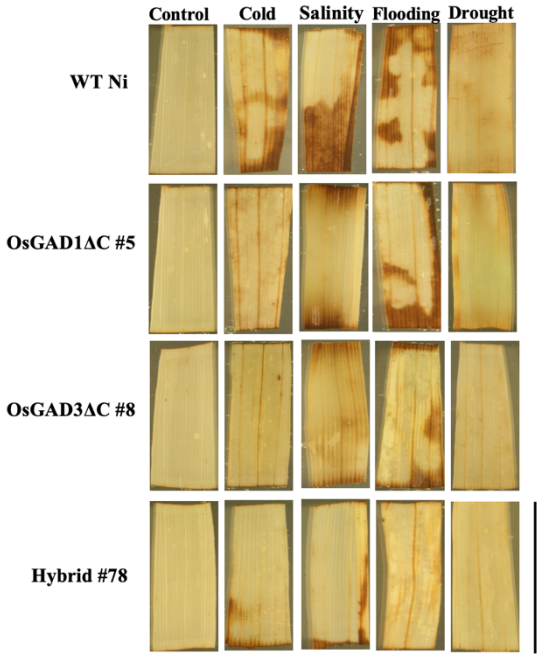

Fig. 11 Detection of H_2O_2 accumulation in rice leaf tissues using DAB staining under abiotic stress. DAB (3,3′-diaminobenzidine) staining was performed to detect hydrogen peroxide (H_2O_2) accumulation in the leaf tissues of four rice lines: WT Nipponbare (WT Ni), OsGAD1ΔC #5, OsGAD3ΔC #8, and Hybrid #78 under various abiotic stress treatments. Detached leaves were treated with DAB solution and incubated under light for 8 hours. Brown coloration indicates H_2O_2 accumulation, reflecting oxidative damage. Leaf samples were collected from seedlings exposed to cold (4°C, 5 days), salinity (150 mM NaCl, 2 days), flooding (submergence in MS liquid, 3 days), and drought (dehydration on a dry surface, 6 hours). Scale bar = 1 cm.

3.8 Transcriptomic alterations induced by combined *OsGAD1* and *OsGAD3* CaMBD truncation in Hybrid #78

To explore the molecular basis of the enhanced stress tolerance observed in Hybrid #78, we conducted a comparative transcriptome analysis using shoot tissues from Hybrid #78, its parental lines (OsGAD1ΔC #5 and OsGAD3ΔC #8), and WT Nipponbare (WT Ni) grown under control conditions. The objective was to determine whether truncation of the calmodulin-binding domain (CaMBD) in both

OsGAD1 and *OsGAD3* in the hybrid line results in distinct gene expression patterns that could contribute to its superior stress adaptation.

As illustrated in Fig. 12a, the median expression levels of transcripts were generally comparable across all four genotypes, suggesting that the central tendencies in gene activity remained relatively unaffected. However, a closer examination of the interquartile range (IQR) revealed notable differences. In particular, Hybrid #78 displayed a wider IQR, indicating greater dispersion in gene expression levels. This increased variability may reflect more dynamic regulatory processes, possibly contributing to its enhanced physiological plasticity. Moreover, Hybrid #78 exhibited the largest number of outliers, with highly expressed genes extending well beyond the upper range observed in the parental lines or WT Ni. Such an extensive spread in gene expression may reflect the influence of novel regulatory interactions triggered by the combined truncation of *OsGAD1* and *OsGAD3*. Previous studies have suggested that greater expression variability can be associated with improved environmental adaptability and stress responsiveness in plants (Smith et al., 2015). While both OsGAD1ΔC #5 and OsGAD3ΔC #8 also showed an increased number of outliers compared to WT, their expression distributions were more constrained than those of the hybrid. WT Ni, by contrast, displayed the least variability, with tightly clustered expression values and minimal outliers, indicating a more conservative transcriptional profile.

To further investigate expression-level relationships among the genotypes, hierarchical clustering heatmap analysis was performed (Fig. 12b). The resulting heatmap clearly demonstrated distinct transcriptional profiles for each genotype, with Hybrid #78 forming a separate cluster, indicating significant divergence from WT and the parental lines. This divergence suggests that the simultaneous removal of the CaMBD from both *OsGAD1* and *OsGAD3* resulted in a unique transcriptional reprogramming not observed in the single mutants.

In addition, a Venn diagram analysis (Fig. 12c) was conducted to compare the number of differentially expressed genes (DEGs) unique to each genotype. Hybrid #78 showed the highest number of uniquely expressed genes, further supporting the idea that dual truncation of CaMBD domains has a synergistic effect on transcriptome reorganization. The presence of genotype-specific genes in all lines, particularly in the hybrid, implies that each genetic background triggers distinct transcriptional responses, likely influenced by differences in stress signaling, metabolism, and regulatory feedback mechanisms.

To understand the biological relevance of these expression changes, a gene ontology (GO) enrichment analysis was performed, focusing on DEGs from each line. As shown in Fig. 12d, enriched GO terms in Hybrid #78 were predominantly associated with molecular function, including terms related to catalytic activity, ion binding, and oxidoreductase function. These functional categories are often implicated in stress perception, signal transduction, and detoxification pathways. The altered expression of genes in these categories suggests that CaMBD truncation impacts genes involved in key molecular

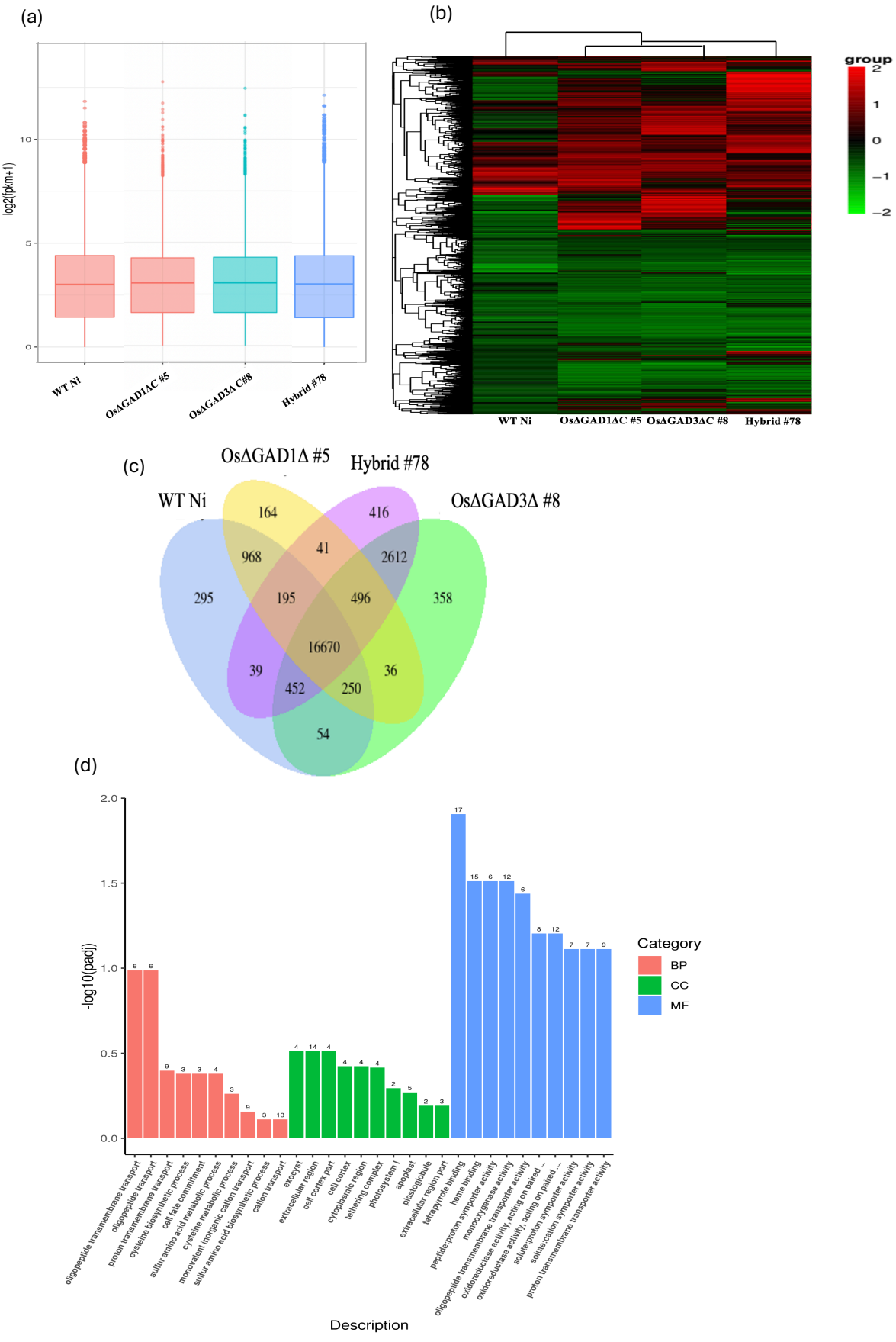
(a)
log2((fpkm+1)
10
5
0
WT Ni
OsΔGAD1ΔC #5
OsΔGAD3Δ C#8
Hybrid #78
(b)
group
2
1
0
−1
−2
WT Ni
OsΔGAD1ΔC #5
OsΔGAD3ΔC #8
Hybrid #78
(c)
OsΔGAD1Δ #5
Hybrid #78
WT Ni
OsΔGAD3Δ #8
164
416
41
968
2612
295
195
496
358
16670
39
36
452
250
54
(d)
-log10(padj)
2.0
1.5
1.0
0.5
0.0
Category
BP
CC
MF
Description
oligopeptide transmembrane transport
oligopeptide transport
proton transmembrane transport
cysteine biosynthetic process
cell fate commitment
sulfur amino acid metabolic process
cysteine metabolic process
monovalent inorganic cation transport
sulfur amino acid biosynthetic process
cation transport
exocyst
extracellular region
cell cortex part
cell cortex
cytoplasmic region
tethering complex
photosystem I
apoplast
plastoglobule
extracellular region part
tetrapyrrole binding
heme binding
monooxygenase activity
peptide:proton symporter activity
oligopeptide transmembrane transporter activity
oxidoreductase activity, acting on paired ...
oxidoreductase activity, acting on paired ...
solute:proton symporter activity
solute:cation symporter activity
proton transmembrane transporter activity

Fig. 12 Analysis of gene expression and functional enrichment across WT Ni, OsGAD1ΔC #5, OsGAD3ΔC #8, and Hybrid #78 in control conditions. **(a)** Box plots representing the log-transformed gene expression levels (log_2(FPKM+1)) for four different groups: WT Ni, OsGAD1ΔC #5, OsGAD3ΔC #8, and Hybrid #78. The central line in each box represents the median expression level, the box limits represent the interquartile range (IQR), and the whiskers extend to 1.5 times the IQR. Outliers are represented by individual points. **(b)** Heatmap of differentially expressed genes (DEGs) across the four groups. The color scale ranges from red (high expression) to green (low expression). The dendrograms indicate hierarchical clustering of both genes and samples, revealing distinct expression patterns and group similarities. **(c)** Venn diagram illustrating the overlap and uniqueness of DEGs among the four groups: WT Ni, OsGAD1ΔC #5, Hybrid #78, and OsGAD3ΔC #8. Each circle represents the DEGs for one group, with numbers indicating the count of unique and shared genes. The intersections highlight common DEGs, providing insights into shared regulatory pathways and responses. **(d)** Gene ontology (GO) enrichment analysis for upregulated DEGs in Hybrid #78 vs WT Ni, categorized into biological processes (BP), cellular components (CC), and molecular functions (MF). The bar chart shows the -log_{10}(*p*-value) for each GO term, with red, green, and blue bars representing BP, CC, and MF categories, respectively. Significant terms indicate key biological processes and functions affected by the genetic modifications.

processes, which may underlie the enhanced stress tolerance observed in the hybrid. Similar findings have been reported in stress-resilient crop varieties, where transcriptomic shifts promote adaptive responses to fluctuating environments (M. Sharma et al., 2024).

3.9 Altered metabolic pathways and functional gene expression following CaMBD truncation in *OsGAD1* and *OsGAD3*

To gain further insights into the molecular mechanisms underlying the enhanced stress tolerance of Hybrid #78, KEGG pathway enrichment analysis was conducted using transcriptome data obtained under control conditions. This analysis revealed a substantial number of upregulated genes in Hybrid #78 when compared to WT Nipponbare (WT Ni) (Table S1), highlighting the broad transcriptional reprogramming induced by CaMBD truncation in *OsGAD1* and *OsGAD3*. The enriched genes were associated with a wide range of biological processes, including primary metabolism, biosynthetic pathways, signaling cascades, molecular interactions, and degradation systems all of which are integral to cellular stress adaptation. The number of genes associated with each pathway is detailed in Table S1, and many of these genes are functionally linked to GABA biosynthesis and metabolic pathways that support stress resilience.

Several key upregulated genes are particularly notable. For example, Os08g0423500, Os08g0423600, and Os08g0468700 are implicated in nitrogen metabolism, which plays a critical role in maintaining intracellular glutamate pools, a direct precursor for GABA synthesis. Enhanced glutamate availability is known to bolster the GABA shunt, thereby contributing to stress response efficiency (Signorelli et al., 2021; Ansari et al., 2021). In addition, Os04g0389800 is involved in 2-oxocarboxylic acid metabolism (KEGG Pathway: ko01210), a pathway that generates intermediates feeding into the GABA

shunt, thereby linking carbon and nitrogen metabolism and promoting GABA biosynthesis. Furthermore, Os11g0210600 is associated with gluconeogenesis, a process that provides essential precursors for the TCA cycle, indirectly supporting sustained GABA production under stress. Similarly, Os10g0465700 is linked to starch and sucrose metabolism, contributing to glycolytic activity, which provides carbon skeletons and energy required for the activation of the GABA pathway (Chen et al., 2020). Collectively, the upregulation of these genes in Hybrid #78 suggested that CaMBD truncation in both *OsGAD1* and *OsGAD3* facilitates a coordinated reprogramming of metabolic pathways. This reprogramming enhances substrate availability and pathway fluxes toward GABA synthesis, contributing to the elevated GABA accumulation and improved stress resilience observed in the hybrid line.

The dot plot visualization (Fig. 13) summarizes these findings by illustrating the enriched KEGG pathways. Among the enriched pathways, phenylpropanoid biosynthesis exhibited the highest significance, characterized by the largest GeneRatio (~0.12) and lowest padj value (padj < 0.001). This pathway, known for its role in producing secondary metabolites that enhance plant defense, was represented by 15 upregulated genes. Similarly, plant pathogen interaction and plant hormone signal transduction pathways showed high enrichment (GeneRatio ~0.10–0.11) and strong statistical support, indicating active modulation of immune and signaling processes in Hybrid #78 under normal growth conditions. Several primary metabolic pathways were also significantly enriched, including nitrogen metabolism, β-alanine metabolism, and α-linolenic acid metabolism, suggesting enhanced flux through carbon and nitrogen processing pathways. These enrichments are functionally consistent with the observed upregulation of GABA biosynthesis-related genes and support the hypothesis that CaMBD truncation promotes a transcriptionally primed state conducive to stress resilience.

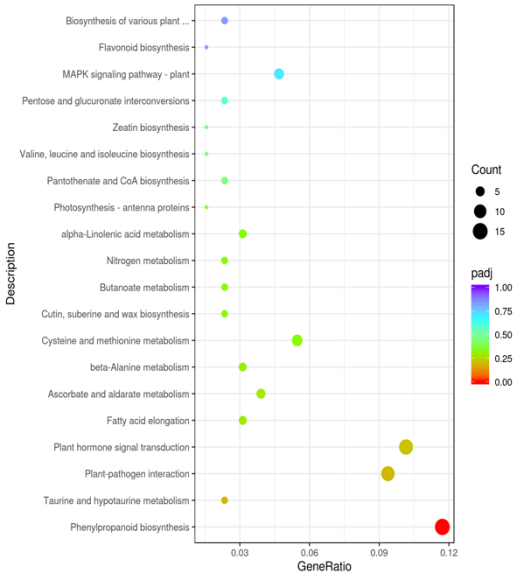

Fig. 13 KEGG pathway enrichment analysis of upregulated genes in Hybrid #78 compared to WT Nipponbare under control conditions. The dot plot visualizes significantly enriched KEGG pathways based on differentially upregulated genes in the shoot transcriptome of Hybrid #78 relative to WT Nipponbare. The x-axis represents the GeneRatio, calculated as the proportion of upregulated genes involved in each pathway relative to the total number of genes annotated in that pathway. Dot size corresponds to the number of upregulated genes, while dot color indicates the adjusted p-value (padj), with red denoting higher statistical significance and blue indicating less significant enrichment.

3.10 Upregulation of stress-responsive genes in genome-edited and hybrid lines

In addition to pathway-level changes, transcript analysis revealed the upregulation of several stress-responsive genes in the genome-edited lines OsGAD1ΔC #5, OsGAD3ΔC #8, and Hybrid #78 when compared to WT Ni under control conditions (Fig. 14). These genes are associated with tolerance to abiotic stresses such as drought, salinity, and oxidative damage, indicating a primed transcriptional state in the edited lines. Among these, *OsNAC3*, a transcription factor known to mediate drought and salinity stress responses, showed variable expression levels across genotypes. Hybrid #78 exhibited the highest expression of *OsNAC3*, suggesting a pre-activated defense response that may contribute to its superior performance under these stresses. OsGAD3ΔC #8 displayed intermediate expression, while both WT Ni and OsGAD1ΔC #5 had relatively low levels, indicating a less robust preparatory response. Similarly, *OsDST*, another gene associated with drought and salt tolerance, was markedly upregulated in Hybrid #78, whereas expression in the other lines remained considerably lower. This suggests that the combined truncation of CaMBD in *OsGAD1* and *OsGAD3* may enhance regulatory mechanisms that facilitate adaptive stress responses, especially those linked to water deficit and ion imbalance. Expression of *OsSGL*, a gene involved in sugar metabolism and general stress adaptation, was also elevated in both Hybrid #78 and OsGAD3ΔC #8, but not in WT Ni or OsGAD1ΔC #5. This upregulation may reflect metabolic reprogramming in these genotypes to better support energy balance

and cellular stability under stress. Furthermore, *HSP70,* encoding a heat shock protein that plays a crucial role in protein folding and protection against cellular damage, was expressed at its highest level in Hybrid #78. This suggests that the hybrid line may possess an enhanced capacity to maintain proteostasis and limit protein aggregation during stress, a feature closely associated with stress resilience in crops (Kumar et al., 2024).

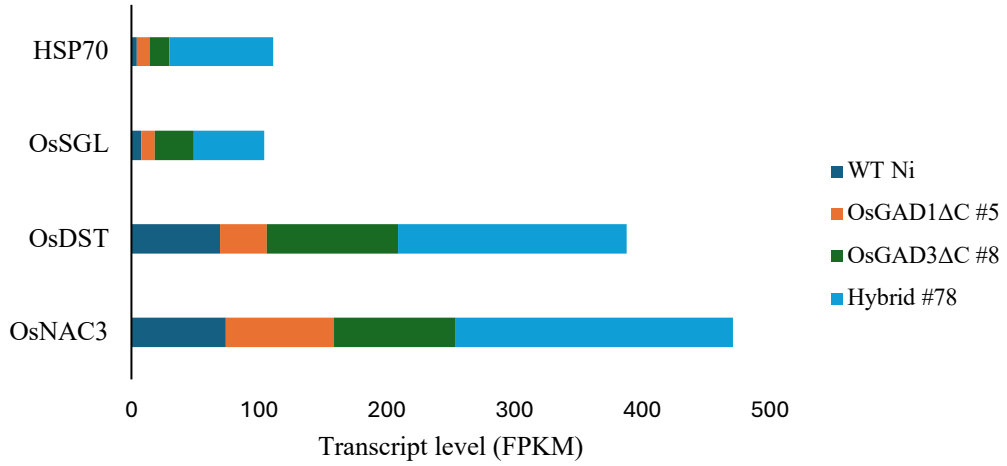

Fig. 14 Expression levels of stress-related genes derived from transcriptome analysis. The bar chart illustrates the expression levels of various stress-related genes in WT Ni (wild-type), OsGAD1ΔC #5, OsGAD3ΔC #8, and Hybrid #78 control conditions. Expression levels are represented as $\log_2$ (FPKM+1) values.

RT-qPCR analysis revealed a notable upregulation of several abiotic stress-related genes in the genome-edited rice lines OsGAD1ΔC #5, OsGAD3ΔC #8, and especially in the Hybrid #78, when compared to the wild-type WT Ni. This transcriptional activation was evident even under control conditions, suggesting a primed defense state in the edited and hybrid lines. Stress-specific markers showed increased expression across various categories of abiotic stress. For cold stress, genes such as *OsADC1, OsTAF2, and OsSAP1* were significantly upregulated in the edited lines, with the highest expression observed in Hybrid #78 (Fig. 15), consistent with earlier reports of their roles in cold tolerance (Peremarti et al., 2010; Kothari et al., 2016). In the context of flooding stress, genes including *OsGolS1, OsERF68, and OsRAB16A* also exhibited elevated expression, particularly in Hybrid #78 (Fig. 16), which aligns with findings that associate these genes with anaerobic stress adaptation (Martins et al., 2022; Haque et al., 2023; García et al., 2024). Similarly, salinity-responsive genes such as *OsMYB30, OsHAK5, and OsNAC3* were strongly induced in the genome-edited lines (Fig. 17), with Hybrid #78 showing the highest levels.

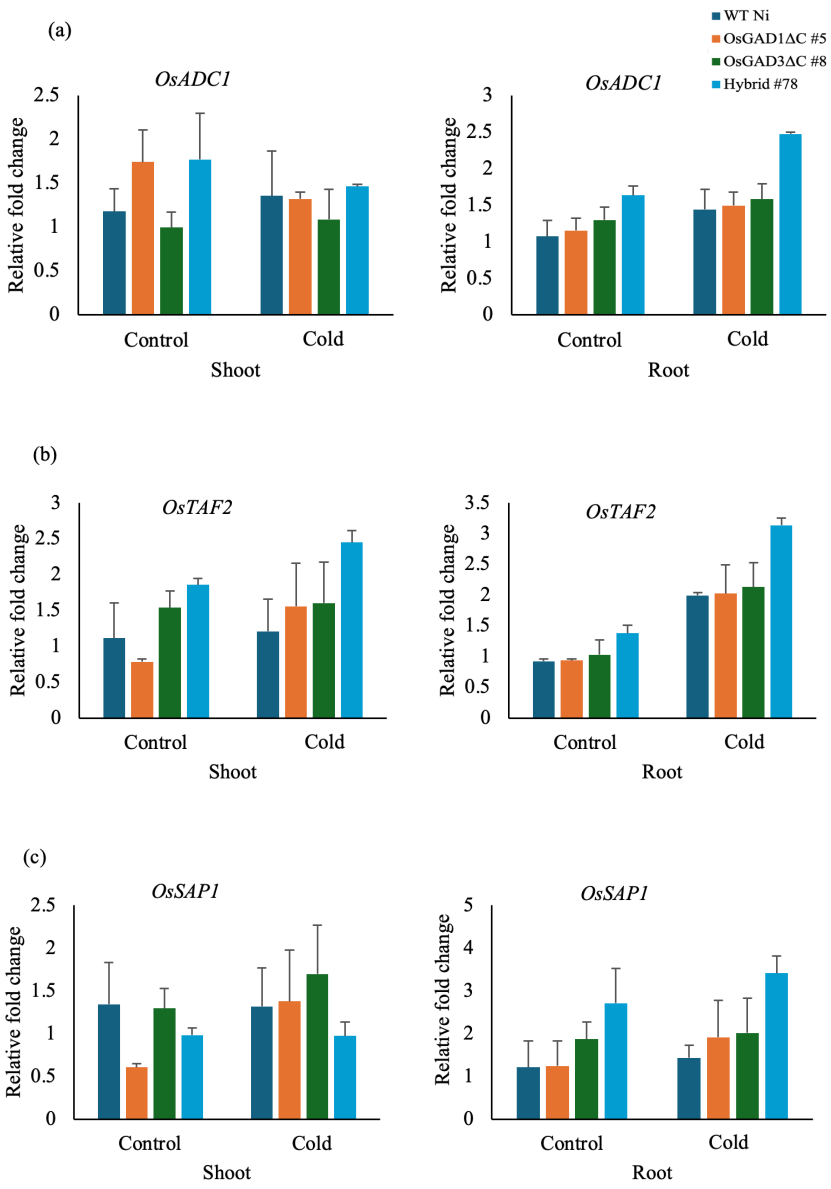

Fig. 15 Relative expression of cold stress-related genes in rice seedlings. (a) *OsADC*, (b) *OsTAF2*, and (c) *OsSAP1* expression in shoot and root tissues of WT Ni (wild-type), OsGAD1ΔC #5, OsGAD3ΔC #8, and Hybrid #78 in control conditions (without stress) followed by the exposure to cold (4°C) for 12 h. Bars represent the mean ± standard deviation (SD) (n=3) of relative fold change. Expression levels were analyzed using the $2^{-\Delta\Delta Ct}$ method, where TATA-binding protein 2(*TBP-2*) was used as an internal control.

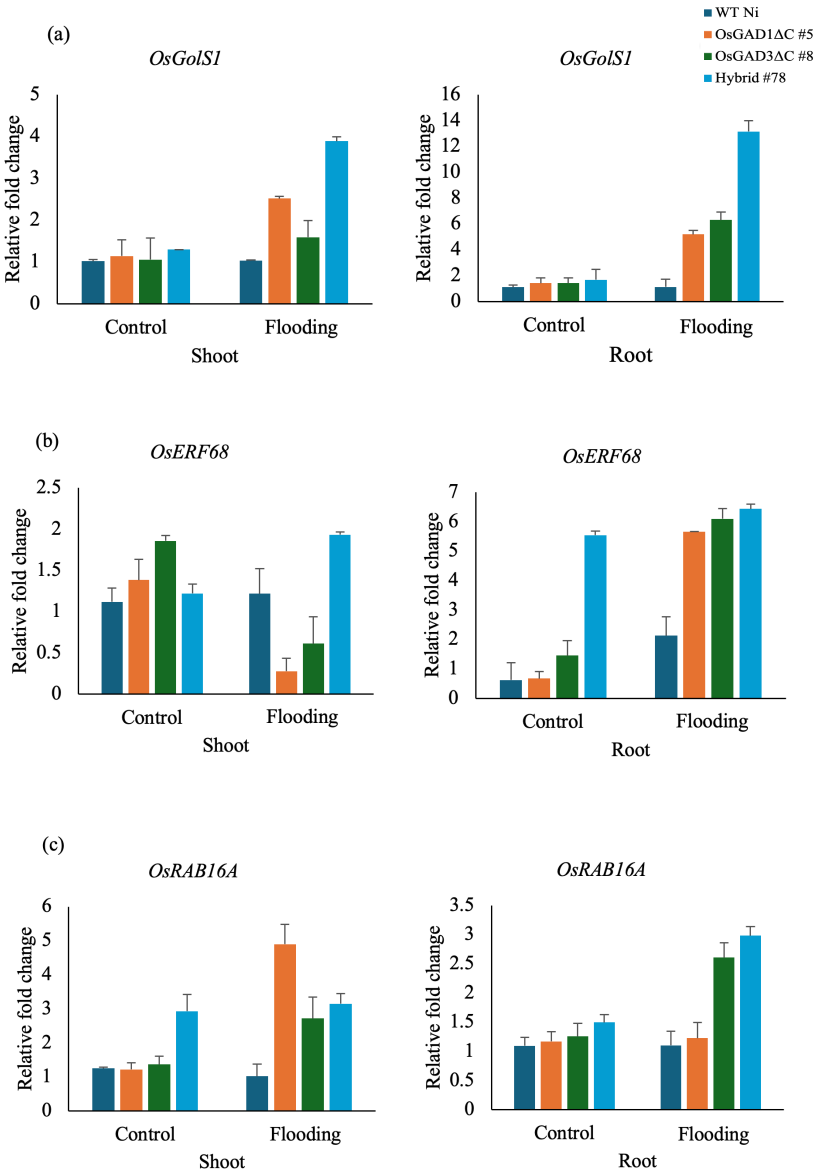

Fig. 16 Relative expression of flooding stress-related genes in rice seedlings. (a) *OsGolS1*, (b) *OsERF68*, and (c) *OsRAB16A* expression in shoot and root tissues of WT Ni (wild-type), OsGAD1ΔC #5, OsGAD3ΔC #8, and Hybrid #78 in control conditions (without stress) followed by exposure to flooding conditions for 3 h. Bars represent the mean ± standard deviation (SD) (n=3) of relative fold change. Expression levels were analyzed using the $2^{-\Delta\Delta Ct}$ method, where TATA-binding protein 2(*TBP-2*) was used as an internal control.

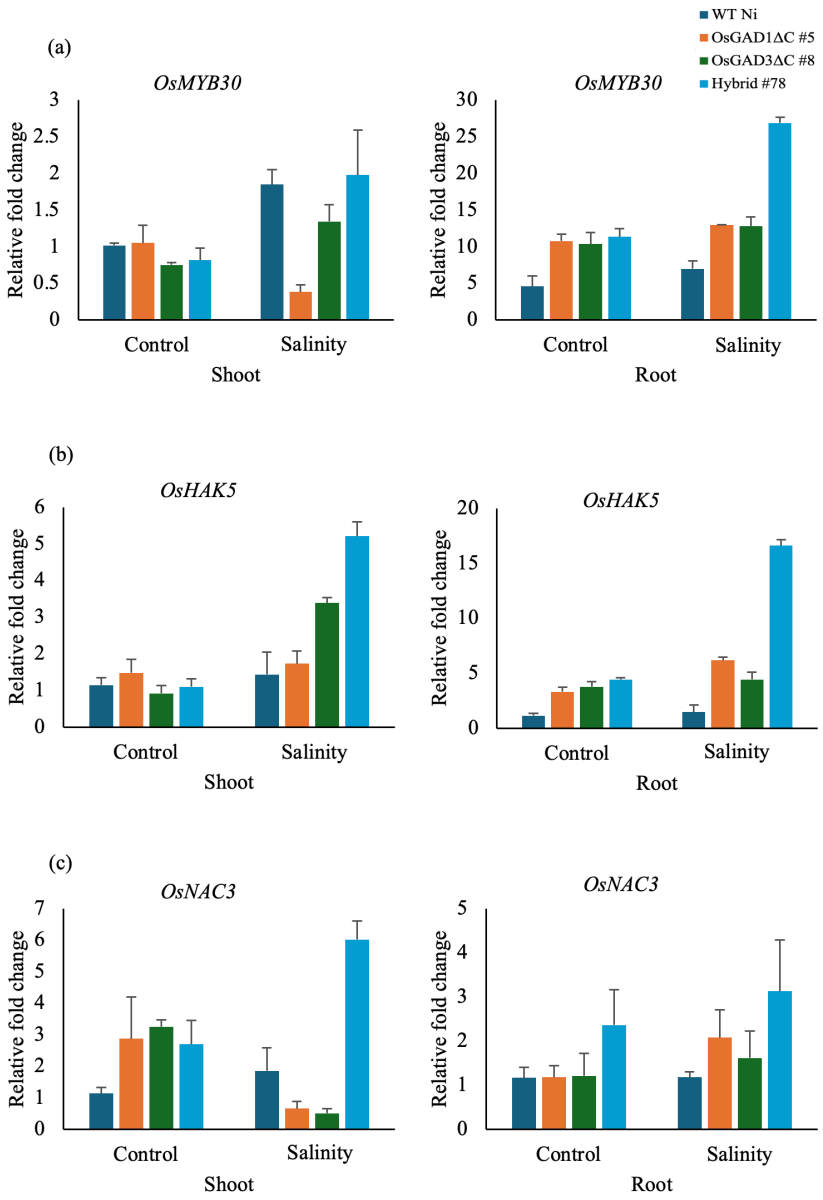

Fig. 17 Relative expression of salinity stress-related genes in rice seedlings. (a) *OsMYB30*, (b) *OsHAK5*, and (c) *OsNAC3* expression in shoot and root tissue of WT Ni (wild-type), OsGAD1ΔC #5, OsGAD3ΔC #8, and Hybrid #78 in control conditions (without stress) followed by exposure to salinity condition (150 mM NaCl) for 3 h. Bars represent the mean ± standard deviation (SD) (n=3) of relative fold change. Expression levels were analyzed using the $2^{-\Delta\Delta Ct}$ method, where TATA-binding protein 2 (*TBP-2*) was used as an internal control.

Under drought stress, the expression of key regulators such as *OsDREB2B, OsDST, and OsHSF13* was also significantly higher in the genome-edited lines, especially in Hybrid #78 (Fig. 18), corroborating their established roles in dehydration response and stress recovery (Matsukura et al., 2010; Santosh et al., 2020; Sirohi et al., 2020).

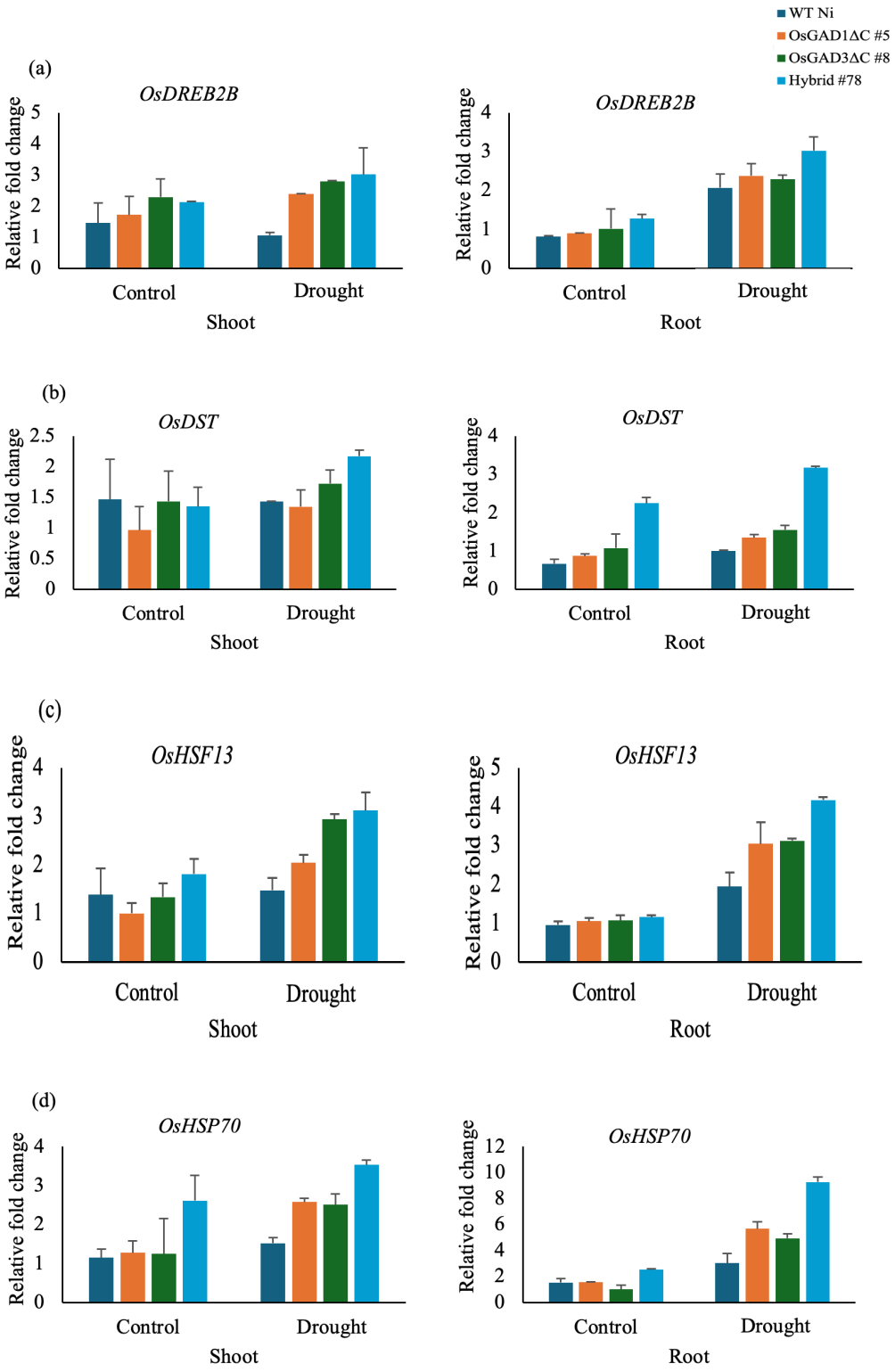

Fig. 18 Relative expression of drought stress-related genes in rice seedlings. (a) *OsDREB2B*, (b) *OsDST*, (c) *OsHSF13*, and (d) *OsOsHSP70* expression in shoot and root tissues of WT Ni (wild-type), OsGAD1ΔC #5, OsGAD3ΔC #8, and Hybrid #78 in control conditions (without stress) followed by exposure to drought conditions for 24 h. Bars represent the mean ± standard deviation (SD) (n=3) of relative fold change. Expression levels were analyzed using the $2^{-\Delta\Delta Ct}$ method, where TATA-binding protein 2(*TBP-2*) was used as an internal control.

These results suggested that the removal of the autoinhibitory CaMBD domain in *OsGAD1* and *OsGAD3* has a broader impact on gene regulation beyond GABA biosynthesis, potentially enhancing stress signaling pathways and transcriptional preparedness. This is further supported by previous studies in *Arabidopsis*, where *CAMTA3*, a calmodulin-binding transcription activator, was shown to regulate biotic stress-related genes, demonstrating the link between CaM-binding domains and transcriptional activation (Galon et al., 2008).

Chapter 4: Discussion

This study demonstrates that targeted truncation of the C-terminal CaMBD in OsGAD1 and OsGAD3 via CRISPR/Cas9 is an effective strategy to enhance GABA accumulation and improve abiotic stress tolerance in rice. The development and characterization of a dual genome-edited hybrid line (Hybrid #78), which contains both OsGAD1ΔC and OsGAD3ΔC alleles, revealed significantly elevated GABA levels and superior tolerance under diverse abiotic stress conditions. These findings extend current knowledge on the role of GAD-mediated GABA biosynthesis and provide strong evidence for the application of genome editing in rice improvement.

4.1 Synergistic effects of OsGAD1 and OsGAD3 editing on GABA biosynthesis

Quantification of GABA levels in the CRISPR/Cas9-edited lines (OsGAD1ΔC and OsGAD3ΔC) revealed substantial accumulation under both control and stress conditions (Fig. 7), with the hybrid line (Hybrid #78) exhibiting the most pronounced increase. Specifically, GABA concentrations in Hybrid #78 roots under stress were up to five times higher than in wild-type Nipponbare and approximately twice as high as in each of the parental genome-edited lines. This suggests a possible additive or synergistic effect arising from the combined truncation of OsGAD1 and OsGAD3. Given that OsGAD1 is predominantly expressed in vegetative tissues and OsGAD3 is more active in seeds (Akama et al., 2020), the hybrid line benefits from complementary, tissue-specific GABA biosynthesis, enabling broader and more efficient GABA accumulation across developmental stages and organ systems.

These observations are in alignment with prior investigations, including the work by Akama et al. (2020), which reported a seven-fold increase in GABA levels in rice grains following CRISPR/Cas9-mediated truncation of the CaMBD in OsGAD3. Similarly, Akter et al. (2024) demonstrated that the deletion of the CaMBD in OsGAD4 significantly enhanced GABA accumulation and contributed to improved abiotic stress tolerance in rice seedlings. Together, these findings reinforce the role of CaMBD truncation as an effective approach to constitutively activate GAD enzymes and boost GABA biosynthesis under both normal and stress conditions. Our findings add further evidence to the growing body of research supporting the utility of GAD manipulation to enhance the GABA shunt pathway and associated metabolic functions. This is further supported by studies in other species, where constitutive GAD activity has similarly led to elevated GABA levels and enhanced stress resilience. For instance, Renault et al. (2010) found that constitutive GAD activity in *Arabidopsis* led to enhanced GABA levels and stress tolerance. Similarly, GABA improved oxidative damage and salinity tolerance in maize and tomato (Wu et al., 2020; Wang et al., 2024 and Seifikalhor et al., 2020).

Unlike studies employing transgenic overexpression or exogenous GABA application, our use of gene editing targets endogenous enzymatic regulation, representing a more sustainable and regulatory-compliant approach. The current study shows that endogenous manipulation of GAD activity through CaMBD truncation, without overexpression or promoter modification, can similarly enhance stress resilience while maintaining a transgene-free background. The combined editing strategy further improves upon single-gene modification by leveraging the spatial and developmental expression differences between *OsGAD1* and *OsGAD3*, thereby maximizing total GABA output.

4.2 Conserved role of *GAD* gene expression in abiotic stress tolerance

RT-qPCR analysis demonstrated that both *OsGAD1* and *OsGAD3* were markedly upregulated in response to abiotic stress, with Hybrid #78 exhibiting the strongest expression among all tested lines (Fig. 8). Under drought conditions, *OsGAD1* expression increased nearly 18-fold and *OsGAD3* by around 12-fold in root tissues compared to wild-type Nipponbare. This strong transcriptional response, alongside the constitutive activation of GAD enzymes through CaMBD truncation, suggests that GABA biosynthesis in the hybrid line is regulated at multiple levels. Similar stress-induced activation of GAD genes has been observed in other crops. In rice, drought conditions were shown to increase *GAD* expression and promote stress adaptation by improving water-use efficiency (Akter et al., 2024). In tomato, cold stress enhanced *SlGAD* transcription and contributed to better membrane integrity and survival (Wang et al., 2024). Maize also responds to drought with increased *GAD* expression, supporting downstream stress-responsive pathways (Zhang et al., 2017). These findings point to a conserved mechanism where *GAD* genes contribute to abiotic stress resilience through both enzymatic and regulatory functions.

4.3 Improved survival and biomass retention linked to elevated GABA levels

Under abiotic stress, Hybrid #78 exhibited substantially higher survival rates (Table 6) and reduced biomass loss (Table 7) compared to the wild-type and parental lines. This enhanced resilience is primarily attributed to increased GABA accumulation resulting from CaMBD truncation in OsGAD1 and OsGAD3. Increased levels of GABA have been implicated in enhancing plant tolerance to abiotic stress by facilitating osmotic balance, stabilizing cellular membranes, and neutralizing reactive oxygen species (ROS), which together contribute to improved cellular homeostasis under adverse environmental conditions (Bouché & Fromm, 2004; Shelp et al., 2021). In our study, the range of survival improvements (25–83%) aligns with earlier findings demonstrating that higher GABA content supports stress mitigation across diverse plant systems (Akter et al., 2024).

These physiological responses are further substantiated by studies in other crops. Wu et al. (2020) showed that GABA treatment improved salt tolerance in tomato by preserving root growth and reducing

ionic toxicity. Similarly, GABA accumulation under cold stress in tea (Zhu et al., 2019) and during drought in maize (Seifikalhor et al., 2020) has been linked to enhanced plant survival. Such cross-species consistency underscores the conserved role of GABA in abiotic stress adaptation and reinforces the utility of our genome-editing approach in rice.

4.4 Transcriptomic insights into GABA-mediated regulation of stress adaptation

Transcriptomic data revealed extensive changes in gene expression in Hybrid #78. KEGG pathway enrichment analysis highlighted key metabolic processes, including nitrogen metabolism, glycolysis, and amino acid biosynthesis (Table S1). These observations align with findings from Fait et al. (2011) who reported that GABA-enriched *Arabidopsis* plants underwent metabolic reprogramming that enhanced nitrogen utilization and energy production. Similarly, Wu et al. (2020) demonstrated that GABA accumulation in tomato modulated cellular redox balance and transcriptional regulation of key metabolic pathways, underscoring the conserved role of GABA in orchestrating stress-adaptive gene networks.

The upregulation of key stress-responsive genes, including *OsDREB*, *OsNAC3*, *OsDST*, *OsSGL*, and *HSP70*, in Hybrid #78 suggests a potential regulatory role of GABA in stress signaling pathways. These genes are associated with abscisic acid (ABA)-mediated signaling, reactive oxygen species (ROS) scavenging, and protein stabilization, critical processes that enhance plant adaptation to abiotic stresses. RT-qPCR results (Fig. 15, Fig. 16, Fig. 17, Fig.18) suggest that increased endogenous GABA levels may influence the activation or modulation of these pathways. This proposed interaction is reinforced by findings from Liu et al. (2021), who reported that elevated GABA concentrations modulated ABA biosynthesis and signaling under drought conditions. Additionally, Zhang et al. (2017) demonstrated that GABA could induce the expression of key stress transcription factors in maize, providing further evidence for its conserved regulatory role across monocots and dicots.

4.5 Potential of CaMBD-truncated OsGAD lines for agronomic improvement

The dual-editing strategy employed in our study offers a powerful approach to pyramid metabolic traits without transgenic constructs. Combining OsGAD1ΔC and OsGAD3ΔC in a hybrid line captured tissue-specific expression advantages while avoiding possible gene silencing or overexpression penalties. The enhanced survival, improved GABA profiles, and gene expression plasticity suggest that similar approaches could be extended to other gene families involved in secondary metabolism or signaling.

While the findings of this research are encouraging, one limitation must be acknowledged. The current evaluations were conducted exclusively at the seedling stage under controlled laboratory conditions. To

fully assess the effectiveness of the genome-edited lines, it will be necessary to conduct field trials and evaluate plant performance across developmental stages under diverse environmental conditions. This will be essential to determine the long-term agronomic potential of the genome-edited lines.

Chapter 5: Conclusion

In this study, we investigated whether targeted genetic modifications in the glutamate decarboxylase genes *OsGAD1* and *OsGAD3*, key regulators of γ-aminobutyric acid (GABA) biosynthesis, could enhance abiotic stress tolerance in rice. Using CRISPR/Cas9-based genome editing, physiological assays, biochemical profiling, and transcriptome analyses, this work provided new insights into the functional role of GABA and GAD enzymes in stress adaptation.

5.1 Genome-editing of *OsGAD1* enhanced GABA biosynthesis

CRISPR/Cas9 genome editing was employed to truncate the calmodulin-binding domain (CaMBD) of *OsGAD1*, a region known to exert autoinhibitory control over GAD enzymatic activity. The resulting genome-edited line, *OsGAD1ΔC #5*, exhibited significantly higher levels of GABA under normal growth conditions. This indicates that removal of the CaMBD effectively abolished the enzyme's dependency on calcium-mediated activation. These findings suggested the critical regulatory function of the CaMBD and demonstrate its potential as a precise molecular target for enhancing metabolic flux through the GABA shunt. The constitutive activation of GAD achieved through CaMBD truncation offers a promising strategy for strengthening GABA-mediated metabolic and stress response pathways in rice.

5.2 Hybrid line exhibited additive effects of dual CaMBD truncation of OsGAD1 and OsGAD3

To assess the combined impact of *OsGAD1* and *OsGAD3* activation, *OsGAD1ΔC #5* was crossed with *OsGAD3ΔC #8* to develop Hybrid #78, which inherited both truncated alleles. Hybrid #78 demonstrated consistently higher GABA accumulation than either parent, confirming a synergistic enhancement of GABA biosynthesis when both GAD enzymes were activated.

5.3 Enhanced physiological, biochemical, and molecular response under abiotic stress

Under multiple abiotic stress conditions, including drought, salinity, cold, and flooding, the genome-edited rice lines exhibited substantial physiological improvements compared to the wild-type, with the most pronounced effects observed in the hybrid line, Hybrid #78. This line consistently maintained significantly higher survival rates, with 83% survival under both drought and flooding conditions, 33% under salinity, and 25% under cold stress. In contrast, the survival rates of the wild-type and single-edited lines were markedly lower, highlighting the enhanced resilience conferred by the dual CaMBD truncation in Hybrid #78.

In addition to improved survival, Hybrid #78 also exhibited reduced stress-induced biomass loss, suggesting better maintenance of growth and water retention under adverse conditions. This was further

supported by DAB staining, which revealed substantially lower hydrogen peroxide accumulation in the hybrid line compared to the wild-type, indicating a more effective oxidative stress response and enhanced reactive oxygen species (ROS) detoxification capacity.

RT-qPCR analysis demonstrated a strong upregulation of both *OsGAD1* and *OsGAD3* transcripts in Hybrid #78 under stress. This suggests that CaMBD truncation not only releases enzymatic activity from calcium/calmodulin regulation but may also influence gene expression, possibly through feedback mechanisms involving GABA or associated stress signaling pathways.

Moreover, GC-MS analysis of free amino acid profiles showed significantly elevated concentrations of stress-associated amino acids in the hybrid line, particularly proline, glutamate, alanine, and valine. These amino acids play critical roles in osmotic adjustment, nitrogen storage, and stabilization of cellular structures during stress. The coordinated increase in these metabolites, alongside elevated GABA levels, indicates that the dual GAD modification promotes a broader reprogramming of amino acid metabolism. This metabolic adjustment likely contributes to improved osmoprotection, cellular integrity, and overall stress tolerance.

5.4 Transcriptional reprogramming in the hybrid line reflected a primed defense state

Transcriptome analysis under control conditions revealed substantial reprogramming in Hybrid #78 compared with WT Ni. The hybrid showed the greatest number of uniquely expressed genes, higher expression variability, and significant enrichment of stress-related KEGG pathways, including phenylpropanoid biosynthesis, nitrogen metabolism, hormone signal transduction, and amino acid metabolism. Gene ontology analysis further highlighted changes in molecular function and catalytic activity, reflecting transcriptional plasticity. In addition, RT-qPCR confirmed the constitutive upregulation of key abiotic stress-related genes (*OsNAC3, OsDST, OsHAK5, OsDREB2B, OsSAP1, OsADC1,* and *HSP70*), suggesting that Hybrid #78 operates in a transcriptionally primed state even before stress exposure. This transcriptional readiness likely contributes to its rapid and effective stress response.

5.5 Role of genome-edited OsGAD1 and OsGAD3 in GABA-mediated stress tolerance in rice

Collectively, this study demonstrates that CRISPR/Cas9-mediated truncation of the CaMBD domains in *OsGAD1* and *OsGAD3* enhances rice abiotic stress tolerance through a coordinated regulatory mechanism centered on GABA metabolism (Fig. 19). The hybrid line integrating both edits displayed enhanced GABA accumulation, increased expression of stress-responsive genes, metabolic adjustments, and superior physiological responses under a range of abiotic stresses. These outcomes establish a direct link between genetic modifications of GAD enzymes and improved plant stress resilience.

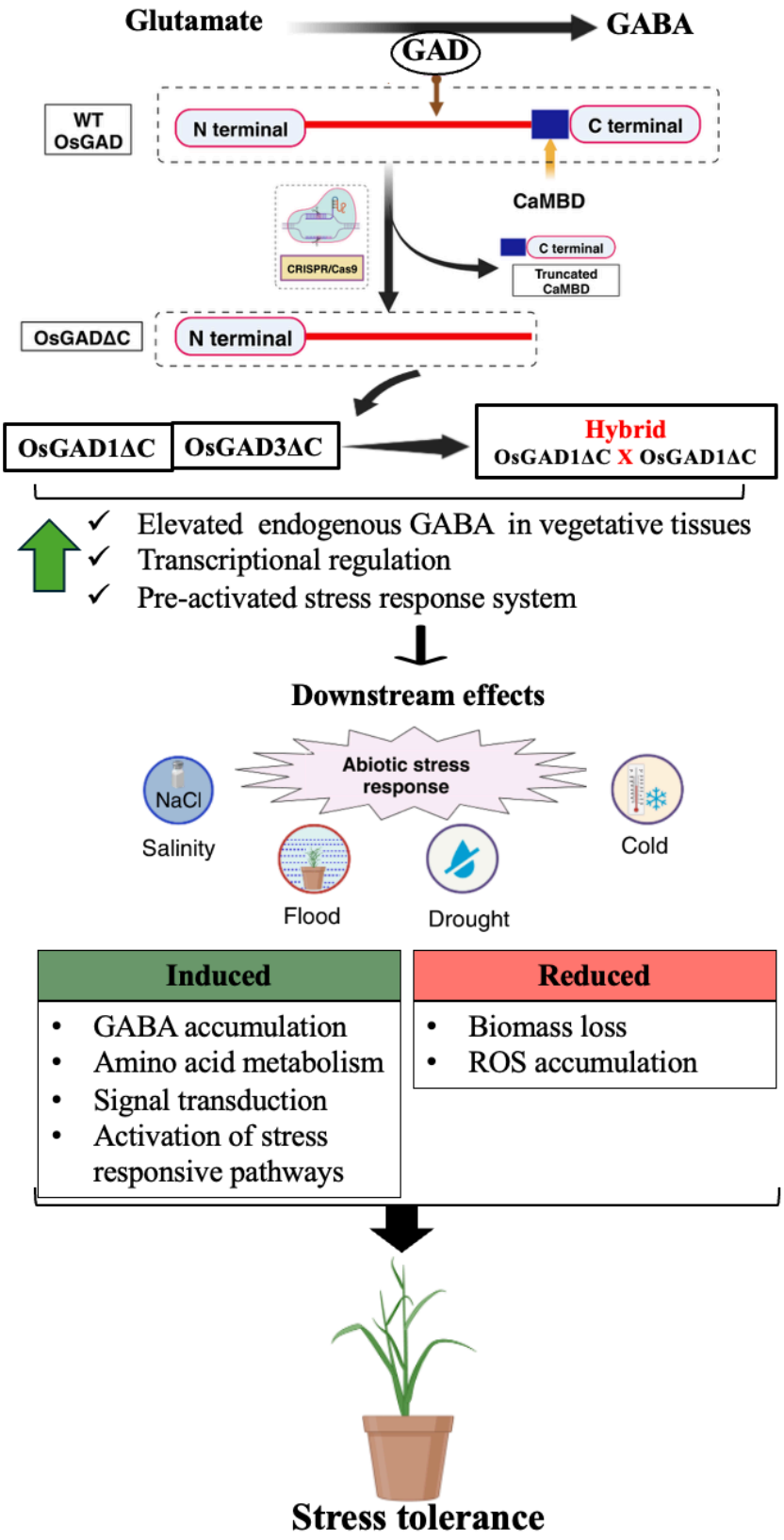

Fig. 19 Overview of OsGAD-CaMBD truncation-mediated stress tolerance in rice. Schematic illustration of the downstream effects following CRISPR/Cas9-mediated truncation of the calmodulin-binding domain (CaMBD) in OsGAD1 and OsGAD3, leading to elevated GABA accumulation, activation of stress-responsive pathways, and enhanced tolerance to salinity, drought, cold, and flooding in rice.

Reference

Abdullah, Wani, K. I., Naeem, M., & Aftab, T. (2025). From Neurotransmitter to Plant Protector: The Intricate World of GABA Signaling and its Diverse Functions in Stress Mitigation. *Journal of Plant Growth Regulation*, *44*(2), 403–418. https://doi.org/10.1007/s00344-024-11470-0

Ahmed, M., Fayyaz-ul-Hassan, & Ahmad, S. (2017). Climate Variability Impact on Rice Production: Adaptation and Mitigation Strategies. In M. Ahmed & C. O. Stockle (Eds.), *Quantification of Climate Variability, Adaptation and Mitigation for Agricultural Sustainability* (pp. 91–111). Springer International Publishing. https://doi.org/10.1007/978-3-319-32059-5_5

Akama, K., Akihiro, T., Kitagawa, M., & Takaiwa, F. (2001). Rice (Oryza sativa) contains a novel isoform of glutamate decarboxylase that lacks an authentic calmodulin-binding domain at the C-terminus. *Biochimica Et Biophysica Acta*, *1522*(3), 143–150. https://doi.org/10.1016/s0167-4781(01)00324-4

Akama, K., Akter, N., Endo, H., Kanesaki, M., Endo, M., & Toki, S. (2020). An In Vivo Targeted Deletion of the Calmodulin-Binding Domain from Rice Glutamate Decarboxylase 3 (OsGAD3) Increases γ-Aminobutyric Acid Content in Grains. *Rice*, *13*(1), 20. https://doi.org/10.1186/s12284-020-00380-w

Akama, K., Kanetou, J., Shimosaki, S., Kawakami, K., Tsuchikura, S., & Takaiwa, F. (2009). Seed-specific expression of truncated OsGAD2 produces GABA-enriched rice grains that influence a decrease in blood pressure in spontaneously hypertensive rats. *Transgenic Research*, *18*(6), 865–876. https://doi.org/10.1007/s11248-009-9272-1

Akama, K., & Takaiwa, F. (2007). C-terminal extension of rice glutamate decarboxylase (OsGAD2) functions as an autoinhibitory domain and overexpression of a truncated mutant results in the accumulation of extremely high levels of GABA in plant cells. *Journal of Experimental Botany*, *58*(10), 2699–2707. https://doi.org/10.1093/jxb/erm120

Akter, N., Kulsum, U., Moniruzzaman, M., Yasuda, N., & Akama, K. (2024). Truncation of the calmodulin binding domain in rice glutamate decarboxylase 4 (OsGAD4) leads to accumulation of γ-aminobutyric acid and confers abiotic stress tolerance in rice seedlings. *Molecular Breeding: New Strategies in Plant Improvement*, *44*(3), 21. https://doi.org/10.1007/s11032-024-01460-1

Amin, M. W., Aryan, S., Habibi, N., Kakar, K., & Zahid, T. (2022). Elucidation of photosynthesis and yield performance of rice (Oryza sativa L.) under drought stress conditions. *Plant Physiology Reports*, *27*(1), 143–151. https://doi.org/10.1007/s40502-021-00613-0

Anders, S., & Huber, W. (2010). Differential expression analysis for sequence count data. *Genome Biology*, *11*(10), R106. https://doi.org/10.1186/gb-2010-11-10-r106

Ansari, M. I., Jalil, S. U., Ansari, S. A., & Hasanuzzaman, M. (2021). GABA shunt: A key-player in mitigation of ROS during stress. *Plant Growth Regulation*, *94*(2), 131–149. https://doi.org/10.1007/s10725-021-00710-y

Anzano, A., Bonanomi, G., Mazzoleni, S., & Lanzotti, V. (2022). Plant metabolomics in biotic and abiotic stress: A critical overview. *Phytochemistry Reviews*, *21*(2), 503–524. https://doi.org/10.1007/s11101-021-09786-w

Arazi, T., Baum, G., Snedden, W. A., Shelp, B. J., & Fromm, H. (1995). Molecular and biochemical analysis of calmodulin interactions with the calmodulin-binding domain of plant glutamate decarboxylase. *Plant Physiology*, *108*(2), 551–561. https://doi.org/10.1104/pp.108.2.551

Aslam, M. M., Raja, S., Saeed, S., Farhat, F., Tariq, A., Rai, H. M., Javaid, A., Shahzadi, I., Asim, M., Zulfiqar, S., Siddiqui, M. A., & Iqbal, R. (2022). Revisiting the Crucial Role of Reactive Oxygen Species and Antioxidant Defense in Plant Under Abiotic Stress. In T. Aftab & K. R. Hakeem (Eds.), *Antioxidant Defense in Plants: Molecular Basis of Regulation* (pp. 397–419). Springer Nature. https://doi.org/10.1007/978-981-16-7981-0_18

Aswathi, K. P. R., Jisha, K. C., Veena, M., Sen, A., Sarath, N. G., & Puthur, J. T. (2025). GABA Priming Induced Modulations in the Redox Homeostasis of Plants under Osmotic Stress. In *GABA in Plants* (pp. 173–187). John Wiley & Sons, Ltd. https://doi.org/10.1002/9781394217786.ch10

Bahariah, B., Masani, M. Y. A., Rasid, O. A., & Parveez, G. K. A. (2021). Multiplex CRISPR/Cas9-mediated genome editing of the FAD2 gene in rice: A model genome editing system for oil palm. *Journal of Genetic Engineering & Biotechnology*, *19*, 86. https://doi.org/10.1186/s43141-021-00185-4

Bartoli, C. G., Buet, A., Gergoff Grozeff, G., Galatro, A., & Simontacchi, M. (2017). Ascorbate-Glutathione Cycle and Abiotic Stress Tolerance in Plants. In M. A. Hossain, S. Munné-Bosch, D. J. Burritt, P. Diaz-Vivancos, M. Fujita, & A. Lorence (Eds.), *Ascorbic Acid in Plant Growth, Development and Stress Tolerance* (pp. 177–200). Springer International Publishing. https://doi.org/10.1007/978-3-319-74057-7_7

Baum, G., Chen, Y., Arazi, T., Takatsuji, H., & Fromm, H. (1993). A plant glutamate decarboxylase containing a calmodulin binding domain. Cloning, sequence, and functional analysis. *Journal of Biological Chemistry*, *268*(26), 19610–19617. https://doi.org/10.1016/S0021-9258(19)36560-3

Baum, G., Lev-Yadun, S., Fridmann, Y., Arazi, T., Katsnelson, H., Zik, M., & Fromm, H. (1996). Calmodulin binding to glutamate decarboxylase is required for regulation of glutamate and GABA metabolism and normal development in plants. *The EMBO Journal*, *15*(12), 2988–2996.

Bhattacharjee, S., Bhowmick, R., Kant, L., & Paul, K. (2023). Strategic transgene-free approaches of CRISPR-based genome editing in plants. *Molecular Genetics and Genomics*, *298*(3), 507–520. https://doi.org/10.1007/s00438-023-01998-3

Bouché, N., & Fromm, H. (2004). GABA in plants: Just a metabolite? *Trends in Plant Science*, *9*(3), 110–115. https://doi.org/10.1016/j.tplants.2004.01.006

Chen, B.-X., Fu, H., Gao, J.-D., Zhang, Y.-X., Huang, W.-J., Chen, Z.-J., Qi-Zhang, Yan, S.-J., & Liu, J. (2022). Identification of Metabolomic Biomarkers of Seed Vigor and Aging in Hybrid Rice. *Rice*, *15*(1), 7. https://doi.org/10.1186/s12284-022-00552-w

Chen, J., Miao, Z., Kong, D., Zhang, A., Wang, F., Liu, G., Yu, X., Luo, L., & Liu, Y. (2024). Application of CRISPR/Cas9 Technology in Rice Germplasm Innovation and Genetic Improvement. *Genes*, *15*(11), Article 11. https://doi.org/10.3390/genes15111492

Chen, W., Meng, C., Ji, J., Li, M.-H., Zhang, X., Wu, Y., Xie, T., Du, C., Sun, J., Jiang, Z., & Shi, S. (2020). Exogenous GABA promotes adaptation and growth by altering the carbon and nitrogen metabolic flux in poplar seedlings under low nitrogen conditions. *Tree Physiology*, *40*(12), 1744–1761. https://doi.org/10.1093/treephys/tpaa101

Dabravolski, S. A., & Isayenkov, S. V. (2023). The Role of the γ-Aminobutyric Acid (GABA) in Plant Salt Stress Tolerance. *Horticulturae*, *9*(2), Article 2. https://doi.org/10.3390/horticulturae9020230

Davis, T. N., Urdea, M. S., Masiarz, F. R., & Thorner, J. (1986). Isolation of the yeast calmodulin gene: Calmodulin is an essential protein. *Cell*, *47*(3), 423–431. https://doi.org/10.1016/0092-8674(86)90599-4

Fait, A., Nesi, A. N., Angelovici, R., Lehmann, M., Pham, P. A., Song, L., Haslam, R. P., Napier, J. A., Galili, G., & Fernie, A. R. (2011). Targeted Enhancement of Glutamate-to-γ-Aminobutyrate Conversion in Arabidopsis Seeds Affects Carbon-Nitrogen Balance and Storage Reserves in a Development-Dependent Manner. *Plant Physiology*, *157*(3), 1026–1042. https://doi.org/10.1104/pp.111.179986

FOOD AND AGRICULTURE 2023: STATISTICAL YEARBOOK. https://doi.org/10.4060/CC8166EN

Fromm, H. (2020). GABA signaling in plants: Targeting the missing pieces of the puzzle. *Journal of Experimental Botany*, *71*(20), 6238–6245. https://doi.org/10.1093/jxb/eraa358

Galon, Y., Nave, R., Boyce, J. M., Nachmias, D., Knight, M. R., & Fromm, H. (2008). Calmodulin-binding transcription activator (CAMTA) 3 mediates biotic defense responses in Arabidopsis. *FEBS Letters*, *582*(6), 943–948. https://doi.org/10.1016/j.febslet.2008.02.037

García, P., Singh, S., & Graciet, E. (2024). New Insights into the Connections between Flooding/Hypoxia Response and Plant Defenses against Pathogens. *Plants*, *13*(16), Article 16. https://doi.org/10.3390/plants13162176

Gu, Z., & Han, B. (2024). Unlocking the mystery of heterosis opens the era of intelligent rice breeding. *Plant Physiology*, *196*(2), 735–744. https://doi.org/10.1093/plphys/kiae385

Guo, Z., Dzinyela, R., Yang, L., & Hwarari, D. (2024). bZIP Transcription Factors: Structure, Modification, Abiotic Stress Responses and Application in Plant Improvement. *Plants*, *13*(15), Article 15. https://doi.org/10.3390/plants13152058

Haque, M. A., Rafii, M. Y., Yusoff, M. M., Ali, N. S., Yusuff, O., Arolu, F., & Anisuzzaman, M. (2023). Flooding tolerance in Rice: Adaptive mechanism and marker-assisted selection breeding approaches. *Molecular Biology Reports*, *50*(3), 2795–2812. https://doi.org/10.1007/s11033-022-07853-9

Heinemann, B., & Hildebrandt, T. M. (2021). The role of amino acid metabolism in signaling and metabolic adaptation to stress-induced energy deficiency in plants. *Journal of Experimental Botany*, *72*(13), 4634–4645. https://doi.org/10.1093/jxb/erab182

Hood, E. E., Gelvin, S. B., Melchers, L. S., & Hoekema, A. (1993). NewAgrobacterium helper plasmids for gene transfer to plants. *Transgenic Research*, *2*(4), 208–218. https://doi.org/10.1007/BF01977351

Hu, Y., Huang, X., Xiao, Q., Wu, X., Tian, Q., Ma, W., Shoaib, N., Liu, Y., Zhao, H., Feng, Z., & Yu, G. (2024). Advances in Plant GABA Research: Biological Functions, Synthesis Mechanisms and Regulatory Pathways. *Plants*, *13*(20), Article 20. https://doi.org/10.3390/plants13202891

Huang, L., Li, Q., Zhang, C., Chu, R., Gu, Z., Tan, H., Zhao, D., Fan, X., & Liu, Q. (2020). Creating novel Wx alleles with fine-tuned amylose levels and improved grain quality in rice by promoter editing using CRISPR/Cas9 system. *Plant Biotechnology Journal*, *18*(11), 2164–2166. https://doi.org/10.1111/pbi.13391

International Rice Genome Sequencing Project. (2005). The map-based sequence of the rice genome. *Nature*, *436*(7052), 793–800. https://doi.org/10.1038/nature03895

Islam, S. N. ul, Kouser, S., Hassan, P., Asgher, M., Shah, A. A., & Khan, N. A. (2024). Gamma-aminobutyric acid interactions with phytohormones and its role in modulating abiotic and biotic stress in plants. *Stress Biology*, *4*(1), 36. https://doi.org/10.1007/s44154-024-00180-y

Jain, M., Nagar, P., Goel, P., Singh, A. K., Kumari, S., & Mustafiz, A. (2018). Second Messengers: Central Regulators in Plant Abiotic Stress Response. In S. M. Zargar & M. Y. Zargar (Eds.), *Abiotic Stress-Mediated Sensing and Signaling in Plants: An Omics Perspective* (pp. 47–94). Springer. https://doi.org/10.1007/978-981-10-7479-0_2

Ji, J., Shi, Z., Xie, T., Zhang, X., Chen, W., Du, C., Sun, J., Yue, J., Zhao, X., Jiang, Z., & Shi, S. (2020). Responses of GABA shunt coupled with carbon and nitrogen metabolism in poplar under NaCl and CdCl2 stresses. *Ecotoxicology and Environmental Safety*, *193*, 110322. https://doi.org/10.1016/j.ecoenv.2020.110322

Kawahara, Y., Oono, Y., Wakimoto, H., Ogata, J., Kanamori, H., Sasaki, H., Mori, S., Matsumoto, T., & Itoh, T. (2016). TENOR: Database for Comprehensive mRNA-Seq Experiments in Rice. *Plant & Cell Physiology*, *57*(1), e7. https://doi.org/10.1093/pcp/pcv179

Kim, M. C., Chung, W. S., Yun, D.-J., & Cho, M. J. (2009). Calcium and calmodulin-mediated regulation of gene expression in plants. *Molecular Plant*, *2*(1), 13–21. https://doi.org/10.1093/mp/ssn091

Komatsu, S., Egishi, M., & Ohno, T. (2024). The Changes of Amino-Acid Metabolism between Wheat and Rice during Early Growth under Flooding Stress. *International Journal of Molecular Sciences*, *25*(10), 5229. https://doi.org/10.3390/ijms25105229

Kothari, K. S., Dansana, P. K., Giri, J., & Tyagi, A. K. (2016). Rice Stress Associated Protein 1 (OsSAP1) Interacts with Aminotransferase (OsAMTR1) and Pathogenesis-Related 1a Protein (OsSCP) and Regulates Abiotic Stress Responses. *Frontiers in Plant Science*, *7*, 1057. https://doi.org/10.3389/fpls.2016.01057

Kowaka, E., Shimajiri, Y., Kawakami, K., Tongu, M., & Akama, K. (2015). Field trial of GABA-fortified rice plants and oral administration of milled rice in spontaneously hypertensive rats. *Transgenic Research*, *24*(3), 561–569. https://doi.org/10.1007/s11248-014-9859-z

Kreps, J. A., Wu, Y., Chang, H.-S., Zhu, T., Wang, X., & Harper, J. F. (2002). Transcriptome Changes for Arabidopsis in Response to Salt, Osmotic, and Cold Stress,. *Plant Physiology*, *130*(4), 2129–2141. https://doi.org/10.1104/pp.008532

Kruthika, N., & Jithesh, M. N. (2023). Response of rice to salinity risk- from a physiological outlook to laboratory focussed experimental approach. *Cereal Research Communications*, *51*(1), 29–43. https://doi.org/10.1007/s42976-022-00291-0

Kumar, K., Raina, S. K., & Sultan, S. M. (2020). Arabidopsis MAPK signaling pathways and their cross talks in abiotic stress response. *Journal of Plant Biochemistry and Biotechnology*, *29*(4), 700–714. https://doi.org/10.1007/s13562-020-00596-3

Kumar, P., Paul, D., Jhajhriya, S., Kumar, R., Dutta, S., Siwach, P., & Das, S. (2024). Understanding heat-shock proteins' abundance and pivotal function under multiple abiotic stresses. *Journal of Plant Biochemistry and Biotechnology*, *33*(4), 492–513. https://doi.org/10.1007/s13562-024-00932-x

Lata, C., & Prasad, M. (2011). Role of DREBs in regulation of abiotic stress responses in plants. *Journal of Experimental Botany*, *62*(14), 4731–4748. https://doi.org/10.1093/jxb/err210

Li, L., Dou, N., Zhang, H., & Wu, C. (2021). The versatile GABA in plants. *Plant Signaling & Behavior*, *16*(3), 1862565. https://doi.org/10.1080/15592324.2020.1862565

Liao, Y., Smyth, G. K., & Shi, W. (2014). featureCounts: An efficient general purpose program for assigning sequence reads to genomic features. *Bioinformatics (Oxford, England)*, *30*(7), 923–930. https://doi.org/10.1093/bioinformatics/btt656

Liu, C., Wang, H., Zhang, X., Ma, F., Guo, T., & Li, C. (2021). Activation of the ABA Signal Pathway Mediated by GABA Improves the Drought Resistance of Apple Seedlings. *International Journal of Molecular Sciences*, *22*(23), 12676. https://doi.org/10.3390/ijms222312676

Liu, M., Gao, J., Wang, N., Yan, Y., Zhang, G., Chen, Y., & Zhang, M. (2024). Effects of exogenous GABA on physiological characteristics of licorice seedlings under saline-alkali stress. *Plant Stress*, *11*, 100364. https://doi.org/10.1016/j.stress.2024.100364

Livak, K. J., & Schmittgen, T. D. (2001). Analysis of relative gene expression data using real-time quantitative PCR and the 2(-Delta Delta C(T)) Method. *Methods (San Diego, Calif.)*, *25*(4), 402–408. https://doi.org/10.1006/meth.2001.1262

Lu, J., & Xia, S. (2025). Metabolomics and Plant Defense. *Metabolites*, *15*(3), Article 3. https://doi.org/10.3390/metabo15030171

Luo, J., Amin, B., Wu, B., Wu, B., Huang, W., Salmen, S. H., & Fang, Z. (2024). Blocking of awn development-related gene OsGAD1 coordinately boosts yield and quality of Kam Sweet Rice. *Physiologia Plantarum*, *176*(2), e14229. https://doi.org/10.1111/ppl.14229

Ma, R., Liu, B., Geng, X., Ding, X., Yan, N., Sun, X., Wang, W., Sun, X., & Zheng, C. (2023). Biological Function and Stress Response Mechanism of MYB Transcription Factor Family Genes. *Journal of Plant Growth Regulation*, *42*(1), 83–95. https://doi.org/10.1007/s00344-021-10557-2

Majeed, A., & Muhammad, Z. (2019). Salinity: A Major Agricultural Problem—Causes, Impacts on Crop Productivity and Management Strategies. In M. Hasanuzzaman, K. R. Hakeem, K. Nahar, & H. F. Alharby (Eds.), *Plant Abiotic Stress Tolerance: Agronomic, Molecular and Biotechnological Approaches* (pp. 83–99). Springer International Publishing. https://doi.org/10.1007/978-3-030-06118-0_3

Martins, C. P. S., Fernandes, D., Guimarães, V. M., Du, D., Silva, D. C., Almeida, A.-A. F., Jr, F. G. G., Otoni, W. C., & Costa, M. G. C. (2022). Comprehensive analysis of the GALACTINOL SYNTHASE (GolS) gene family in citrus and the function of CsGolS6 in stress tolerance. *PLOS ONE*, *17*(9), e0274791. https://doi.org/10.1371/journal.pone.0274791

Matsukura, S., Mizoi, J., Yoshida, T., Todaka, D., Ito, Y., Maruyama, K., Shinozaki, K., & Yamaguchi-Shinozaki, K. (2010). Comprehensive analysis of rice DREB2-type genes that encode transcription factors involved in the expression of abiotic stress-responsive genes. *Molecular Genetics and Genomics: MGG*, *283*(2), 185–196. https://doi.org/10.1007/s00438-009-0506-y

McCormack, E., Tsai, Y.-C., & Braam, J. (2005). Handling calcium signaling: Arabidopsis CaMs and CMLs. *Trends in Plant Science*, *10*(8), 383–389. https://doi.org/10.1016/j.tplants.2005.07.001

McLean, M. D., Yevtushenko, D. P., Deschene, A., Van Cauwenberghe, O. R., Makhmoudova, A., Potter, J. W., Bown, A. W., & Shelp, B. J. (2003). Overexpression of glutamate decarboxylase in transgenic tobacco plants confers resistance to the northern root-knot nematode. *Molecular Breeding*, *11*(4), 277–285. https://doi.org/10.1023/A:1023483106582

Melotto, M., Zhang, L., Oblessuc, P. R., & He, S. Y. (2017). Stomatal Defense a Decade Later. *Plant Physiology*, *174*(2), 561–571. https://doi.org/10.1104/pp.16.01853

Michaeli, S., & Fromm, H. (2015). Closing the Loop on the GABA Shunt in Plants: Are GABA metabolism and signaling entwined? *Frontiers in Plant Science*, *6*. https://doi.org/10.3389/fpls.2015.00419

Mikami, M., Toki, S., & Endo, M. (2015). Comparison of CRISPR/Cas9 expression constructs for efficient targeted mutagenesis in rice. *Plant Molecular Biology*, *88*(6), 561–572. https://doi.org/10.1007/s11103-015-0342-x

Mortazavi, A., Williams, B. A., McCue, K., Schaeffer, L., & Wold, B. (2008). Mapping and quantifying mammalian transcriptomes by RNA-Seq. *Nature Methods*, *5*(7), 621–628. https://doi.org/10.1038/nmeth.1226

Murashige, T., & Skoog, F. (1962). A Revised Medium for Rapid Growth and Bio Assays with Tobacco Tissue Cultures. *Physiologia Plantarum*, *15*(3), 473–497. https://doi.org/10.1111/j.1399-3054.1962.tb08052.x

Murray, M. G., & Thompson, W. F. (1980). Rapid isolation of high molecular weight plant DNA. *Nucleic Acids Research*, *8*(19), 4321–4325. https://doi.org/10.1093/nar/8.19.4321

Nuruzzaman, M., Sharoni, A. M., & Kikuchi, S. (2013). Roles of NAC transcription factors in the regulation of biotic and abiotic stress responses in plants. *Frontiers in Microbiology*, *4*. https://doi.org/10.3389/fmicb.2013.00248

Ozawa, K. (2009). Establishment of a high efficiency Agrobacterium-mediated transformation system of rice (Oryza sativa L.). *Plant Science: An International Journal of Experimental Plant Biology*, *176*(4), 522–527. https://doi.org/10.1016/j.plantsci.2009.01.013

Paliwal, A., Tiwari, H., Singh, M. K., Nigam, A. K., Gour, J. K., Kumar, R., & Kumar, D. (2021). Compatible Solute Engineering: An Approach for Plant Growth Under Climate Change. In S. H. Wani, M. P. Gangola, & B. R. Ramadoss (Eds.), *Compatible Solutes Engineering for Crop Plants Facing Climate Change* (pp. 241–257). Springer International Publishing. https://doi.org/10.1007/978-3-030-80674-3_11

Pandey, P., Irulappan, V., Bagavathiannan, M. V., & Senthil-Kumar, M. (2017). Impact of Combined Abiotic and Biotic Stresses on Plant Growth and Avenues for Crop Improvement by Exploiting Physio-morphological Traits. *Frontiers in Plant Science*, *8*. https://doi.org/10.3389/fpls.2017.00537

Pandita, D. (2023). Transgenic Approaches for Stress Tolerance in Crops. In M. Hasanuzzaman (Ed.), *Climate-Resilient Agriculture, Vol 2: Agro-Biotechnological Advancement for Crop Production* (pp. 793–818). Springer International Publishing. https://doi.org/10.1007/978-3-031-37428-9_35

Parkhomchuk, D., Borodina, T., Amstislavskiy, V., Banaru, M., Hallen, L., Krobitsch, S., Lehrach, H., & Soldatov, A. (2009). Transcriptome analysis by strand-specific sequencing of complementary DNA. *Nucleic Acids Research*, *37*(18), e123. https://doi.org/10.1093/nar/gkp596

Peremarti, A., Bassie, L., Zhu, C., Christou, P., & Capell, T. (2010). Molecular characterization of the Arginine decarboxylase gene family in rice. *Transgenic Research*, *19*(5), 785–797. https://doi.org/10.1007/s11248-009-9354-0

Phukan, U. J., Jeena, G. S., & Shukla, R. K. (2016). WRKY Transcription Factors: Molecular Regulation and Stress Responses in Plants. *Frontiers in Plant Science*, *7*, 760. https://doi.org/10.3389/fpls.2016.00760

Pingali, P. L. (2012). Green Revolution: Impacts, limits, and the path ahead. *Proceedings of the National Academy of Sciences*, *109*(31), 12302–12308. https://doi.org/10.1073/pnas.0912953109

Qian, Z., Lu, L., Zihan, W., Qianyue, B., Chungang, Z., Shuheng, Z., Jiali, P., Jiaxin, Y., Shuang, Z., & Jian, W. (2024). Gamma-aminobutyric acid (GABA) improves salinity stress tolerance in soybean seedlings by modulating their mineral nutrition, osmolyte contents, and ascorbate-glutathione cycle. *BMC Plant Biology*, *24*(1), 365. https://doi.org/10.1186/s12870-024-05023-6

Radha, B., Sunitha, N. C., Sah, R. P., T. P., M. A., Krishna, G. K., Umesh, D. K., Thomas, S., Anilkumar, C., Upadhyay, S., Kumar, A., Ch L. N., M., S., B., Marndi, B. C., & Siddique, K. H. M. (2023). Physiological and molecular implications of multiple abiotic stresses on yield and quality of rice. *Frontiers in Plant Science*, *13*. https://doi.org/10.3389/fpls.2022.996514

Rahman, M. M., Ibrahim, Md., Muktadir, M. A., Sadeque, A., Abdel Latef, A. A. H., & Ashrafuzzaman, M. (2022). Rice: Role and Responses Under Abiotic Stress. In A. A. H. Abdel Latef (Ed.), *Sustainable Remedies for Abiotic Stress in Cereals* (pp. 125–147). Springer Nature. https://doi.org/10.1007/978-981-19-5121-3_6

Rai, V. K. (2002). Role of Amino Acids in Plant Responses to Stresses. *Biologia Plantarum*, *45*(4), 481–487. https://doi.org/10.1023/A:1022308229759

Ramesh, S. A., Kamran, M., Sullivan, W., Chirkova, L., Okamoto, M., Degryse, F., McLaughlin, M., Gilliham, M., & Tyerman, S. D. (2018). Aluminum-Activated Malate Transporters Can Facilitate GABA Transport. *The Plant Cell*, *30*(5), 1147–1164. https://doi.org/10.1105/tpc.17.00864

Ray, D. K., Mueller, N. D., West, P. C., & Foley, J. A. (2013). Yield Trends Are Insufficient to Double Global Crop Production by 2050. *PLOS ONE*, *8*(6), e66428. https://doi.org/10.1371/journal.pone.0066428

Renault, H., Roussel, V., El Amrani, A., Arzel, M., Renault, D., Bouchereau, A., & Deleu, C. (2010). The Arabidopsis pop2-1 mutant reveals the involvement of GABA transaminase in salt stress tolerance. *BMC Plant Biology*, *10*, 20. https://doi.org/10.1186/1471-2229-10-20

Rice Production Course. (n.d.). Retrieved February 8, 2025, from http://www.knowledgebank.irri.org/ericeproduction/bodydefault.htm#Importance_of_Rice.htm

Rossi, S., Chapman, C., Yuan, B., & Huang, B. (2021). Improved heat tolerance in creeping bentgrass by γ-aminobutyric acid, proline, and inorganic nitrogen associated with differential regulation of amino acid metabolism. *Plant Growth Regulation*, *93*(2), 231–242. https://doi.org/10.1007/s10725-020-00681-6

Rajani , MS., Bedair, M. F., Li, H., & Duff, S. M. G. (2021). Phenotypic effects from the expression of a deregulated AtGAD1 transgene and GABA pathway suppression mutants in maize. *PLoS ONE*, *16*(12), e0259365. https://doi.org/10.1371/journal.pone.0259365

Sabar, M., Mustafa, S. E., Ijaz, M., Khan, R. A. R., Shahzadi, F., Saher, H., Javed, H. M., Zafar, S. A., Saleem, M. U., Siddique, S., & Sabir, A. M. (2024). Rice Breeding for Yield Improvement through Traditional and Modern Genetic Tools. *European Journal of Ecology, Biology and Agriculture*, *1*(1), Article 1. https://doi.org/10.59324/ejeba.2024.1(1).02

Sahil, Keshan, R., Patra, A., Mehta, S., Abdelmotelb, K. F., Lavale, S. A., Chaudhary, M., Aggarwal, S. K., & Chattopadhyay, A. (2021). Expression and Regulation of Stress-Responsive Genes in Plants Under Harsh Environmental Conditions. In A. Husen (Ed.), *Harsh Environment and Plant Resilience: Molecular and Functional Aspects* (pp. 25–44). Springer International Publishing. https://doi.org/10.1007/978-3-030-65912-7_2

Santosh Kumar, V. V., Verma, R. K., Yadav, S. K., Yadav, P., Watts, A., Rao, M. V., & Chinnusamy, V. (2020). CRISPR-Cas9 mediated genome editing of drought and salt tolerance (OsDST) gene in indica mega rice cultivar MTU1010. *Physiology and Molecular Biology of Plants*, *26*(6), 1099–1110. https://doi.org/10.1007/s12298-020-00819-w

Sarma, B., Kashtoh, H., Lama Tamang, T., Bhattacharyya, P. N., Mohanta, Y. K., & Baek, K.-H. (2023). Abiotic Stress in Rice: Visiting the Physiological Response and Its Tolerance Mechanisms. *Plants*, *12*(23), Article 23. https://doi.org/10.3390/plants12233948

Seifikalhor, M., Aliniaeifard, S., Bernard, F., Seif, M., Latifi, M., Hassani, B., Didaran, F., Bosacchi, M., Rezadoost, H., & Li, T. (2020). γ-Aminobutyric acid confers cadmium tolerance in maize plants by concerted regulation of polyamine metabolism and antioxidant defense systems. *Scientific Reports*, *10*(1), 3356. https://doi.org/10.1038/s41598-020-59592-1

Seifikalhor, M., Aliniaeifard, S., Hassani, B., Niknam, V., & Lastochkina, O. (2019). Diverse role of γ-aminobutyric acid in dynamic plant cell responses. *Plant Cell Reports*, *38*(8), 847–867. https://doi.org/10.1007/s00299-019-02396-z

Sharma, A., Kumar, V., Shahzad, B., Ramakrishnan, M., Singh Sidhu, G. P., Bali, A. S., Handa, N., Kapoor, D., Yadav, P., Khanna, K., Bakshi, P., Rehman, A., Kohli, S. K., Khan, E. A., Parihar, R. D., Yuan, H., Thukral, A. K., Bhardwaj, R., & Zheng, B. (2020). Photosynthetic Response of Plants Under Different Abiotic Stresses: A Review. *Journal of Plant Growth Regulation*, *39*(2), 509–531. https://doi.org/10.1007/s00344-019-10018-x

Sharma, M., Tisarum, R., Kohli, R. K., Batish, D. R., Cha-um, S., & Singh, H. P. (2024). Inroads into saline-alkaline stress response in plants: Unravelling morphological, physiological, biochemical, and molecular mechanisms. *Planta*, *259*(6), 130. https://doi.org/10.1007/s00425-024-04368-4

Shelp, B. J., Aghdam, M. S., & Flaherty, E. J. (2021). γ-Aminobutyrate (GABA) Regulated Plant Defense: Mechanisms and Opportunities. *Plants*, *10*(9), Article 9. https://doi.org/10.3390/plants10091939

Signorelli, S., Tarkowski, Ł. P., O'Leary, B., Tabares-da Rosa, S., Borsani, O., & Monza, J. (2021). GABA and Proline Metabolism in Response to Stress. In D. K. Gupta & F. J. Corpas (Eds.), *Hormones and Plant Response* (pp. 291–314). Springer International Publishing. https://doi.org/10.1007/978-3-030-77477-6_12

Singh, A., & Satheeshkumar, P. K. (2024). Reactive Oxygen Species (ROS) and ROS Scavengers in Plant Abiotic Stress Response. In A. K. Mishra (Ed.), *Stress Biology in Photosynthetic Organisms: Molecular Insights and Cellular Responses* (pp. 41–63). Springer Nature. https://doi.org/10.1007/978-981-97-1883-2_3

Singh, A., Septiningsih, E. M., Balyan, H. S., Singh, N. K., & Rai, V. (2017). Genetics, Physiological Mechanisms and Breeding of Flood-Tolerant Rice (Oryza sativa L.). *Plant and Cell Physiology*, *58*(2), 185–197. https://doi.org/10.1093/pcp/pcw206

Sirohi, P., Yadav, B. S., Afzal, S., Mani, A., & Singh, N. K. (2020). Identification of drought stress-responsive genes in rice (Oryza sativa) by meta-analysis of microarray data. *Journal of Genetics*, *99*, 35.

Sita, K., & Kumar, V. (2020). Role of Gamma Amino Butyric Acid (GABA) against abiotic stress tolerance in legumes: A review. *Plant Physiology Reports*, *25*(4), 654–663. https://doi.org/10.1007/s40502-020-00553-1

Smith, S., Bubeck, D., Nelson, B., Stanek, J., & Gerke, J. (2015). Genetic Diversity and Modern Plant Breeding. In M. R. Ahuja & S. M. Jain (Eds.), *Genetic Diversity and Erosion in Plants: Indicators and Prevention* (pp. 55–88). Springer International Publishing. https://doi.org/10.1007/978-3-319-25637-5_3

Stéger, A., & Palmgren, M. (2023). Hypothesis paper: The development of a regulatory layer in P2B autoinhibited Ca2+-ATPases may have facilitated plant terrestrialization and animal multicellularization. *Plant Signaling & Behavior*, *18*(1), 2204284. https://doi.org/10.1080/15592324.2023.2204284

Sun, X., Chen, F., Yuan, L., & Mi, G. (2020). The physiological mechanism underlying root elongation in response to nitrogen deficiency in crop plants. *Planta*, *251*(4), 84. https://doi.org/10.1007/s00425-020-03376-4

Thapa, R., Tabien, R. E., Johnson, C. D., & Septiningsih, E. M. (2023). Comparative transcriptomic analysis of germinating rice seedlings to individual and combined anaerobic and cold stress. *BMC Genomics*, *24*(1), 185. https://doi.org/10.1186/s12864-023-09262-z

Thordal-Christensen, H., Zhang, Z., Wei, Y., & Collinge, D. B. (1997). Subcellular localization of H2O2 in plants. H2O2 accumulation in papillae and hypersensitive response during the barley—Powdery mildew interaction. *The Plant Journal*, *11*(6), 1187–1194. https://doi.org/10.1046/j.1365-313X.1997.11061187.x

Trobacher, C. P., Zarei, A., Liu, J., Clark, S. M., Bozzo, G. G., & Shelp, B. J. (2013). Calmodulin-dependent and calmodulin-independent glutamate decarboxylases in apple fruit. *BMC Plant Biology*, *13*, 144. https://doi.org/10.1186/1471-2229-13-144

Trovato, M., Funck, D., Forlani, G., Okumoto, S., & Amir, R. (2021). Editorial: Amino Acids in Plants: Regulation and Functions in Development and Stress Defense. *Frontiers in Plant Science*, *12*, 772810. https://doi.org/10.3389/fpls.2021.772810

Ullah, A., Ali, I., Noor, J., Zeng, F., Bawazeer, S., Eldin, S. M., Asghar, M. A., Javed, H. H., Saleem, K., Ullah, S., & Ali, H. (2023). Exogenous γ-aminobutyric acid (GABA) mitigated salinity-induced impairments in mungbean plants by regulating their nitrogen metabolism and antioxidant potential. *Frontiers in Plant Science*, *13*. https://doi.org/10.3389/fpls.2022.1081188

Usman, B., Nawaz, G., Zhao, N., Liao, S., Liu, Y., & Li, R. (2020). Precise Editing of the OsPYL9 Gene by RNA-Guided Cas9 Nuclease Confers Enhanced Drought Tolerance and Grain Yield in Rice (Oryza sativa L.) by Regulating Circadian Rhythm and Abiotic Stress Responsive Proteins. *International Journal of Molecular Sciences*, *21*(21), 7854. https://doi.org/10.3390/ijms21217854

Wang, F., Wang, C., Liu, P., Lei, C., Hao, W., Gao, Y., Liu, Y.-G., & Zhao, K. (2016). Enhanced Rice Blast Resistance by CRISPR/Cas9-Targeted Mutagenesis of the ERF Transcription Factor Gene OsERF922. *PLOS ONE*, *11*(4), e0154027. https://doi.org/10.1371/journal.pone.0154027

Wang, J., Zhang, Y., Wang, J., Khan, A., Kang, Z., Ma, Y., Zhang, J., Dang, H., Li, T., & Hu, X. (2024). SlGAD2 is the target of SlTHM27, positively regulates cold tolerance by mediating anthocyanin biosynthesis in tomato. *Horticulture Research*, *11*(6), uhae096. https://doi.org/10.1093/hr/uhae096

Wang, J., Zhang, Y., Wang, J., Ma, F., Wang, L., Zhan, X., Li, G., Hu, S., Khan, A., Dang, H., Li, T., & Hu, X. (2024). Promoting γ-aminobutyric acid accumulation to enhances saline-alkali tolerance in tomato. *Plant Physiology*, *196*(3), 2089–2104. https://doi.org/10.1093/plphys/kiae446

Wdowiak, A., Podgórska, A., & Szal, B. (2024). Calcium in plants: An important element of cell physiology and structure, signaling, and stress responses. *Acta Physiologiae Plantarum*, *46*(12), 108. https://doi.org/10.1007/s11738-024-03733-w

Wu, X., Jia, Q., Ji, S., Gong, B., Li, J., Lü, G., & Gao, H. (2020). Gamma-aminobutyric acid (GABA) alleviates salt damage in tomato by modulating Na+ uptake, the GAD gene, amino acid synthesis and reactive oxygen species metabolism. *BMC Plant Biology*, *20*(1), 465. https://doi.org/10.1186/s12870-020-02669-w

Xu, B., Long, Y., Feng, X., Zhu, X., Sai, N., Chirkova, L., Betts, A., Herrmann, J., Edwards, E. J., Okamoto, M., Hedrich, R., & Gilliham, M. (2021). GABA signalling modulates stomatal opening to enhance plant water use efficiency and drought resilience. *Nature Communications*, *12*(1), 1952. https://doi.org/10.1038/s41467-021-21694-3

Xu, G., Moeder, W., Yoshioka, K., & Shan, L. (2022). A tale of many families: Calcium channels in plant immunity. *The Plant Cell*, *34*(5), 1551–1567. https://doi.org/10.1093/plcell/koac033

Yin, M., Wang, S., Wang, Y., Wei, R., Liang, Y., Zuo, L., Huo, M., Huang, Z., Lang, J., Zhao, X., Zhang, F., Xu, J., Fu, B., Li, Z., & Wang, W. (2024). Impact of Abiotic Stress on Rice and the Role of DNA Methylation in Stress Response Mechanisms. *Plants*, *13*(19), Article 19. https://doi.org/10.3390/plants13192700

You, J., & Chan, Z. (2015). ROS Regulation During Abiotic Stress Responses in Crop Plants. *Frontiers in Plant Science*, *6*. https://doi.org/10.3389/fpls.2015.01092

Yu, G., & Chen, Y. (2008). The language of GABA in pollen tube growth and guidance. *Frontiers of Biology in China*, *3*(4), 439–442. https://doi.org/10.1007/s11515-008-0095-x

Yuan, X., Sun, H., Tang, Z., Tang, H., Zhang, H., & Huang, J. (2016). A Novel Little Membrane Protein Confers Salt Tolerance in Rice (Oryza sativa L.). *Plant Molecular Biology Reporter*, *34*(2), 524–532. https://doi.org/10.1007/s11105-015-0944-0

Zarbakhsh, S., & Shahsavar, A. R. (2023). Exogenous γ-aminobutyric acid improves the photosynthesis efficiency, soluble sugar contents, and mineral nutrients in pomegranate plants exposed to drought, salinity, and drought-salinity stresses. *BMC Plant Biology*, *23*(1), 543. https://doi.org/10.1186/s12870-023-04568-2

Zhang, A., Liu, Y., Wang, F., Li, T., Chen, Z., Kong, D., Bi, J., Zhang, F., Luo, X., Wang, J., Tang, J., Yu, X., Liu, G., & Luo, L. (2019). Enhanced rice salinity tolerance via CRISPR/Cas9-targeted mutagenesis of the OsRR22 gene. *Molecular Breeding*, *39*(3), 47. https://doi.org/10.1007/s11032-019-0954-y

Zhang, H., Lang, Z., Zhu, J.-K., & Wang, P. (2025). Tackling abiotic stress in plants: Recent insights and trends. *Stress Biology*, *5*(1), 8. https://doi.org/10.1007/s44154-025-00216-x

Zhang, K., Duan, Y., Cao, Y., Chen, Y., Zou, Z., Li, F., Shen, Q., Yang, X., Ma, Y., Fang, W., & Zhu, X. (2022). CsCuAOs and CsAMADH1 Are Required for Putrescine-Derived γ-Aminobutyric Acid Accumulation in Tea. *Foods (Basel, Switzerland)*, *11*(9), 1356. https://doi.org/10.3390/foods11091356

Zhang, X., Liu, X., Zhang, D., Tang, H., Sun, B., Li, C., Hao, L., Liu, C., Li, Y., Shi, Y., Xie, X., Song, Y., Wang, T., & Li, Y. (2017). Genome-wide identification of gene expression in contrasting maize inbred lines under field drought conditions reveals the significance of transcription factors in drought tolerance. *PLOS ONE*, *12*(7), e0179477. https://doi.org/10.1371/journal.pone.0179477

Zhang, Y., Sultan, H., Shah, A., Mu, Y., Li, Y., Li, L., Huang, Z., Song, S., Tao, Y., Zhou, Z., & Nie, L. (2025). Regulation effect of seed priming on sowing rate of direct seeding of rice under salt stress. *Frontiers in Plant Science*, *16*, 1541736. https://doi.org/10.3389/fpls.2025.1541736

Zhou, C., Bo, W., El-Kassaby, Y. A., & Li, W. (2024). Transcriptome profiles reveal response mechanisms and key role of PsNAC1 in Pinus sylvestris var. Mongolica to drought stress. *BMC Plant Biology*, *24*(1), 343. https://doi.org/10.1186/s12870-024-05051-2

Zhu, X., Li, X., Chen, W., Chen, J., Lu, W., Chen, L., & Fu, D. (2012). Evaluation of new reference genes in papaya for accurate transcript normalization under different experimental conditions. *PloS One*, *7*(8), e44405. https://doi.org/10.1371/journal.pone.0044405

Zhu, X., Liao, J., Xia, X., Xiong, F., Li, Y., Shen, J., Wen, B., Ma, Y., Wang, Y., & Fang, W. (2019). Physiological and iTRAQ-based proteomic analyses reveal the function of exogenous γ-aminobutyric acid (GABA) in improving tea plant (*Camellia sinensis* L.) tolerance at cold temperature. *BMC Plant Biology*, *19*(1), 43. https://doi.org/10.1186/s12870-019-1646-9

Zulfiqar, F., Akram, N. A., & Ashraf, M. (2019). Osmoprotection in plants under abiotic stresses: New insights into a classical phenomenon. *Planta*, *251*(1), 3. https://doi.org/10.1007/s00425-019-03293-1

Annex

Table S1. Descriptions of upregulated genes associated with KEGG pathways in Hybrid #78 compared with WT Ni in control conditions.

	KEGG ID	Description	Gene ID	Number of genes	Kegg ID
Metabolism	dosa00910	Nitrogen metabolism	Os08g0423500/Os08g0423600/ Os08g0468700	3	dosa:Os08t0423500-00/dosa:Os08t0423600-00/dosa:Os08t0468700-00
	dosa01212	Fatty acid metabolism	Os04g0116600	3	dosa:Os04t0116600-01
	dosa00270	Cysteine and methionine metabolism	Os03g0196600/Os06g0564700/ Os06g0175800/Os07g0689600	4	dosa:Os03t0196600-01/dosa:Os06t0564700-01/dosa:Os06t0175800-01/dosa:Os07t0689600-01
	dosa00052	Galactose metabolism	Os07g0687900/Os07g0209100	2	dosa:Os07t0687900-01/dosa:Os07t0209100-01
	dosa00053	Ascorbate and aldarate metabolism	Os04g0361500/Os04g0360500	2	dosa:Os04t0361500-00/dosa:Os04t0360500-01

	dosa00450	Seleno compound metabolism	Os06g0175800	1	dosa:Os06t0175800-01
	dosa00750	Vitamin B6 metabolism	Os02g0226200	1	dosa:Os02t0226200-01
	dosa00650	Butanoate metabolism	Os04g0389800	1	dosa:Os04t0389800-01
	dosa00350	Tyrosine metabolism	Os11g0210600	1	dosa:Os11t0210600-01
	dosa00592	alpha-Linolenic acid metabolism	Os03g0225900	1	dosa:Os03t0225900-01
	dosa01210	2-Oxocarboxylic acid metabolism	Os04g0389800	1	dosa:Os04t0389800-01
	dosa00051	Fructose and mannose metabolism	Os03g0828300	1	dosa:Os03t0828500-01
	dosa00240	Pyrimidine metabolism	Os12g0123500	1	dosa:Os12t0123500-01
	dosa00630	Glyoxylate and dicarboxylate metabolism	Os07g0529000	1	dosa:Os07t0529000-01
	dosa00564	Glycerophospholipid metabolism	Os01g0329000	1	dosa:Os01t0329000-01
	dosa00230	Purine metabolism	Os12g0123500	1	dosa:Os12t0123500-01
	dosa00620	Pyruvate metabolism	Os11g0210600	1	dosa:Os11t0210600-01

	dosa00561	Glycerolipid metabolism	Os01g0329000	1	dosa:Os01t0329000-01
	dosa00010	Glycolysis / gluconeogenesis	Os11g0210600	1	dosa:Os11t0210600-01
	dosa00500	Starch and sucrose metabolism	Os10g0465700	1	dosa:Os10t0465700-01
	dosa00920	Sulfur metabolism	Os03g0196600/Os06g0564700	2	dosa:Os03t0196600-01/dosa:Os06t0564700-01
	dosa00380	Tryptophan metabolism	Os09g0344500	1	dosa:Os09t0344500-01
	dosa01232	Nucleotide metabolism	Os12g0123500	1	dosa:Os12t0123500-01
	dosa00480	Glutathione metabolism	Os10g0527800	1	dosa:Os10t0527800-01
	dosa00500	Starch and sucrose metabolism	Os10g0465700	1	dosa:Os10t0465700-01
Biosynthesis	dosa01230	Biosynthesis of amino acids	Os03g0196600/Os06g0564700/Os06g0175800/Os04g0389800	4	dosa:Os03t0196600-01/dosa:Os06t0564700-01/dosa:Os06t0175800-01/dosa:Os04t0389800-01

	dosa00999	Biosynthesis of various plant secondary metabolites	Os02g0306401/Os07g0689600/ Os04g0167800	3	dosa:Os02t0306401-00/dosa:Os07t0689600-01/dosa:Os04t0167800-01
	dosa00290	Valine, leucine, and isoleucine biosynthesis	Os04g0389800	1	dosa:Os04t0389800-01
	dosa00908	Zeatin biosynthesis	Os10g0178500	1	dosa:Os10t0178500-01
	dosa00941	Flavonoid biosynthesis	Os10g0317900	1	dosa:Os10t0317900-01
	dosa01040	Biosynthesis of unsaturated fatty acids	Os04g0116600	1	dosa:Os04t0116600-01
	dosa00073	Cutin, suberin, and wax biosynthesis	Os04g0354600	1	dosa:Os04t0354600-01
	dosa00904	Diterpenoid biosynthesis	Os03g0856700	1	dosa:Os03t0856700-01
	dosa00130	Ubiquinone and other terpenoid-quinone biosynthesis	Os08g0143300	1	dosa:Os08t0143300-00
	dosa00770	Pantothenate and CoA biosynthesis	Os04g0389800	1	dosa:Os04t0389800-01

	dosa00940	Phenylpropanoid biosynthesis	Os04g0689000/Os10g0512400/Os03g0339300/Os08g0143300	4	dosa:Os04t0689000-01/dosa:Os10t0512400-01/dosa:Os07t0676900-01/dosa:Os08t0143300-00
	dosa01240	Biosynthesis of cofactors	Os04g0361500/Os02g0226200/Os04g0360500	3	dosa:Os04t0361500-00/dosa:Os02t0226200-01/dosa:Os04t0360500-01
Signalling and interaction	dosa00196	Photosynthesis - antenna proteins	Os01g0600900/Os01g0720500	2	dosa:Os01t0600900-02/dosa:Os01t0720500-01
	dosa04626	Plant-pathogen interaction	Os05g0380900/Os01g0955100/Os10g0191300/Os05g0343400/Os03g0382100/Os06g0262800	6	dosa:Os05t0380900-01/dosa:Os01t0955100-01/dosa:Os10t0191300-01/dosa:Os05t0343400-01/dosa:Os03t0382100-01/dosa:Os06t0262800-01
	dosa04016	MAPK signaling pathway - plant	Os10g0191300/Os05g0343400/Os09g0325700	3	dosa:Os10t0191300-01/dosa:Os05t0343400-01/dosa:Os09t0325700-01

	dosa04075	Plant hormone signal transduction	Os02g0643800/Os10g0191300/ Os02g0769100/Os09g0325700	4	dosa:Os02t0643800-01/dosa:Os10t0191300-01/dosa:Os02t0769100-01/dosa:Os09t0325700-01
Degradation/ Utilization	dosa00062	Fatty acid elongation	Os04g0116600/Os03g0382100/ Os06g0262800	3	dosa:Os04t0116600-01/dosa:Os03t0382100-01/dosa:Os06t0262800-01
	dosa04122	Sulfur relay system	Os01g0598900	1	dosa:Os01t0598900-00
	dosa00071	Fatty acid degradation	Os11g0210600	1	dosa:Os11t0210600-01
	dosa03018	RNA degradation	Os04g0684900	1	dosa:Os04t0684900-01
	dosa04120	Ubiquitin-mediated proteolysis	Os01g0124900	1	dosa:Os01t0124900-00
Other cellular process	dosa04146	Peroxisome	Os04g0354600	1	dosa:Os04t0354600-01
	dosa03010	Ribosome	Os07g0565100	1	dosa:Os04t0613600-00